

Introduction to hadronic collisions: theoretical concepts and practical tools for the LHC

*Scuola Normale Superiore,
Pisa, 18-22 February, 2008*

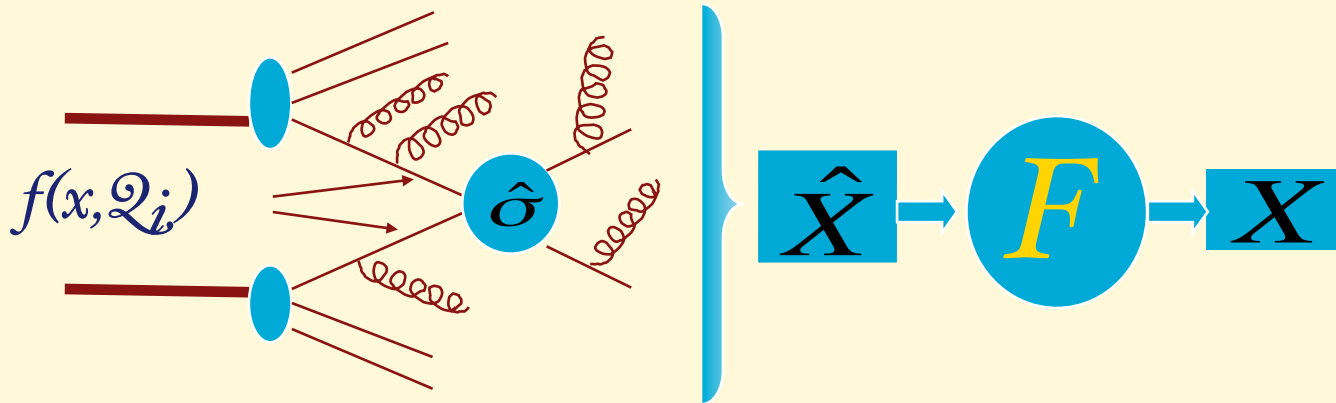
Michelangelo L. Mangano
TH Unit, Physics Dept, CERN
michelangelo.mangano@cern.ch

Contents

- **Lecture I & II:** Define the framework and basic rules
 - Factorization theorem
 - Parton densities
 - Evolution of final states
 - Hard processes
- **Lecture III, IV, V:** Tools and applications:
 - Numerical and Monte Carlo codes
 - Physics objects relevant to the search of BSM phenomena at the LHC:
 - leptons
 - jets
 - top quark
 - W +multijets
 - Example: SUSY searches

Factorization Theorem

$$\frac{d\sigma}{dX} = \sum_{j,k} \int_{\hat{X}} f_j(x_1, Q_i) f_k(x_2, Q_i) \frac{d\hat{\sigma}_{jk}(Q_i, Q_f)}{d\hat{X}} F(\hat{X} \rightarrow X; Q_i, Q_f)$$



$f_j(x, Q)$ Parton distribution functions (PDF)

- sum over all initial state histories leading, at the scale Q , to:

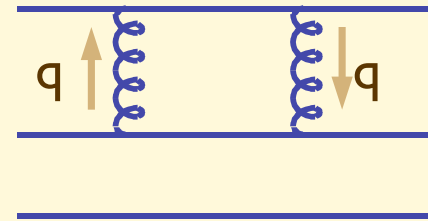
$$\vec{p}_j = x \vec{P}_{proton}$$

$F(\hat{X} \rightarrow X; Q_i, Q_f)$

- transition from partonic final state to the hadronic observable (hadronization, fragm. function, jet definition, etc)
 - Sum over all histories with X in them

Universality of parton densities and factorization, an intuitive view

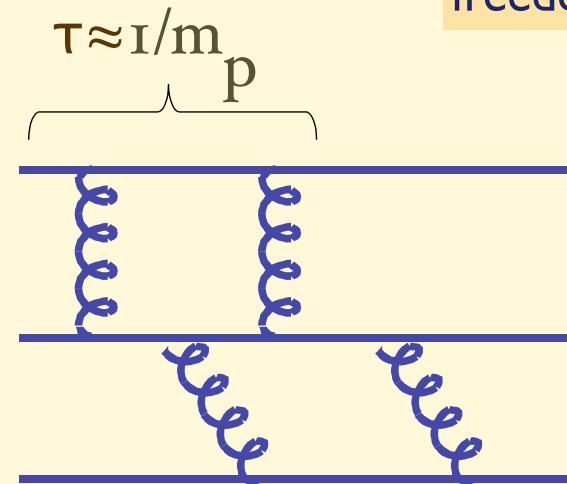
1) Exchange of **hard gluons** among quarks inside the proton is suppressed by powers of $(m_p/Q)^2$



$$q \gtrsim Q \quad \int_Q^\infty \frac{d^4 q}{q^6} \sim \frac{1}{Q^2}$$

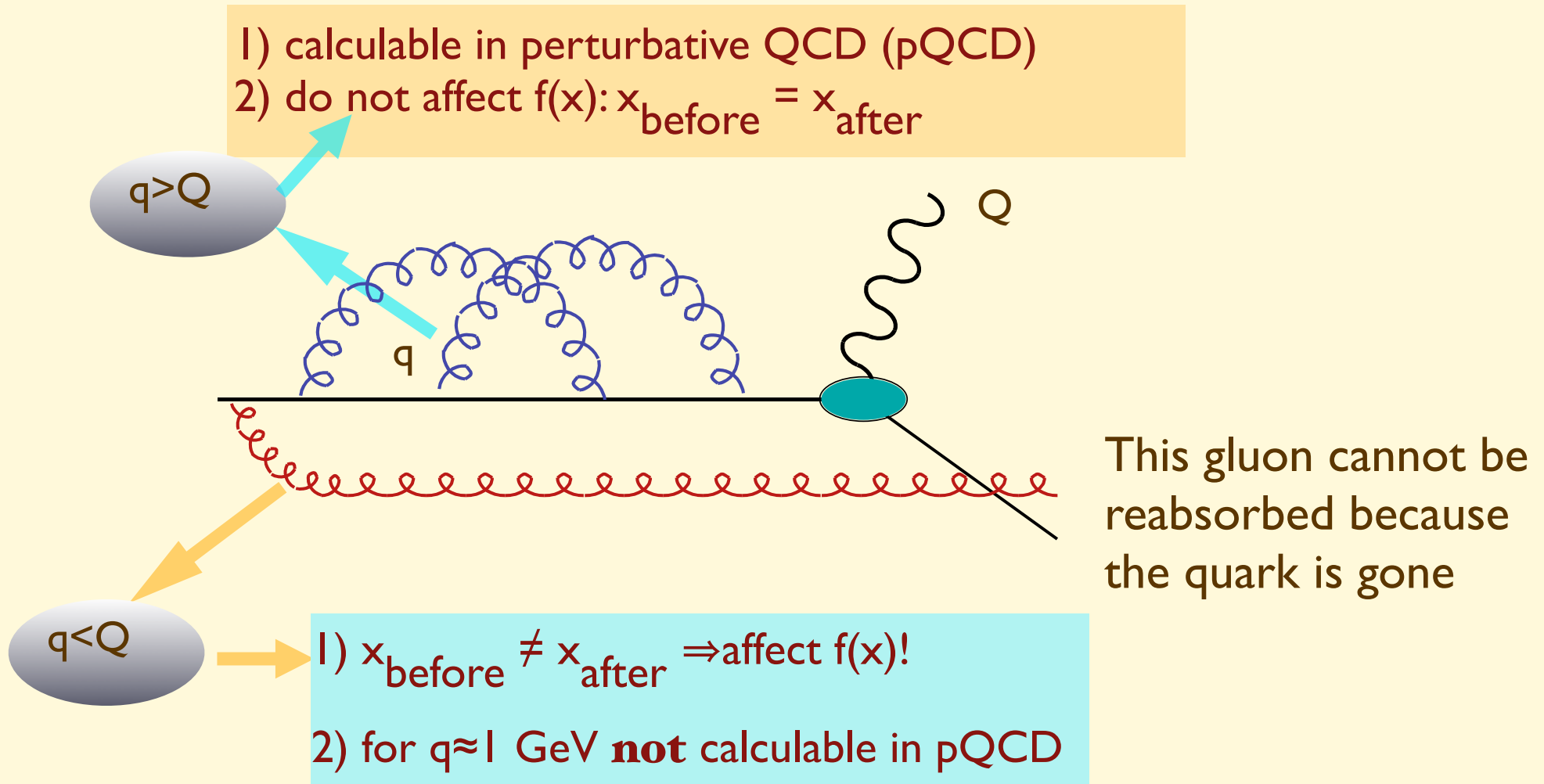
Assuming asymptotic freedom!

2) **Typical time-scale of interactions binding the proton** is therefore of $O(1/m_p)$ (in a frame in which the proton has energy E , $\tau = \gamma/m_p = E/m_p^2$)



3) If a hard probe ($Q \gg m_p$) hits the proton, on a time scale $= 1/Q$, there is no time for quarks to negotiate a coherent response. The struck quark receives no feedback from its pals, and acts as a free particle

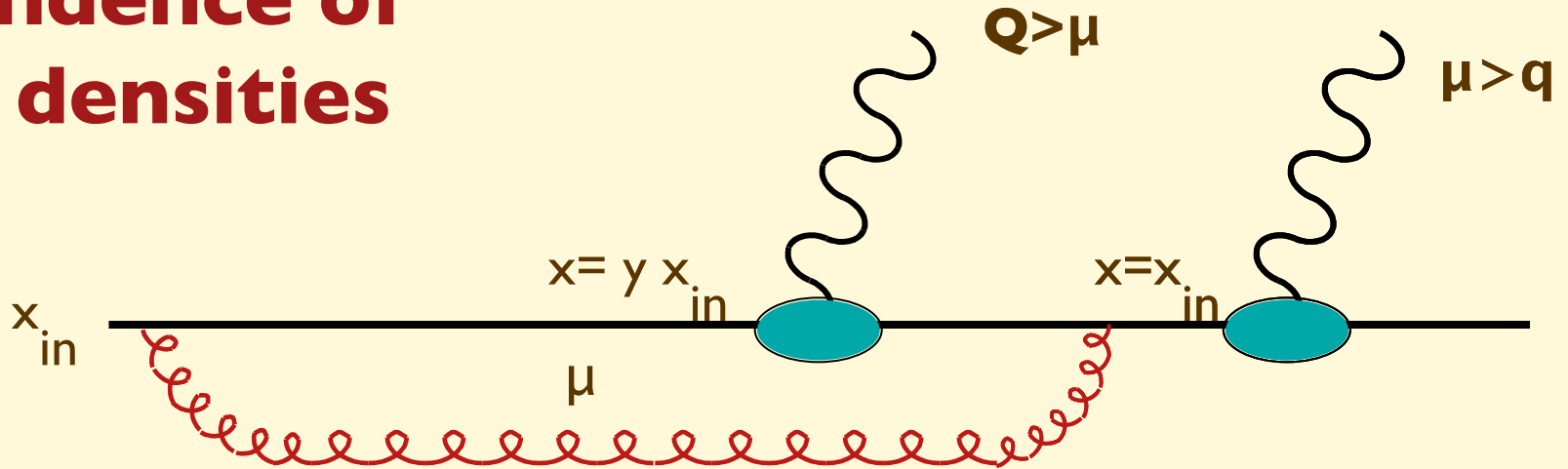
As a result, to study inclusive processes at large Q it is sufficient to consider the interactions between the external probe and a single parton:



However, since $\tau(q \approx 1 \text{ GeV}) \gg 1/Q$, the emission of low-virtuality gluons will take place long before the hard collision, and therefore cannot depend on the detailed nature of the hard probe. While it is not calculable in pQCD, $f(q \ll Q)$ can be measured using a reference probe, and used elsewhere

→ **Universality of $f(x)$**

Q dependence of parton densities



The larger is Q , the more gluons will **not** have time to be reabsorbed

PDF's depend on Q !

$$f(x, Q) = f(x, \mu) + \int_x^1 dx_{in} f(x_{in}, \mu) \int_{\mu}^Q dq^2 \int_0^1 dy P(y, q^2) \delta(x - yx_{in})$$

$$f(x, Q) = f(x, \mu) + \int_x^1 dx_{in} f(x_{in}, \mu) \int_{\mu}^Q dq^2 \int_0^1 dy P(y, q^2) \delta(x - yx_{in})$$

$f(x, Q)$ should be independent of the intermediate scale μ considered:

$$\frac{df(x, Q)}{d\mu^2} = 0 \quad \Rightarrow \quad \frac{df(x, \mu)}{d\mu^2} = \int_x^1 \frac{dy}{y} f(y, \mu) P(x/y, \mu^2)$$

One can prove that:

$$P(x, Q^2) = \frac{\alpha_s}{2\pi} \frac{1}{Q^2} P(x) \quad \leftarrow \text{calculable in pQCD}$$

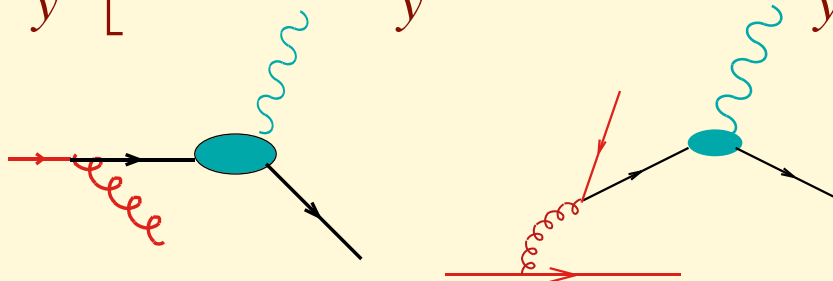
and therefore (Altarelli-Parisi equation):

$$\frac{df(x, \mu)}{d \log \mu^2} = \frac{\alpha_s}{2\pi} \int_x^1 \frac{dy}{y} f(y, \mu) P(x/y)$$

More in general, one should consider additional processes which lead to the evolution of partons at high Q ($t = \log Q^2$):

$$[g(x)]_+ : \int_0^1 dx f(x) g(x)_+ \equiv \int_0^1 [f(x) - f(1)] g(x) dx$$

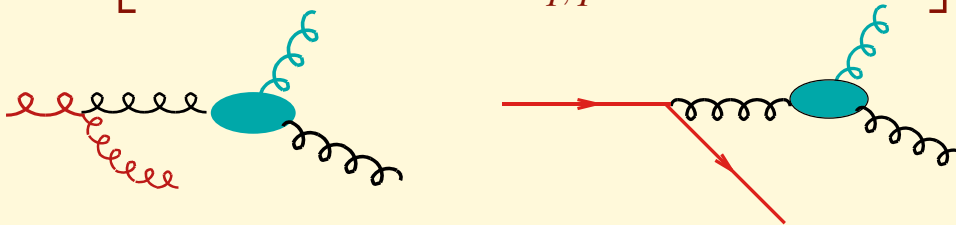
$$\frac{dq(x, Q)}{dt} = \frac{\alpha_s}{2\pi} \int_x^1 \frac{dy}{y} \left[q(y, Q) P_{qq}\left(\frac{x}{y}\right) + g(y, Q) P_{qg}\left(\frac{x}{y}\right) \right]$$



$$P_{qq}(x) = C_F \left(\frac{1+x^2}{1-x} \right)_+$$

$$P_{qg}(x) = \frac{1}{2} [x^2 + (1-x)^2]$$

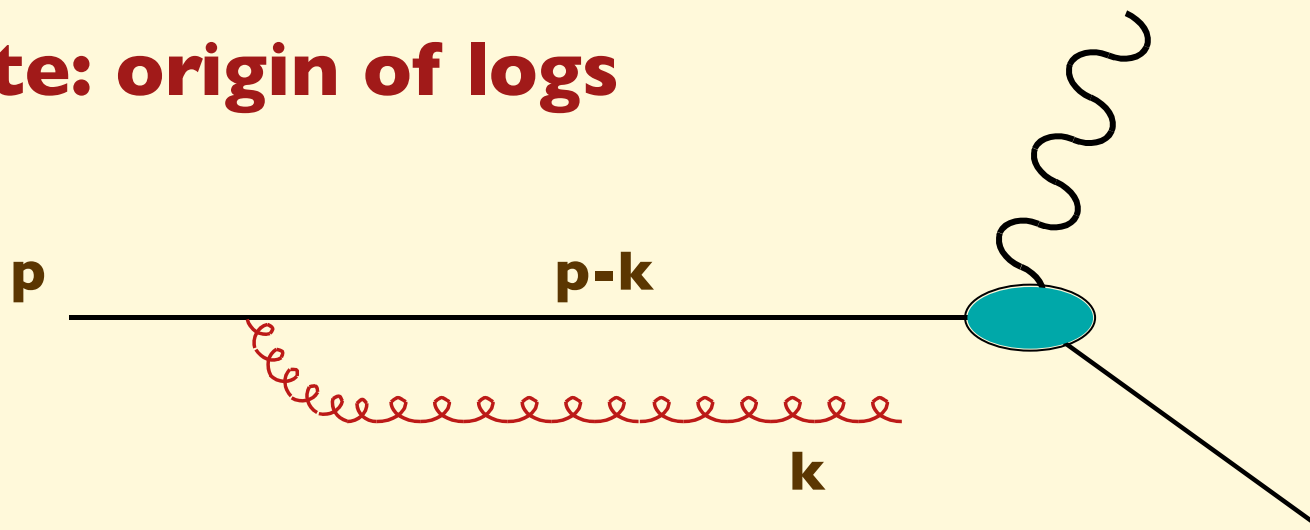
$$\frac{dg(x, Q)}{dt} = \frac{\alpha_s}{2\pi} \int_x^1 \frac{dy}{y} \left[g(y, Q) P_{gg}\left(\frac{x}{y}\right) + \sum_{q, \bar{q}} q(y, Q) P_{gq}\left(\frac{x}{y}\right) \right]$$



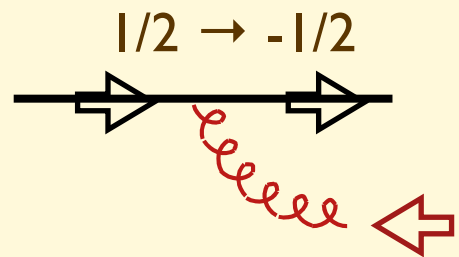
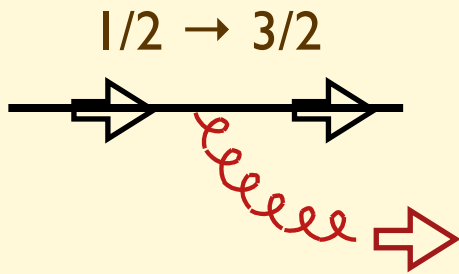
$$P_{gq}(x) = C_F \left(\frac{1 + (1-x)^2}{x} \right)$$

$$P_{gg}(x) = 2N_c \left[\frac{x}{(1-x)_+} + \frac{1-x}{x} + x(1-x) \right] + \delta(1-x) \left(\frac{11N_c - 2n_f}{6} \right)$$

Note: origin of logs



$$(p-k)^2 = -2p^0 k^0 (1 - \cos \theta_{pk})$$



Helicity conservation
 $\sim p \cdot k$

$$|M|^2 \sim \left[\frac{1}{(p-k)^2} \right]^2 \times (p \cdot k)$$

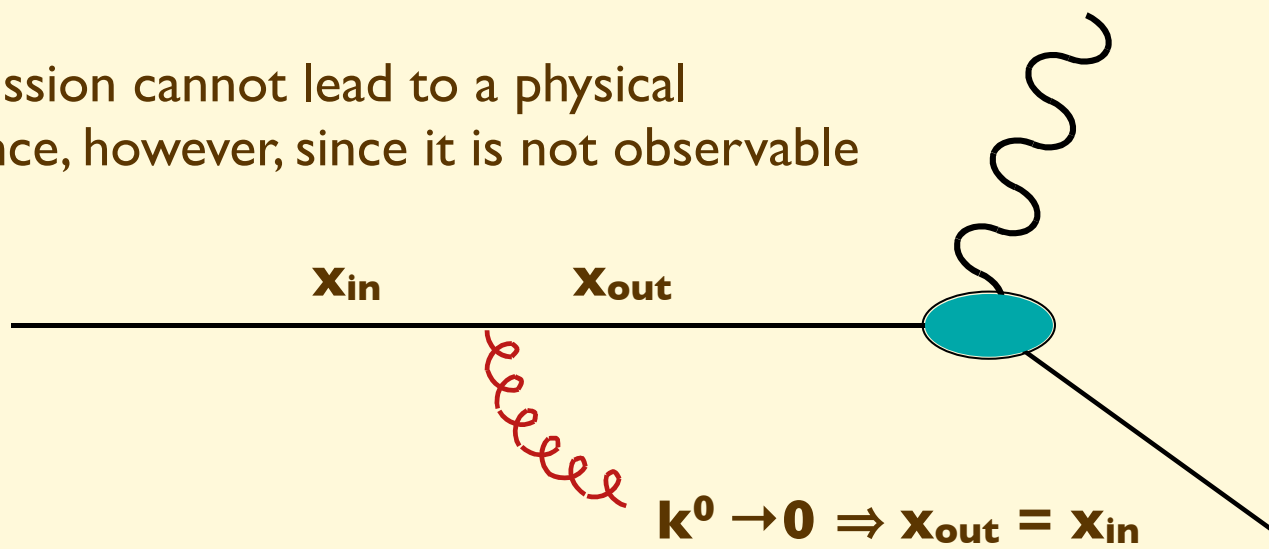
\rightarrow

Soft divergence

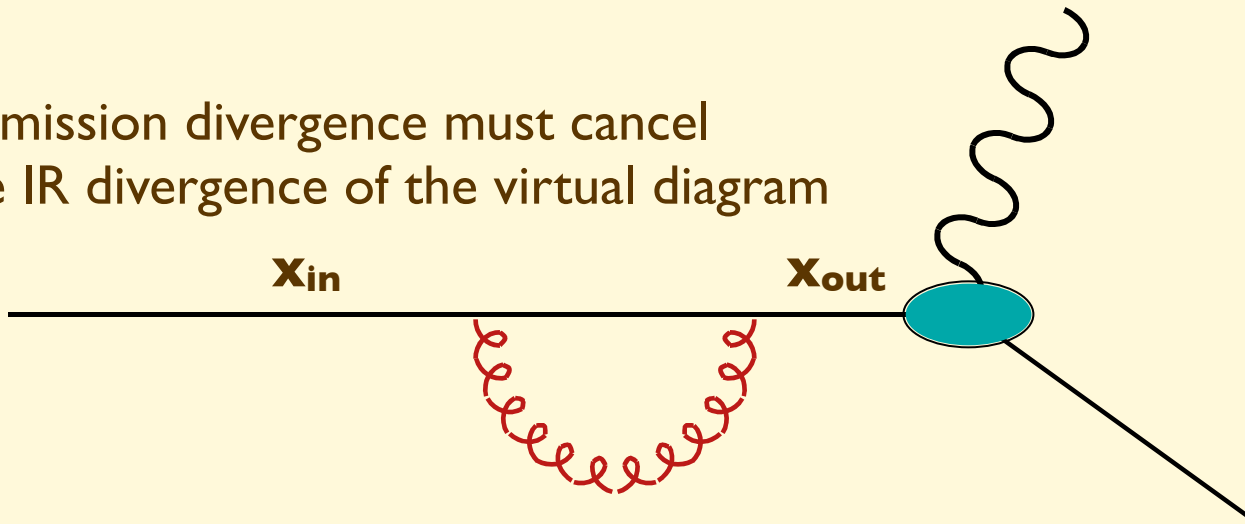
$$\frac{1}{p^0} \frac{dk^0}{k^0} \frac{d\theta}{\theta}$$

Collinear divergence

Soft emission cannot lead to a physical divergence, however, since it is not observable

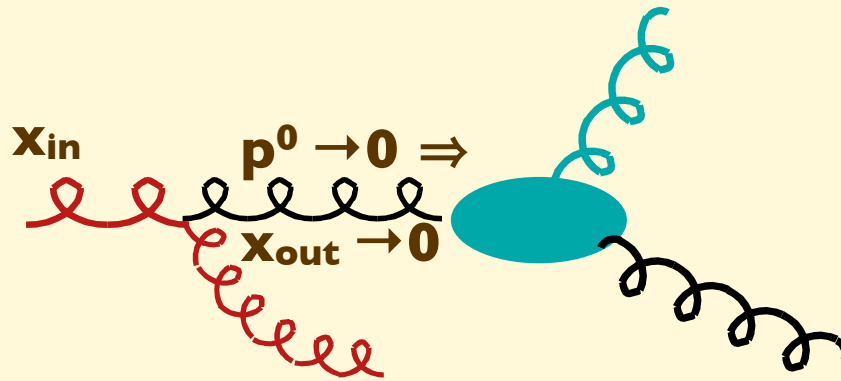


The soft-emission divergence must cancel against the IR divergence of the virtual diagram



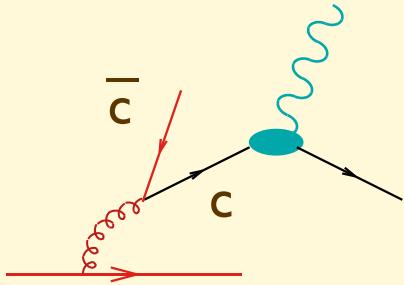
The cancellation cannot take place in the case of collinear divergence, since $\mathbf{x}_{out} \neq \mathbf{x}_{in}$, so virtual and real configurations are not equivalent

Things are different if $\mathbf{p}^0 \rightarrow \mathbf{0}$. In this case, again, $\mathbf{x}_{\text{out}} \neq \mathbf{x}_{\text{in}}$, no virtual-real cancellation takes place, and an extra singularity due to the $1/\mathbf{p}^0$ pole appears



These are called **small- \mathbf{x}** logarithms. They give rise to the double-log growth of the number of gluons at small \mathbf{x} and large \mathbf{Q}

Example: charm in the proton



$$\frac{dc(x, Q)}{dt} = \frac{\alpha_s}{2\pi} \int_x^1 \frac{dy}{y} g(y, Q) P_{qg}\left(\frac{x}{y}\right)$$

Assuming a typical behaviour of the gluon density: $g(x, Q) \sim A/x$

and using $P_{qg}(x) = \frac{1}{2} [x^2 + (1-x)^2]$ we get:

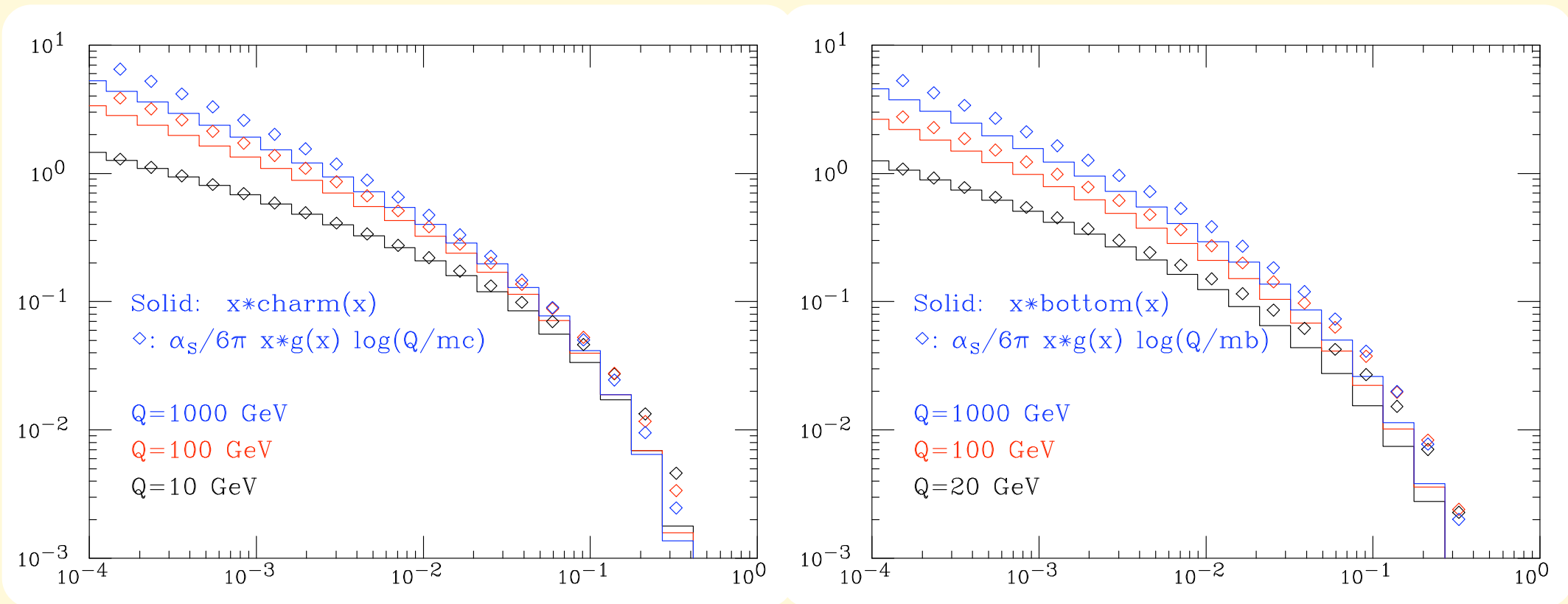
$$\frac{dc(x, Q)}{dt} = \frac{\alpha_s}{2\pi} \int_x^1 \frac{dy}{y} g(x/y, Q) P_{qg}(y) = \frac{\alpha_s}{2\pi} \int_x^1 dy \frac{A}{x} \frac{1}{2} [y^2 + (1-y)^2] = \frac{\alpha_s A}{6\pi x}$$

and therefore:

$$c(x, Q) \sim \frac{\alpha_s}{6\pi} \log\left(\frac{Q^2}{m_c^2}\right) g(x, Q)$$

Corrections to this simple formula will arise due to the Q dependence of $g(x)$ and of α_s

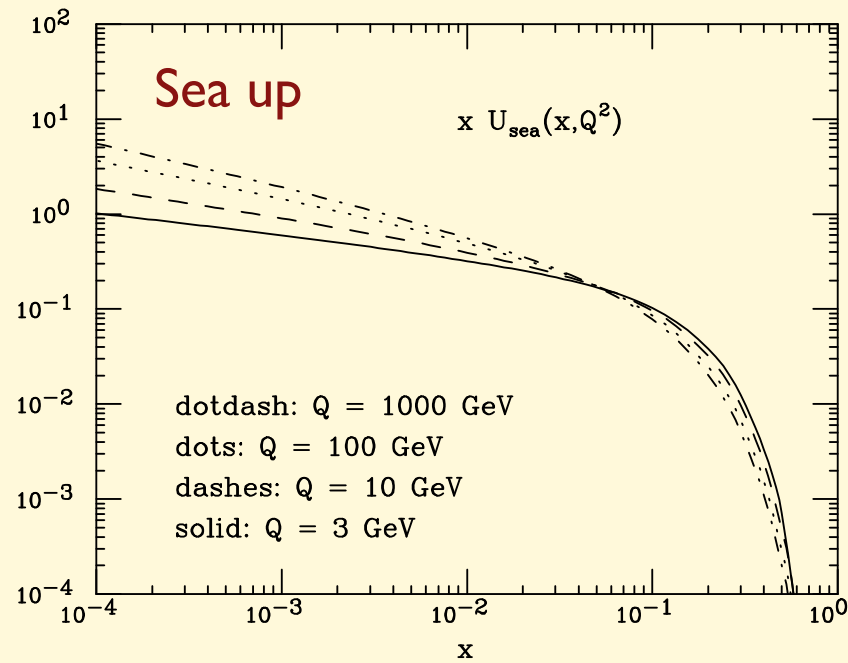
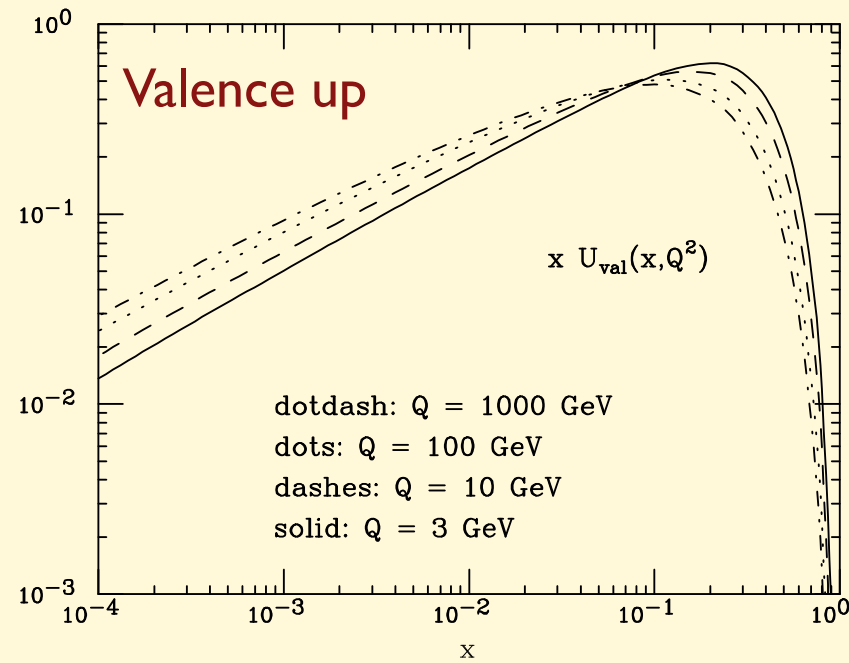
Numerical example



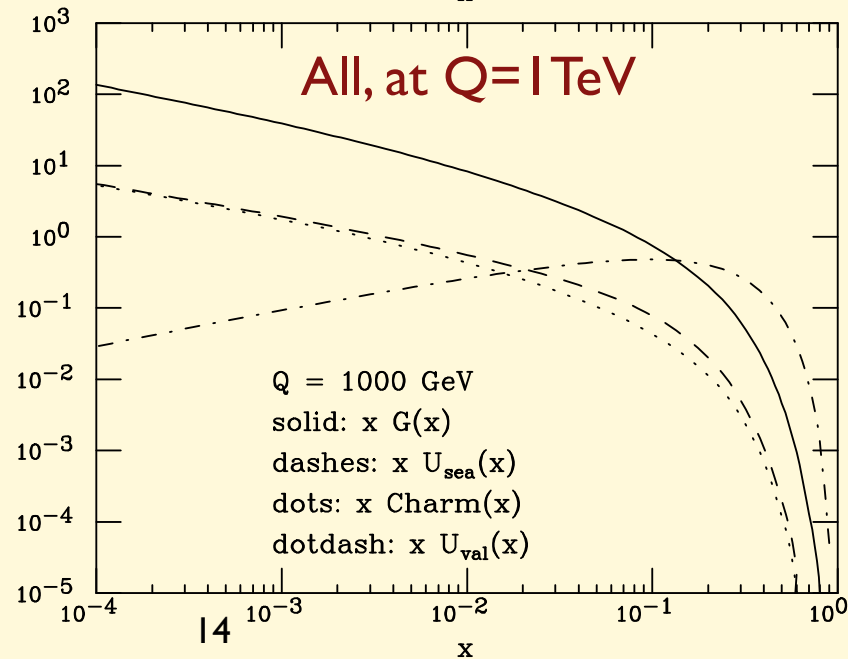
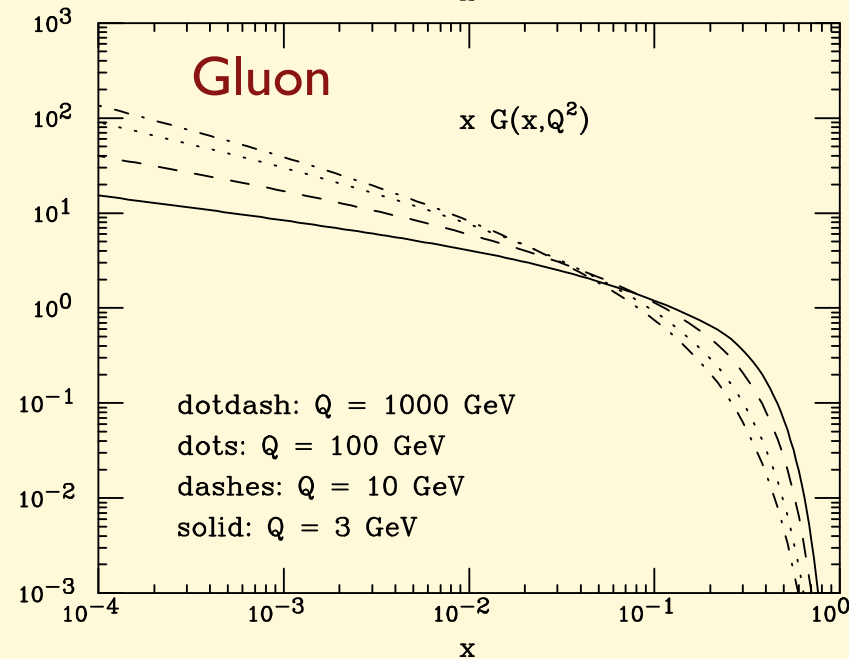
Excellent agreement, given the simplicity of the approximation!

Can be improved by tuning the argument of the log (threshold onset), including a better parameterization of $g(x)$, etc....

Examples of PDFs and their evolution



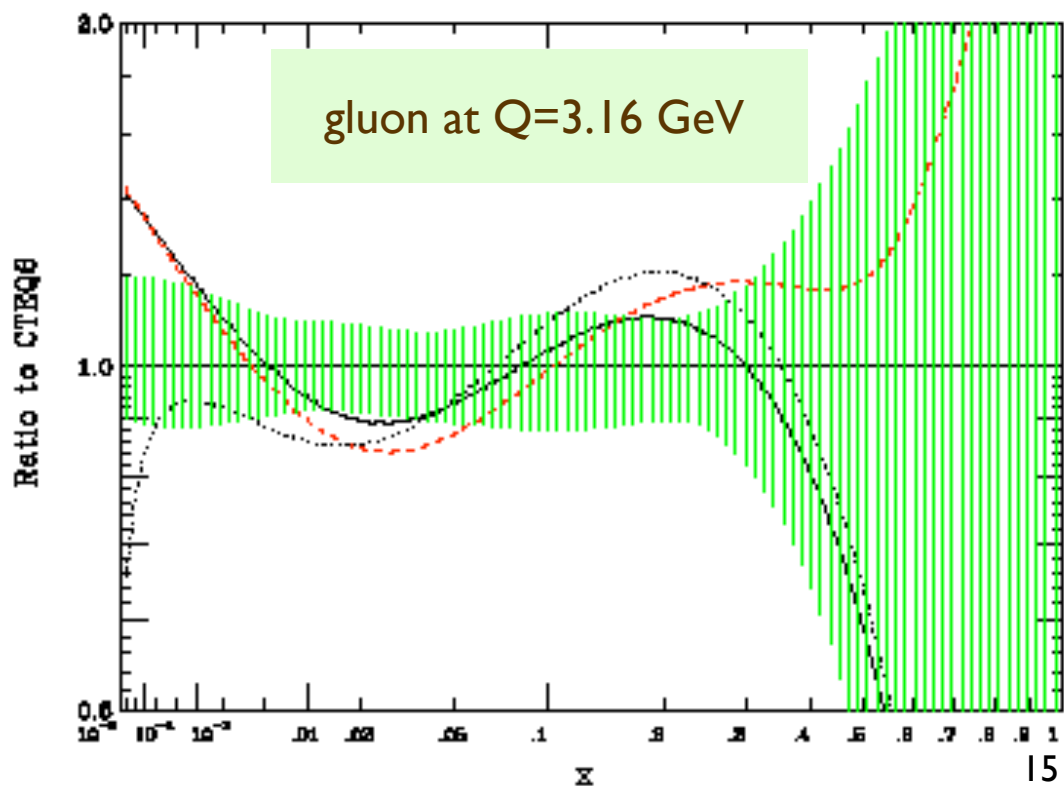
Note:
sea \approx 10% glue



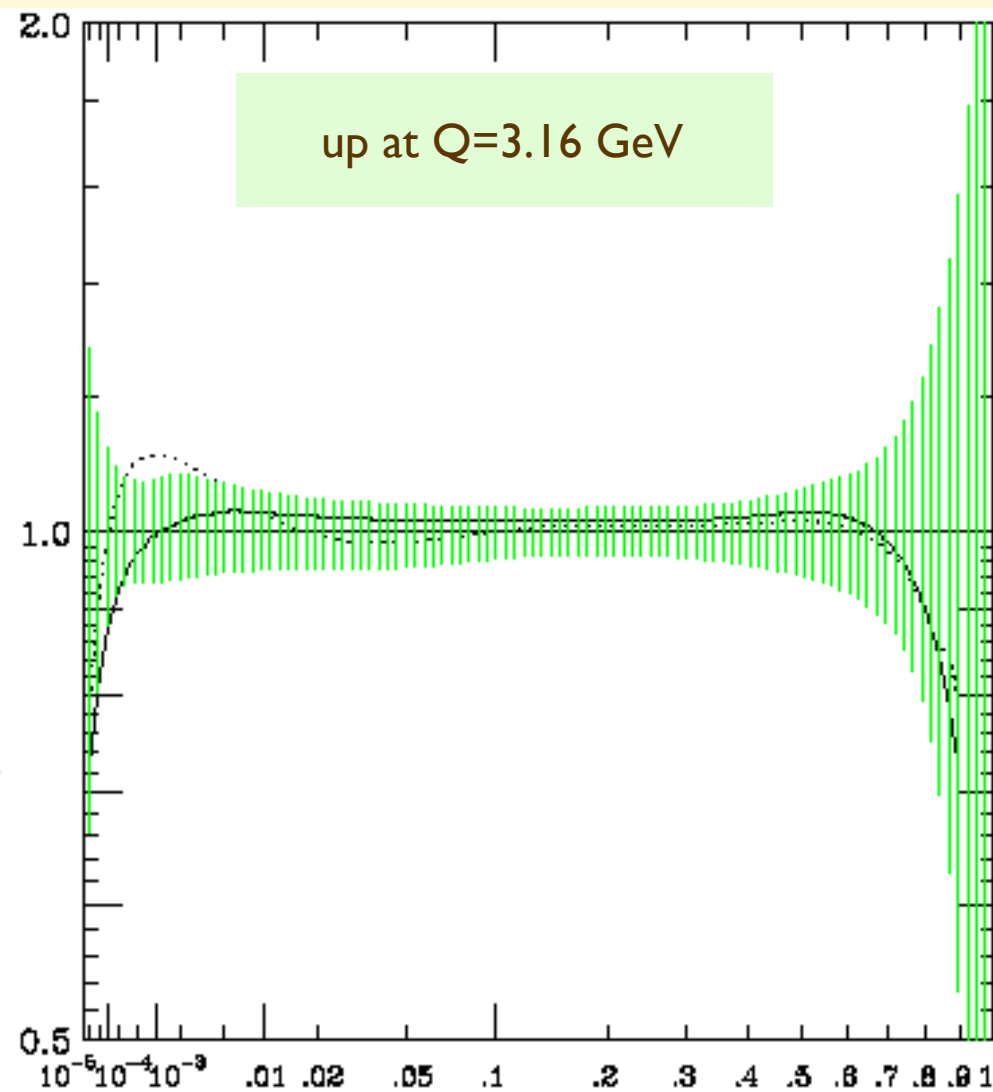
Note:
charm \approx up at high Q

PDF uncertainties

Green bands represent the convolution of theoretical and experimental systematics in the determination of PDFs



Ratio to CTEQ6

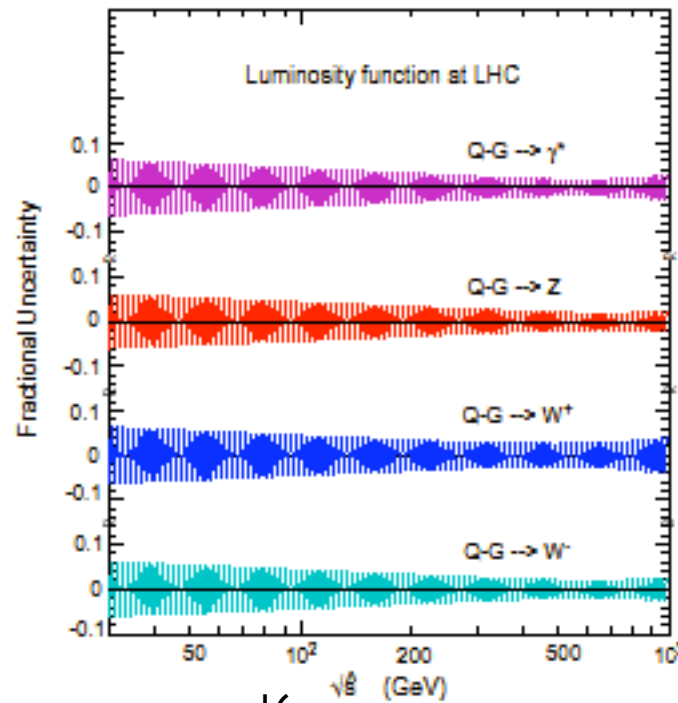
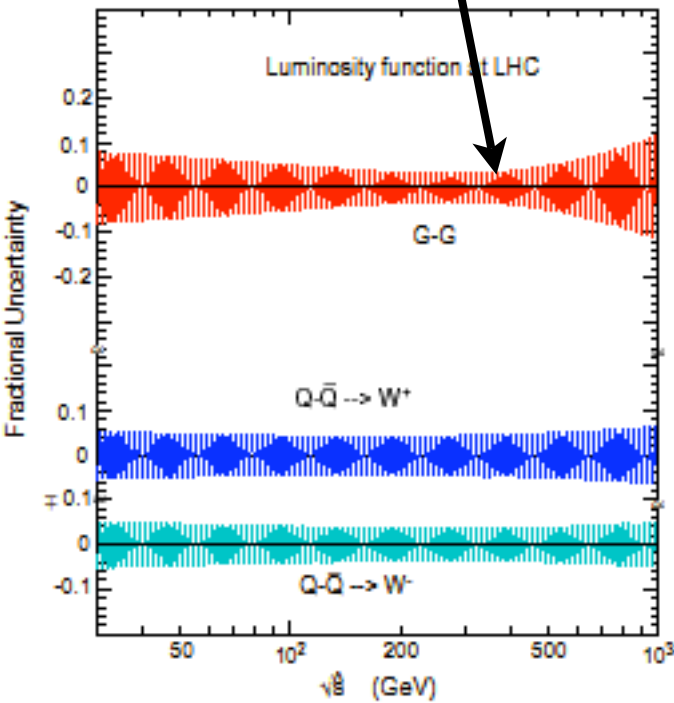
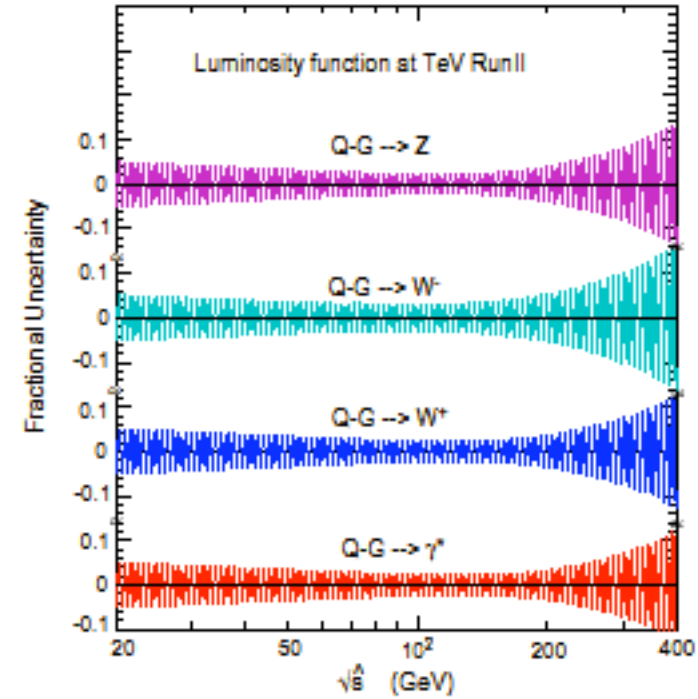
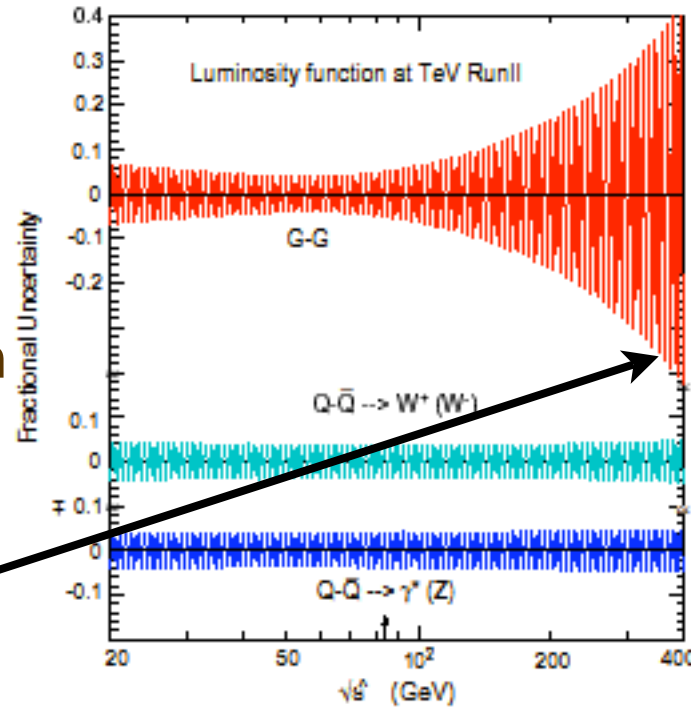


Proton PDFs known to 10-20% for $10^{-3} < x < 0.3$, with uncertainties getting smaller at larger Q

PDF luminosity uncertainties

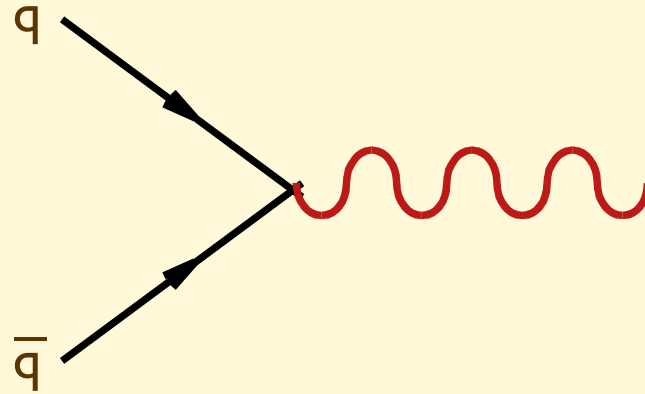
At the Tevatron

tt production, smaller uncertainty at the LHC!



At the LHC

Example: Drell-Yan processes



$$W \rightarrow l\nu$$

$$Z \rightarrow l^+ l^-$$

Properties/Goals of the measurement:

- Clean final state (no hadrons from the hard process)
- Tests of QCD: $\sigma(W,Z)$ known up to NNLO (2-loops)
- Measure $m(W)$ (\rightarrow constrain $m(H)$)
- constrain PDFs (e.g. $f_{\text{up}}(x)/f_{\text{down}}(x)$)
- search for new gauge bosons: $q\bar{q} \rightarrow W', Z'$
- Probe contact interactions: $q\bar{q}l^+l^-$

Some useful relations and definitions

Rapidity: $y = \frac{1}{2} \log \frac{E_W + p_W^z}{E_W - p_W^z}$

Pseudorapidity: $\eta = -\log\left(\tan \frac{\theta}{2}\right)$

where:

$$\tan \theta = \frac{p_T}{p^z} \quad \text{and} \quad p_T = \sqrt{p_x^2 + p_y^2}$$

Exercise: prove that for a massless particle rapidity=pseudorapidity:

Exercise: using $\tau = \frac{\hat{s}}{S} = x_1 x_2$ and

$$\begin{cases} E_W = (x_1 + x_2) E_{beam} \\ p_W^z = (x_1 - x_2) E_{beam} \end{cases} \Rightarrow y = \frac{1}{2} \log \frac{x_1}{x_2}$$

prove the following relations:

$$x_{1,2} = \sqrt{\tau} e^{\pm y} \quad dx_1 dx_2 = dy d\tau$$
$$dy = \frac{dx_1}{x_1} \quad d\tau \delta(\hat{s} - m_W^2) = \frac{1}{S}$$

LO Cross-section calculation

$$\sigma(pp \rightarrow W) = \sum_{q,q'} \int dx_1 dx_2 f_q(x_1, Q) f_{\bar{q}'}(x_2, Q) \frac{1}{2\hat{s}} \int d[PS] \overline{\sum_{spin,col}} |M(q\bar{q}' \rightarrow W)|^2$$

where:

$$\overline{\sum_{spin,col}} |M(q\bar{q}' \rightarrow W)|^2 = \frac{1}{3} \frac{1}{4} 8g_W^2 |V_{qq'}|^2 \hat{s} = \frac{2G_F m_W^2}{3\sqrt{2}} |V_{qq'}|^2 \hat{s}$$

$$\begin{aligned} d[PS] &= \frac{d^3 p_W}{(2\pi)^3 p_W^0} (2\pi)^4 \delta^4(P_{in} - p_W) \\ &= 2\pi d^4 p_W \delta(p_W^2 - m_W^2) \delta^4(P_{in} - p_W) = 2\pi \delta(\hat{s} - m_W^2) \end{aligned}$$

leading to:

$$\sigma(pp \rightarrow W) = \sum_{ij} \frac{\pi A_{ij}}{m_W^2} \tau \int_{\tau}^1 \frac{dx}{x} f_i(x, Q) f_j\left(\frac{\tau}{x}, Q\right) \equiv \sum_{ij} \frac{\pi A_{ij}}{m_W^2} \tau L_{ij}(\tau)$$

where:

$$\frac{\pi A_{u\bar{d}}}{m_W^2} = 6.5 \text{nb} \quad \text{and} \quad \tau = \frac{m_W^2}{S}$$

Exercise: Study the function $\tau L(\tau)$

Assume, for example, that $f(x) \sim \frac{1}{x^{1+\delta}}, \quad 0 < \delta < 1$

Then:
$$L(\tau) = \int_{\tau}^1 \frac{dx}{x} \frac{1}{x^{1+\delta}} \left(\frac{x}{\tau}\right)^{1+\delta} = \frac{1}{\tau^{1+\delta}} \log\left(\frac{1}{\tau}\right)$$

and:
$$\sigma_W = \sigma_W^0 \left(\frac{S}{m_W^2}\right)^{\delta} \log\left(\frac{S}{m_W^2}\right)$$

Therefore the **W** cross-section grows at least logarithmically with the hadronic **CM energy**. This is a typical behavior of cross-sections for production of fixed-mass objects in hadronic collisions, contrary to the case of e^+e^- collisions, where cross-sections tend to decrease with CM energy.

Note also the following relation, which allows the measurement of the total width of the W boson from the determination of the leptonic rates of W and Z bosons,

$$\Gamma_W = \frac{N(e^+e^-)}{N(e^{\pm}\nu)} \left(\frac{\sigma_{W^{\pm}}}{\sigma_Z}\right) \left(\frac{\Gamma_{ev}^W}{\Gamma_{e^+e^-}^Z}\right) \Gamma_Z$$

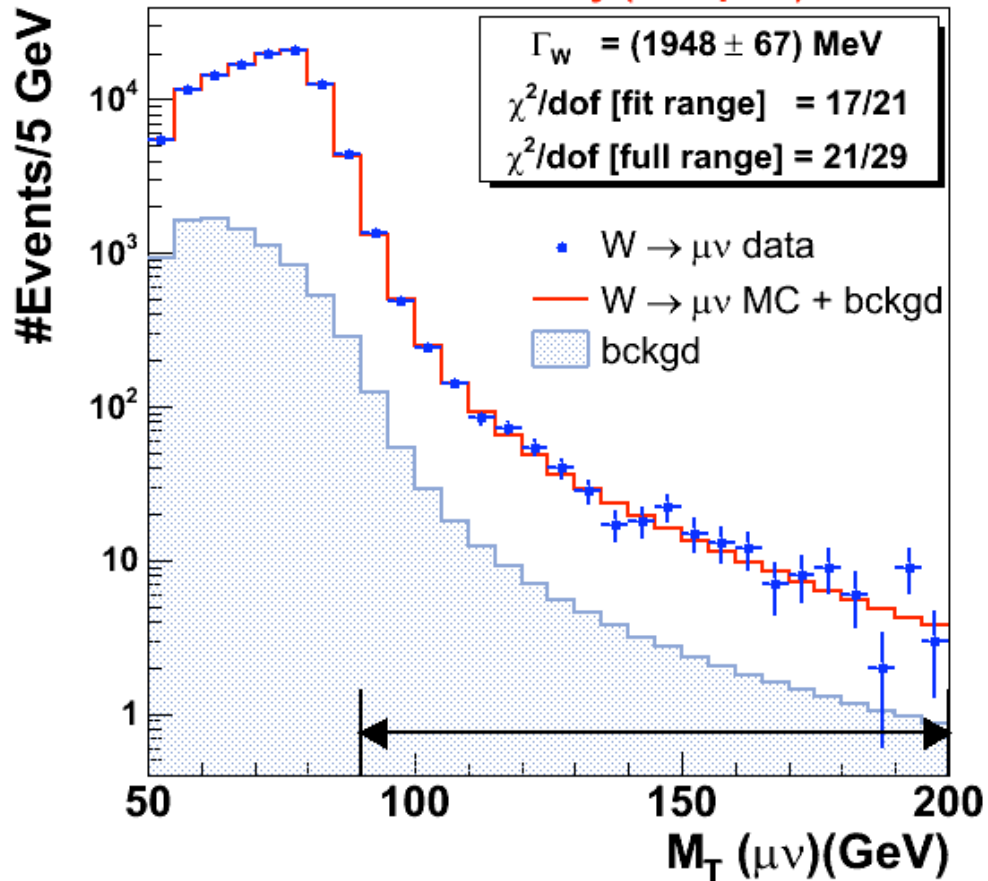
LHC data

20 theory

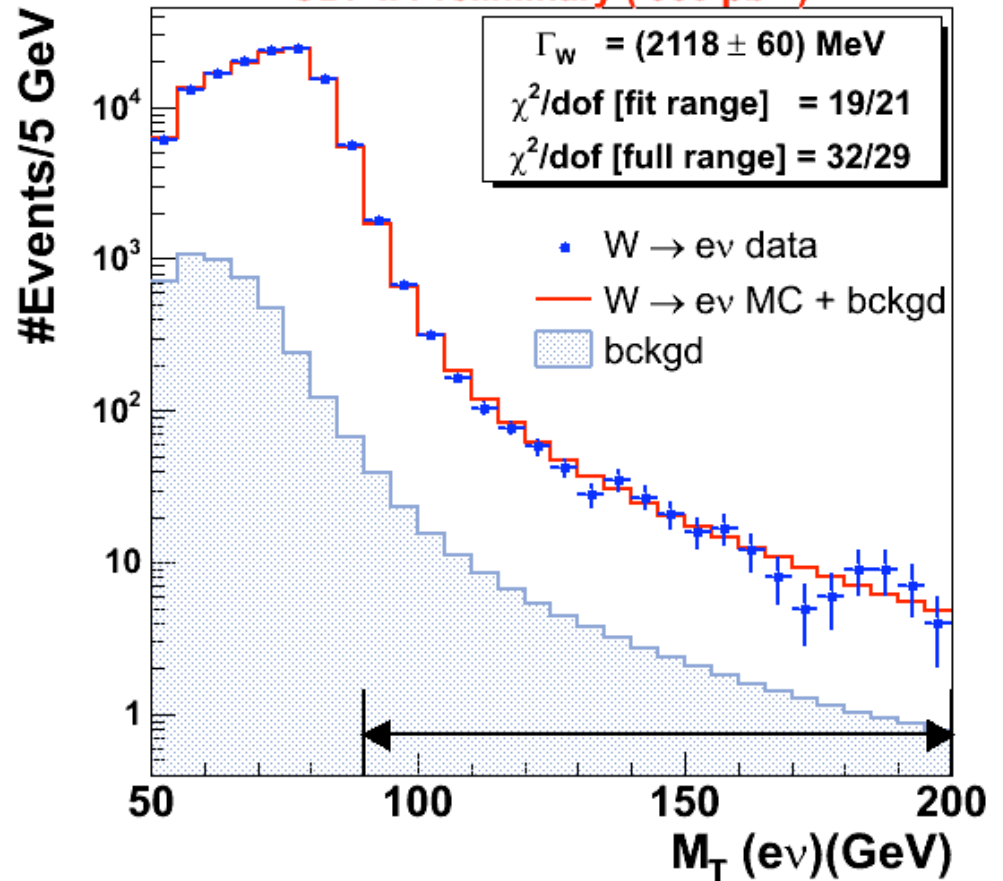
LEP/SLC

Again on the W width

CDF II Preliminary (350 pb⁻¹)

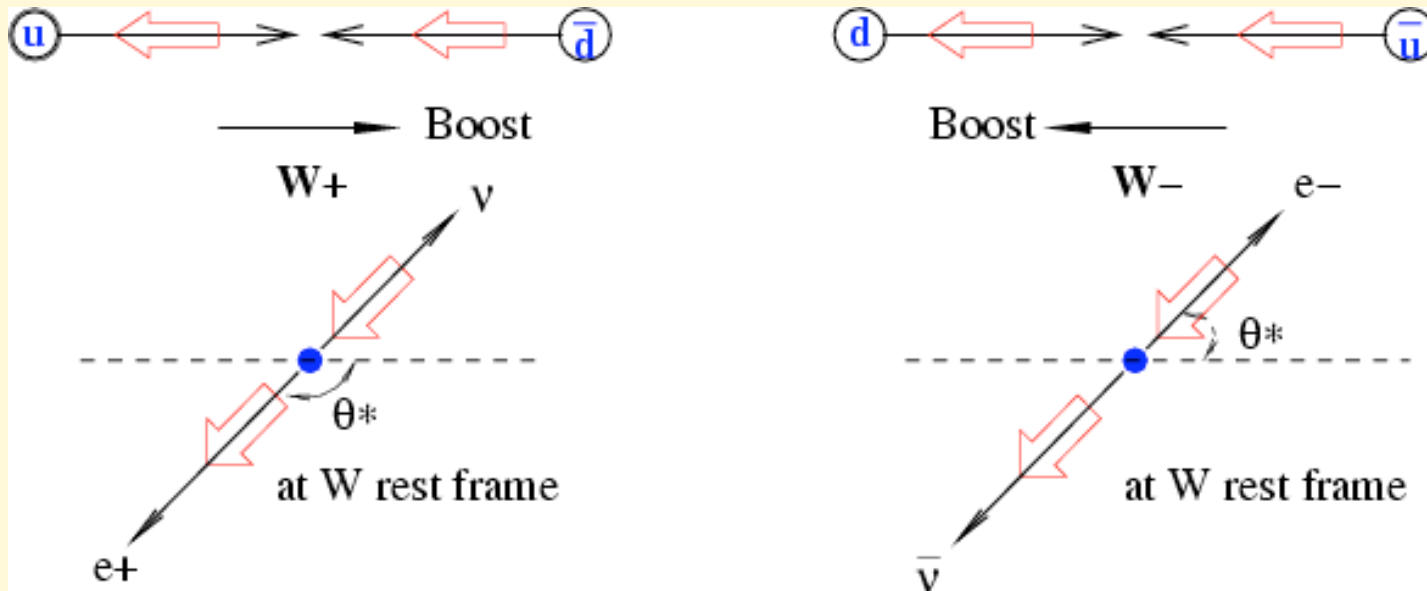


CDF II Preliminary (350 pb⁻¹)



$$\Gamma_W = 2032 \pm 73 \text{ MeV}/c^2$$

Example: W rapidity asymmetry



$$\frac{d\sigma_{W^+}}{dy} \propto f_u^P(x_1) f_{\bar{d}}^{\bar{P}}(x_2) + f_{\bar{d}}^P(x_1) f_u^{\bar{P}}(x_2)$$

$$\frac{d\sigma_{W^-}}{dy} \propto f_{\bar{u}}^P(x_1) f_d^{\bar{P}}(x_2) + f_d^P(x_1) f_{\bar{u}}^{\bar{P}}(x_2)$$

$$f_d(x) = f_u(x) R(x)$$

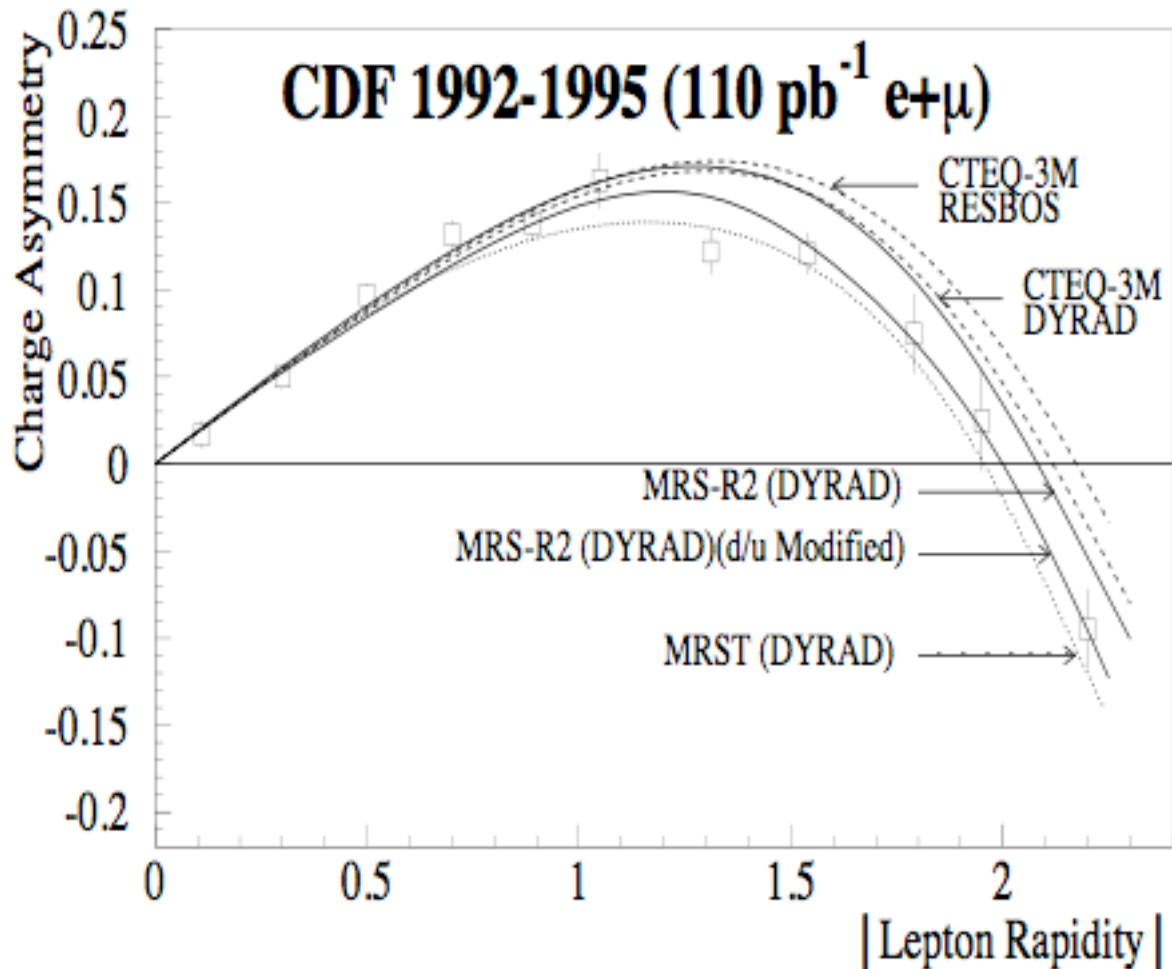
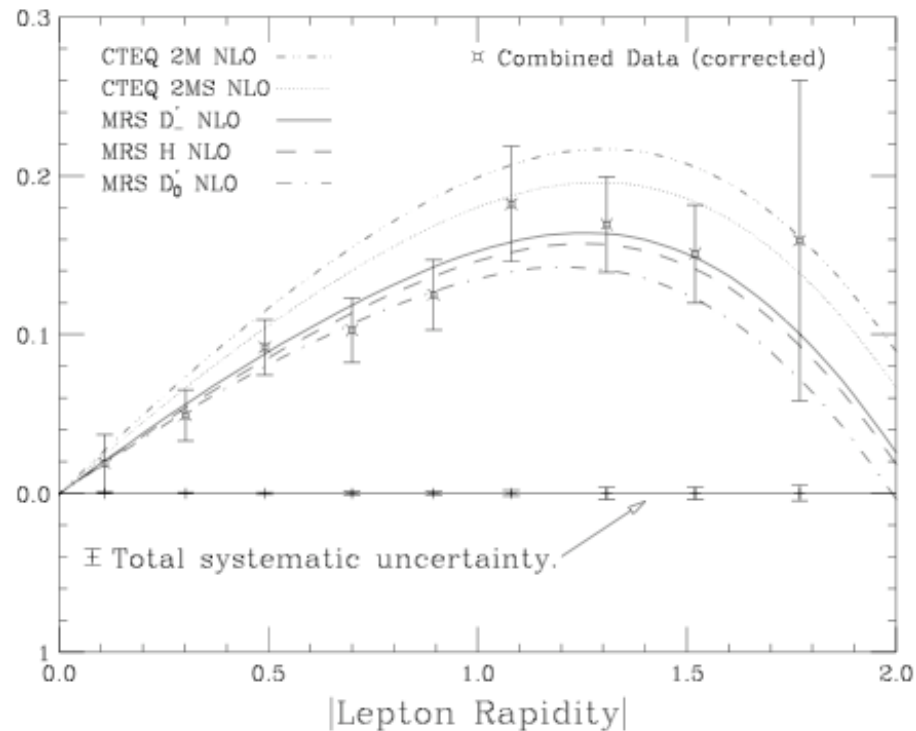
(Assuming dominance of valence contributions)

$$A(y) = \frac{\frac{d\sigma_{W^+}}{dy} - \frac{d\sigma_{W^-}}{dy}}{\frac{d\sigma_{W^+}}{dy} + \frac{d\sigma_{W^-}}{dy}} = \frac{f_u^P(x_1) f_d^{\bar{P}}(x_2) - f_d^P(x_1) f_{\bar{u}}^{\bar{P}}(x_2)}{f_u^P(x_1) f_d^{\bar{P}}(x_2) + f_d^P(x_1) f_{\bar{u}}^{\bar{P}}(x_2)} = \frac{R(x_2) - R(x_1)}{R(x_2) + R(x_1)}$$

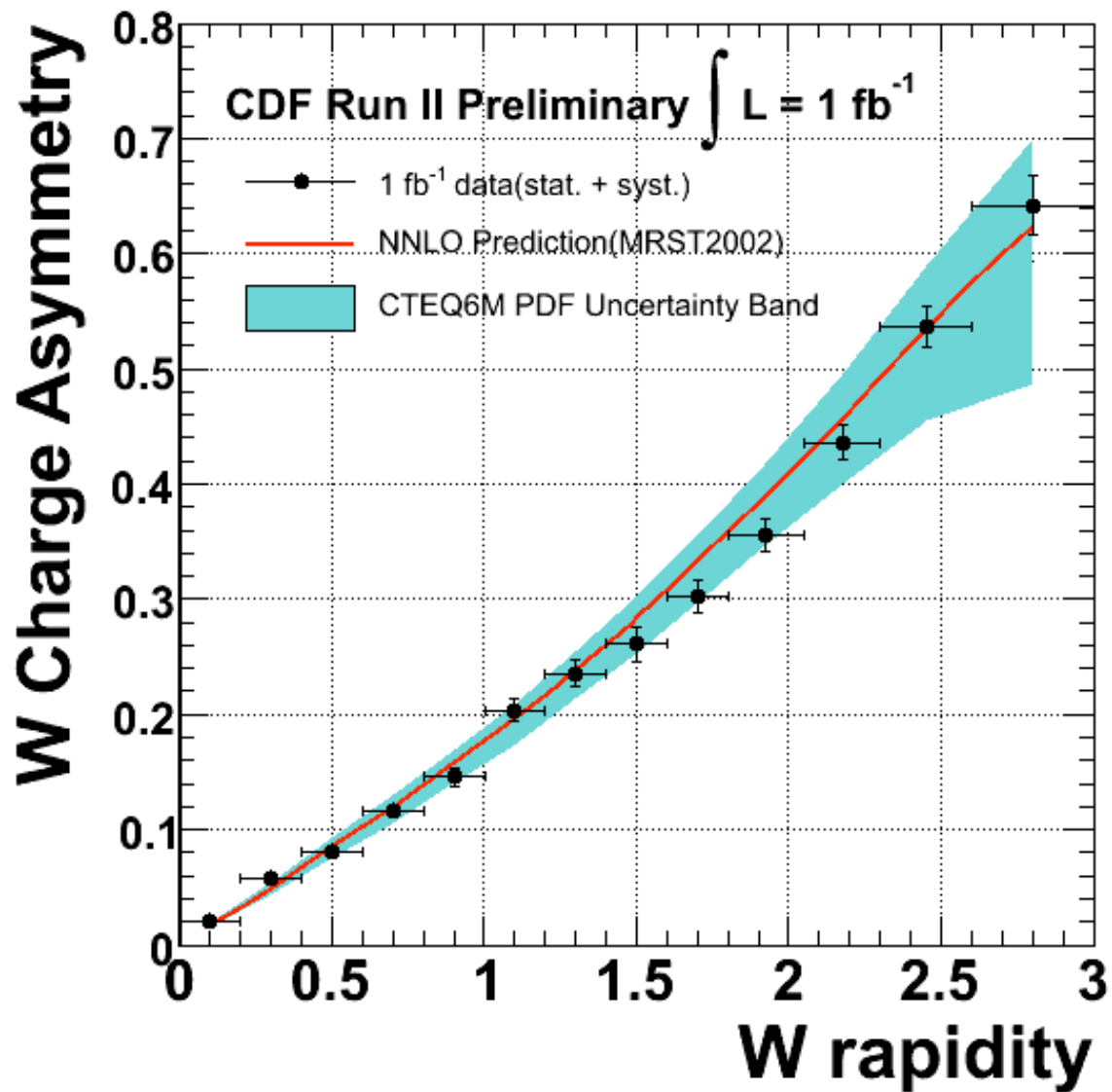
Run I comparisons of leptonic charge asymmetry with previous PDF parameterizations

Early data, no statistical power

Charge Asymmetry



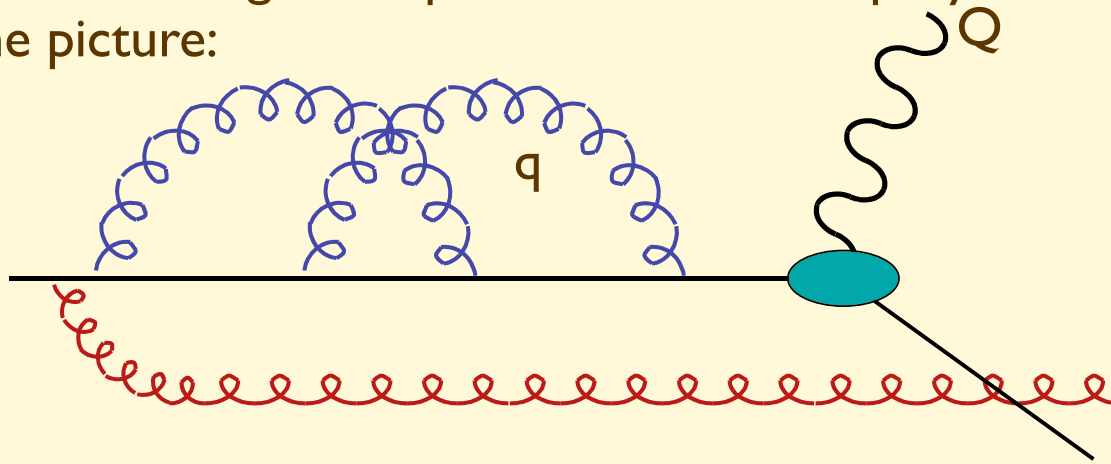
Full dataset, good discrimination



Run II comparison of W charge asymmetry with current PDF parameterizations

Comment

The parton densities are inclusive quantities, namely they say nothing about the number and spectrum of gluons/quarks which accompany the struck parton, like the red gluon in the picture:



Cross-sections obtained with matrix element calculations can therefore only represent inclusive observables. To fully describe, on an event-by-event basis, the multiplicity and kinematics of the emitted radiation requires the so-called parton-shower Monte Carlos.

Occasionally, the gluons emitted during the evolution of the parton towards its hard scattering can themselves be hard, and give rise to what are called “initial state radiation (ISR) jets”. Since these are hard objects, with scales comparable or larger than Q , interference effects with the final state are relevant, and their description in the factorized approximation is not correct.

The separation between these two regimes of ISR amounts to a factorization prescription choice. Reducing the dependence of the prescription and guaranteeing a continuity of distributions across this boundary is the subject of intensive study

Introduction to hadronic collisions: theoretical concepts and practical tools for the LHC

Lecture 2

Michelangelo L. Mangano

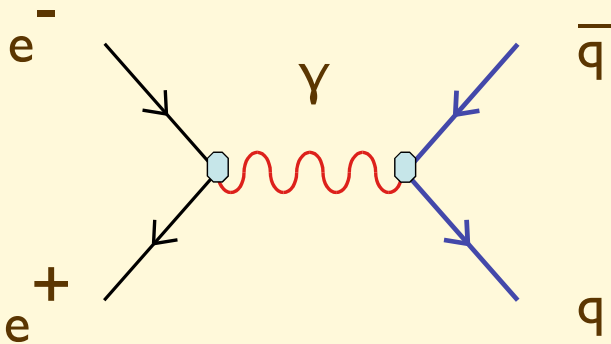
TH Unit, Physics Dept, CERN
michelangelo.mangano@cern.ch

Evolution of hadronic final states

Asymptotic freedom implies that at $E_{CM} \gg 1 \text{ GeV}$

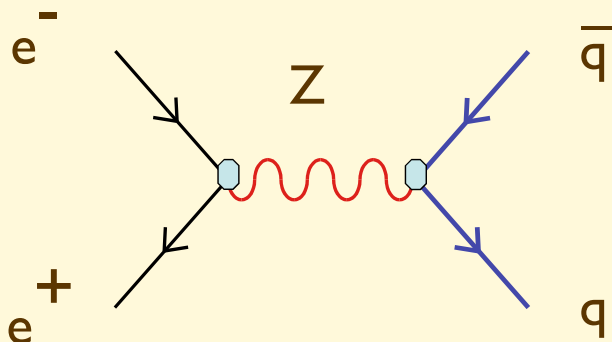
$$\sigma(e^+ e^- \rightarrow \text{hadrons}) \longleftrightarrow \sigma(e^+ e^- \rightarrow \text{quarks/gluons})$$

At the Leading Order (LO) in PT:



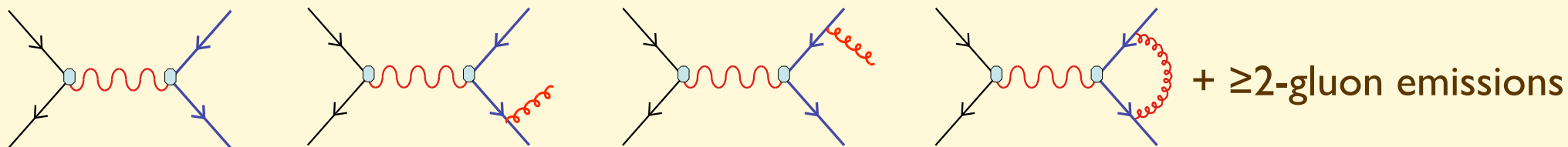
$$\sigma_0(e^+ e^- \rightarrow q\bar{q}) = \frac{4\pi\alpha^2}{9s} N_c \sum_{f=u,d,\dots} e_{q_f}^2$$

$$\frac{\sigma_0(e^+ e^- \rightarrow q\bar{q})}{\sigma_0(e^+ e^- \rightarrow \mu^+ \mu^-)} = N_c \sum_{f=u,d,\dots} e_{q_f}^2$$



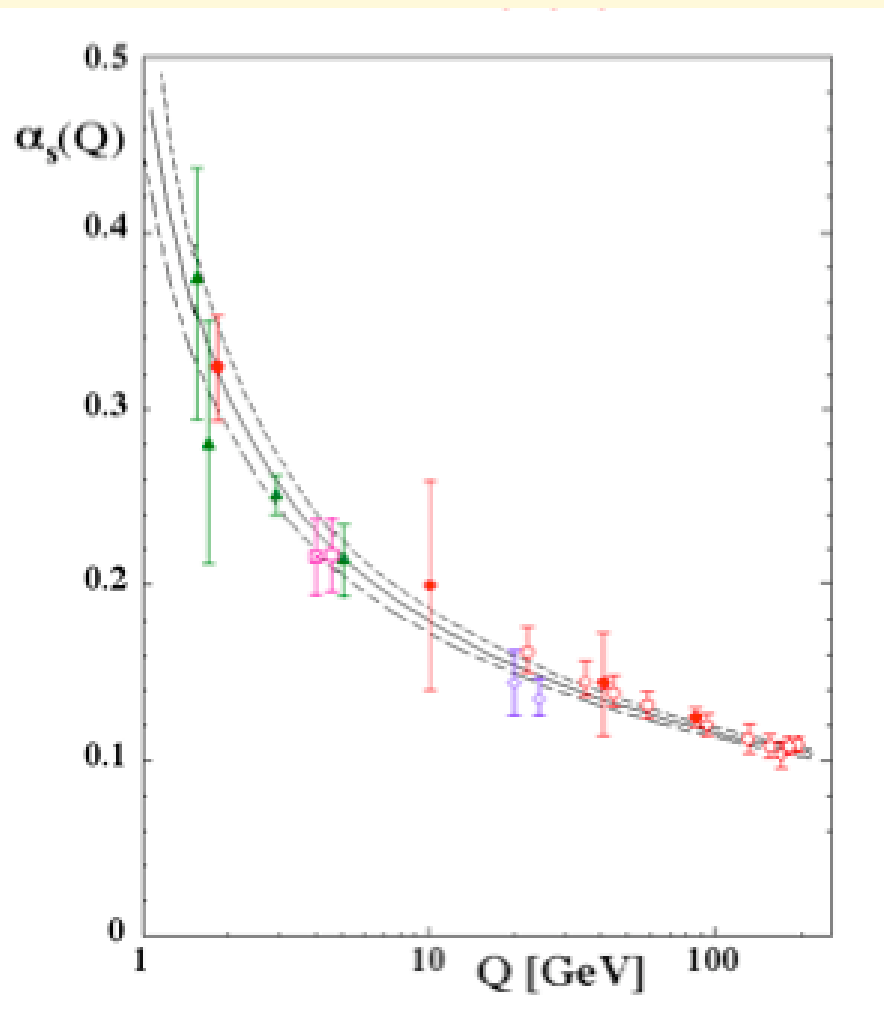
$$\frac{\sigma_0(e^+ e^- \rightarrow Z \rightarrow q\bar{q})}{\sigma_0(e^+ e^- \rightarrow Z \rightarrow \mu^+ \mu^-)} = N_c \frac{\sum_{f=u,d,\dots} (v_{q_f}^2 + a_{q_f}^2)}{(v_\mu^2 + a_\mu^2)}$$

Adding higher-order perturbative terms:



$$\sigma_1(e^+e^- \rightarrow q\bar{q}(g)) = \sigma_0(e^+e^- \rightarrow q\bar{q}) \left(1 + \frac{\alpha_s(E_{CM})}{\pi} + O(\alpha_s^2) \right)$$

O(3%) at M_Z



Excellent agreement with data,

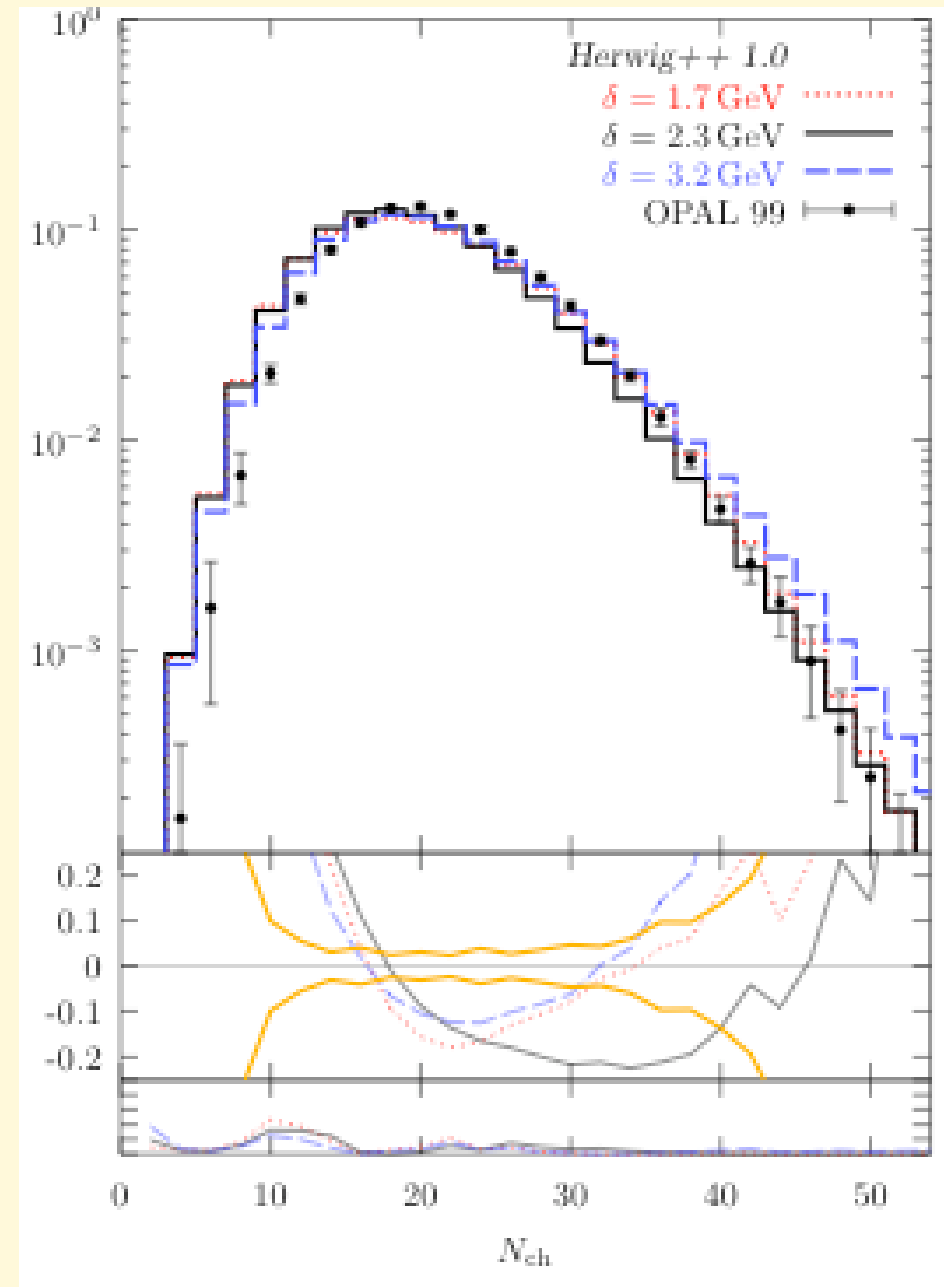
provided $N_c=3$

Extraction of α_s consistent with the Q evolution predicted by QCD

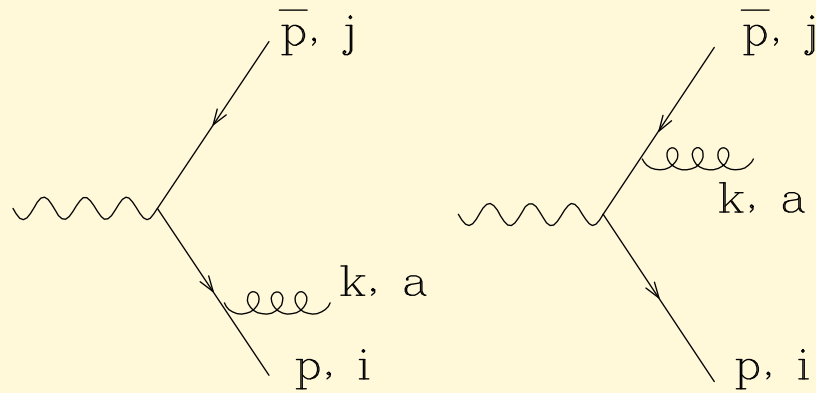
Experimentally, the final states contain a large number of particles, not the 2 or 3 which apparently saturate the perturbative cross-section.

Experimental
multiplicity
distribution

$$\langle n_{\text{charged}} \rangle = 20.9$$



Soft gluon emission



$$\begin{aligned}
 A &= \bar{u}(p)\epsilon(k)(ig) \frac{-i}{\not{p} + \not{k}} \Gamma^\mu v(\bar{p}) \lambda_{ij}^a + \bar{u}(p) \Gamma^\mu \frac{i}{\not{p} + \not{k}} (ig)\epsilon(k) v(\bar{p}) \lambda_{ij}^a \\
 &= \left[\frac{g}{2p \cdot k} \bar{u}(p)\epsilon(k) (\not{p} + \not{k}) \Gamma^\mu v(\bar{p}) - \frac{g}{2\bar{p} \cdot k} \bar{u}(p) \Gamma^\mu (\not{p} + \not{k}) \epsilon(k) v(\bar{p}) \right] \lambda_{ij}^a
 \end{aligned}$$

$p \cdot k = p_0 k_0 (1 - \cos\theta) \Rightarrow$ singularities for collinear ($\cos\theta \rightarrow 1$) or soft ($k_0 \rightarrow 0$) emission

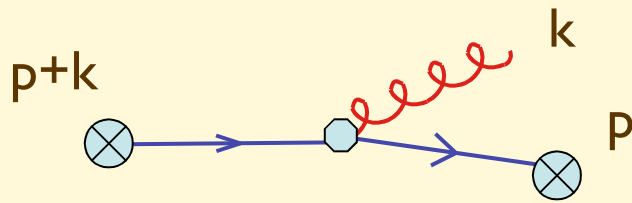
Collinear emission does not alter the global structure of the final state, since it preserves its “pencil-like-ness”. **Soft emission** at large angle, however, could spoil the structure, and leads to strong interferences between emissions from different legs. So soft emission needs to be studied in more detail.

In the soft ($k_0 \rightarrow 0$) limit the amplitude simplifies and factorizes as follows:

$$A_{soft} = g \lambda_{ij}^a \left(\frac{p \cdot \epsilon}{p \cdot k} - \frac{\bar{p} \cdot \epsilon}{\bar{p} \cdot k} \right) A_{Born}$$

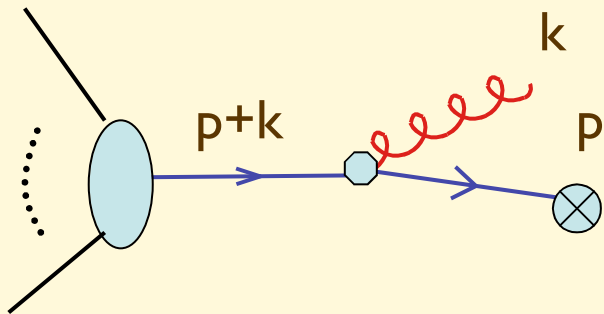
Factorization: it is the expression of the independence of long-wavelength (soft) emission on the nature of the hard (short-distance) process.

Another simple derivation of soft-gluon emission rules

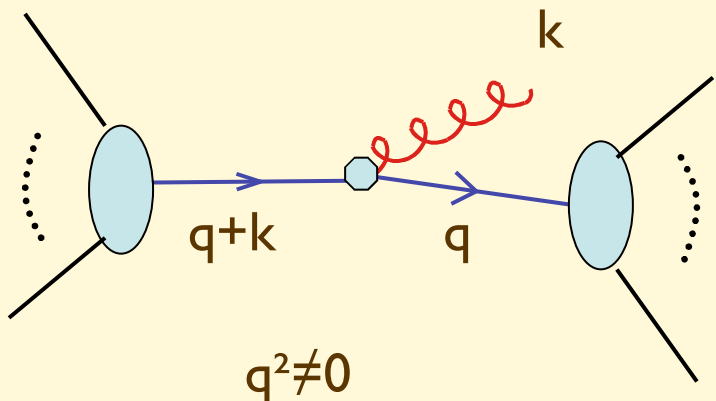


charge current of a free fermion

$$\bar{\Psi}(p) \gamma_{\mu} \Psi(p+k) \varepsilon^{\mu}(k) \xrightarrow{k \rightarrow 0} \bar{\Psi}(p) \gamma_{\mu} \Psi(p) \varepsilon^{\mu}(k) = 2p \cdot \varepsilon$$



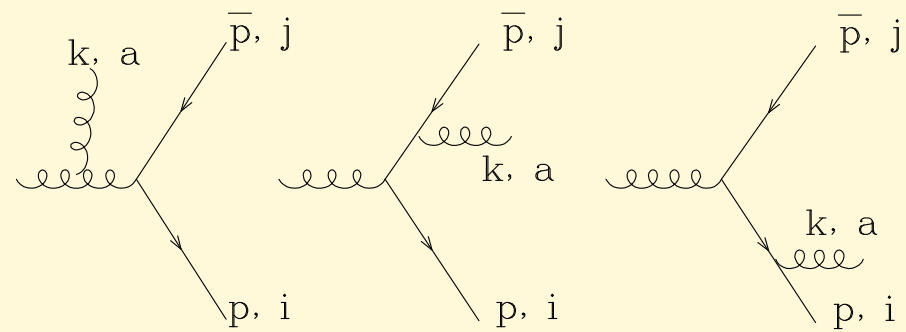
$$\frac{1}{\not{p} + \not{k}} \gamma_{\mu} \Psi(p) \varepsilon^{\mu}(k) \xrightarrow{k \rightarrow 0} \frac{1}{2p \cdot k} \not{p} \gamma_{\mu} \Psi(p) \varepsilon^{\mu}(k) = \frac{p \cdot \varepsilon}{p \cdot k}$$



$$\frac{1}{\not{q} + \not{k}} \gamma_{\mu} \frac{1}{\not{q}} \varepsilon^{\mu}(k) \xrightarrow{q^2 \neq 0, k \rightarrow 0} \frac{1}{q^2} \not{q} \gamma_{\mu} \not{q} \frac{1}{q^2} \varepsilon^{\mu}(k)$$

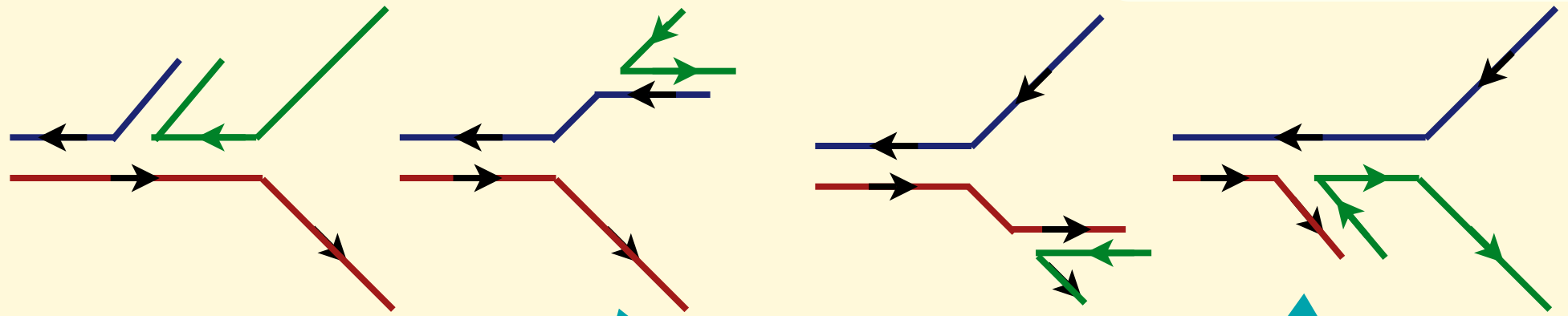
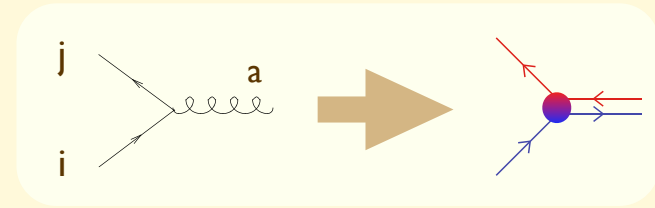
=> finite

Similar, but more structured, result in the case of a fully coloured process:



$$A_{soft} = g (\lambda^a \lambda^b)_{ij} \left[\frac{Q\varepsilon}{Qk} - \frac{\bar{p}\varepsilon}{\bar{p}k} \right] + g (\lambda^b \lambda^a)_{ij} \left[\frac{p\varepsilon}{pk} - \frac{Q\varepsilon}{Qk} \right]$$

The four terms correspond to the two possible ways colour can flow, and to the two possible emissions for each colour flow:



$$A_{soft} = g (\lambda^a \lambda^b)_{ij} \left[\frac{Q\varepsilon}{Qk} - \frac{\bar{p}\varepsilon}{\bar{p}k} \right] + g (\lambda^b \lambda^a)_{ij} \left[\frac{p\varepsilon}{pk} - \frac{Q\varepsilon}{Qk} \right]$$

The interference between the two colour structures

$$\left[\text{Diagram 1} + \text{Diagram 2} \right] \propto (\lambda^a \lambda^b)_{ij} \quad \left[\text{Diagram 3} + \text{Diagram 4} \right] \propto (\lambda^b \lambda^a)_{ij}$$

is suppressed by $1/N_c^2$:

$$\sum_{a,b,i,j} |(\lambda^a \lambda^b)_{ij}|^2 = \sum_{a,b} \text{tr} (\lambda^a \lambda^b \lambda^b \lambda^a) = \frac{N^2 - 1}{2} C_F = O(N^3)$$

$$\sum_{a,b,i,j} (\lambda^a \lambda^b)_{ij} [(\lambda^b \lambda^a)_{ij}]^* = \sum_{a,b} \text{tr} (\lambda^a \lambda^b \lambda^a \lambda^b) = \frac{N^2 - 1}{2} \underbrace{\left(C_F - \frac{C_A}{2} \right)}_{-\frac{1}{2N}} = O(N)$$

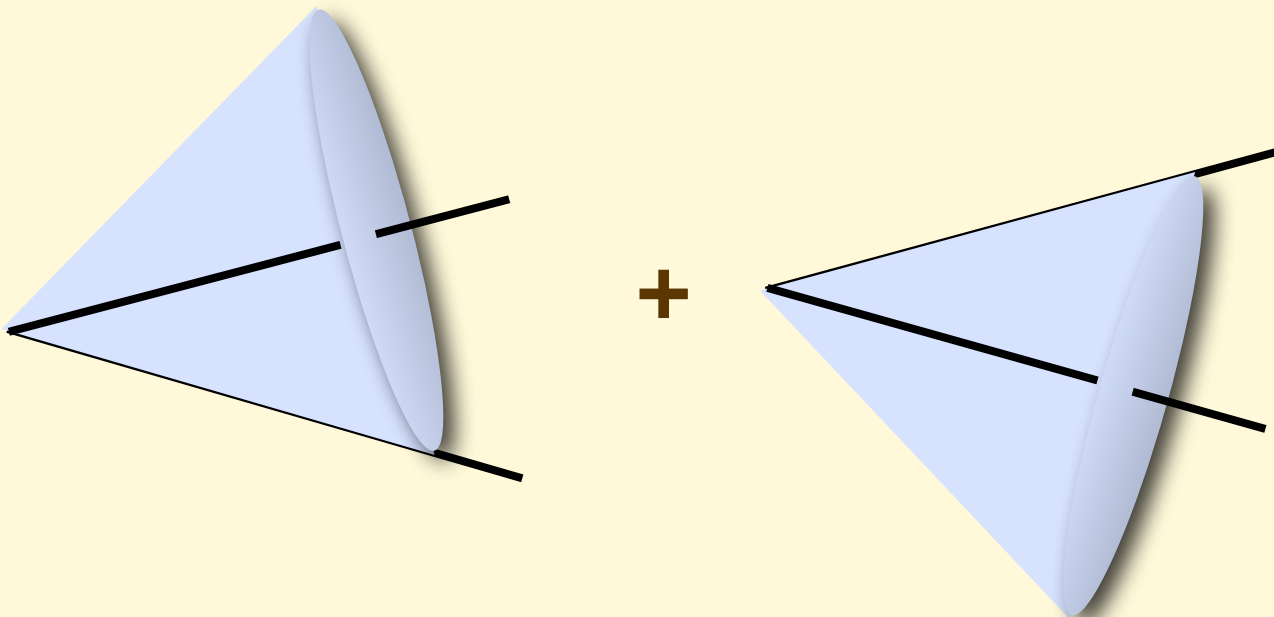
As a result, the emission of a soft gluon can be described, to the leading order in $1/N_c^2$, as the incoherent sum of the emission from the two colour currents

What about the interference between the two diagrams corresponding to the same colour flow? ➡

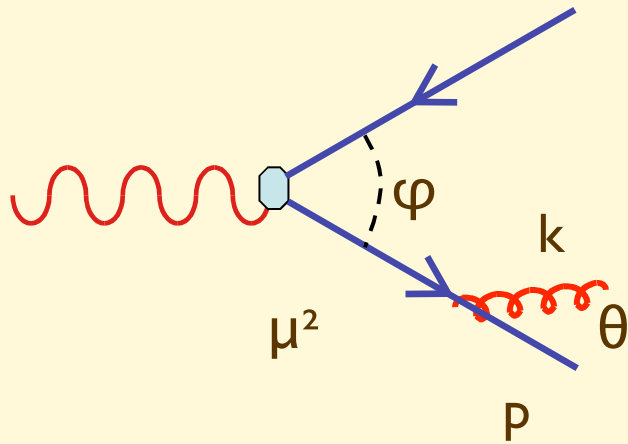
Angular ordering

$$\left| \begin{array}{c} \text{quark} \\ \text{gluon} \end{array} \right|^2 = \left| \begin{array}{c} \text{quark} \\ \text{gluon} \end{array} \right|^2 \Theta(\varphi - \varphi_1) + \left| \begin{array}{c} \text{quark} \\ \text{gluon} \end{array} \right|^2 \Theta(\varphi - \varphi_2)$$

Radiation inside the cones is allowed, and described by the eikonal probability, radiation outside the cones is suppressed and averages to 0 when integrated over the full azimuth



An intuitive explanation of angular ordering



Lifetime of the virtual intermediate state:

$$\tau < \gamma/\mu = E/\mu^2 = 1 / (k_0 \theta^2) = 1/(k_{\perp} \theta)$$

$$\begin{aligned} \mu^2 &= (p+k)^2 = 2E k_0 (1-\cos\theta) \\ &\sim E k_0 \theta^2 \sim E k_{\perp} \theta \end{aligned}$$

Distance between q and $qbar$ after τ :

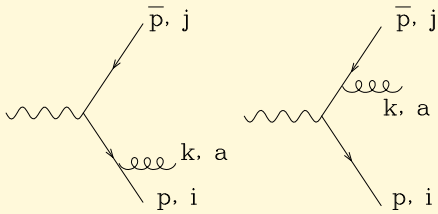
$$d = \varphi\tau = (\varphi/\theta) 1/k_{\perp}$$

If the transverse wavelength of the emitted gluon is longer than the separation between q and $qbar$, the gluon emission is suppressed, because the q $qbar$ system will appear as colour neutral (\Rightarrow dipole-like emission, suppressed)

Therefore $d > 1/k_{\perp}$, which implies

$$\theta < \varphi$$

The formal proof of angular ordering



$$d\sigma_g = \sum |A_{soft}|^2 \frac{d^3k}{(2\pi)^3 2k^0} \sum |A_0|^2 \frac{-2p^\mu \bar{p}^\nu}{(pk)(\bar{p}k)} g^2 \sum \epsilon_\mu \epsilon_\nu^* \frac{d^3k}{(2\pi)^3 2k^0}$$

$$= d\sigma_0 \frac{\alpha_s C_F}{\pi} \frac{dk^0}{k^0} \frac{d\phi}{2\pi} \frac{1 - \cos \theta_{ij}}{(1 - \cos \theta_{ik})(1 - \cos \theta_{jk})} d\cos \theta$$

You can easily prove that:

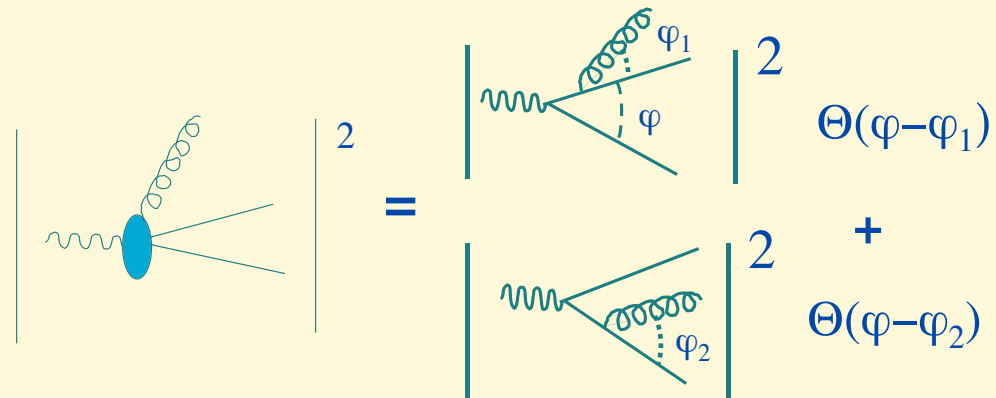
$$\frac{1 - \cos \theta_{ij}}{(1 - \cos \theta_{ik})(1 - \cos \theta_{jk})} = \frac{1}{2} \left[\frac{\cos \theta_{jk} - \cos \theta_{ij}}{(1 - \cos \theta_{ik})(1 - \cos \theta_{jk})} + \frac{1}{1 - \cos \theta_{ik}} \right] + \frac{1}{2} [i \leftrightarrow j] \equiv W_{(i)} + W_{(j)}$$

where:

$$W_{(i)} \rightarrow \text{finite if } k \parallel j \text{ (} \cos \theta_{jk} \rightarrow 1 \text{)}$$

$$W_{(j)} \rightarrow \text{finite if } k \parallel i \text{ (} \cos \theta_{ik} \rightarrow 1 \text{)}$$

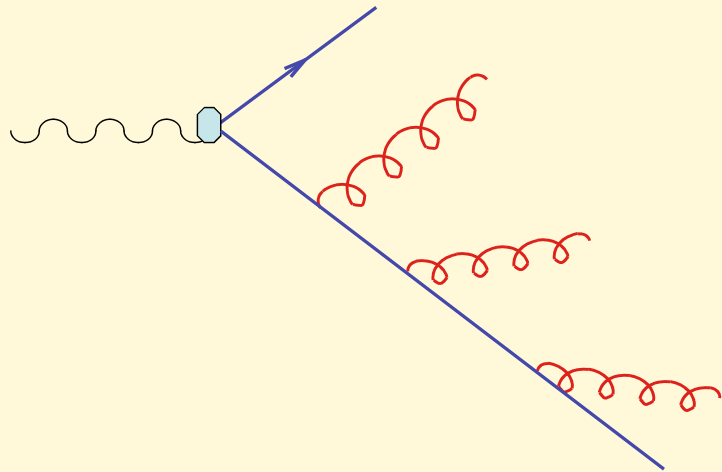
The probabilistic interpretation of $W_{(i)}$ and $W_{(j)}$ is a priori spoiled by their non-positivity. However, you can prove that after azimuthal averaging:



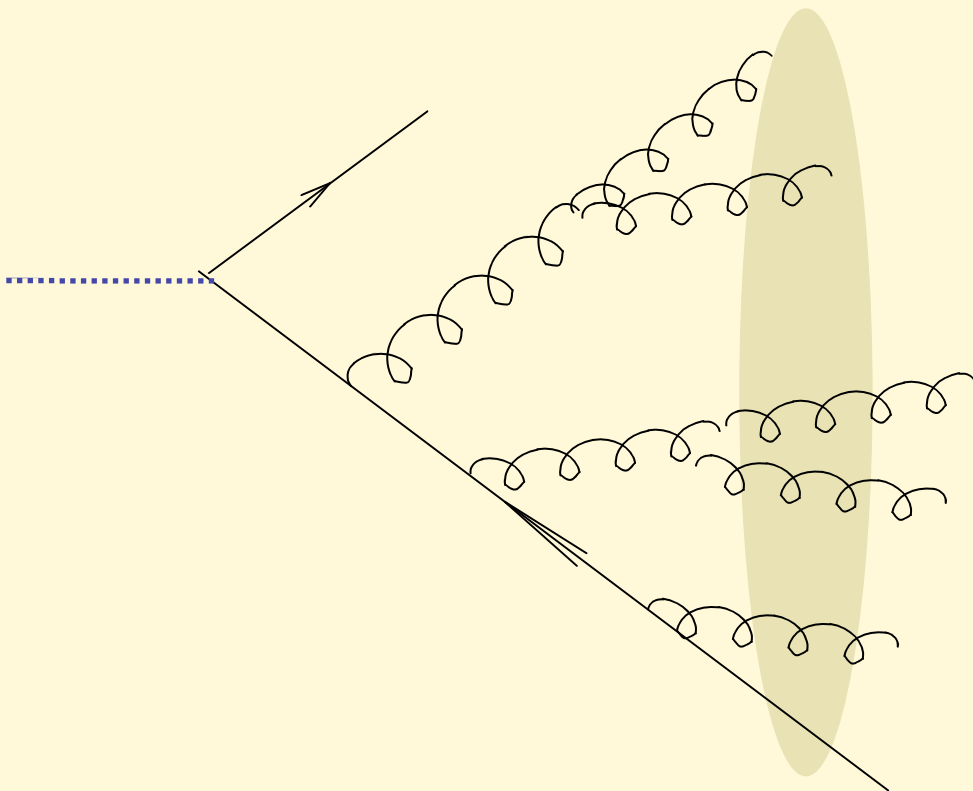
$$\int \frac{d\phi}{2\pi} W_{(i)} = \frac{1}{1 - \cos \theta_{ik}} \text{ if } \theta_{ik} < \theta_{ij}, \quad 0 \text{ otherwise}$$

$$\int \frac{d\phi}{2\pi} W_{(j)} = \frac{1}{1 - \cos \theta_{jk}} \text{ if } \theta_{jk} < \theta_{ij}, \quad 0 \text{ otherwise}$$

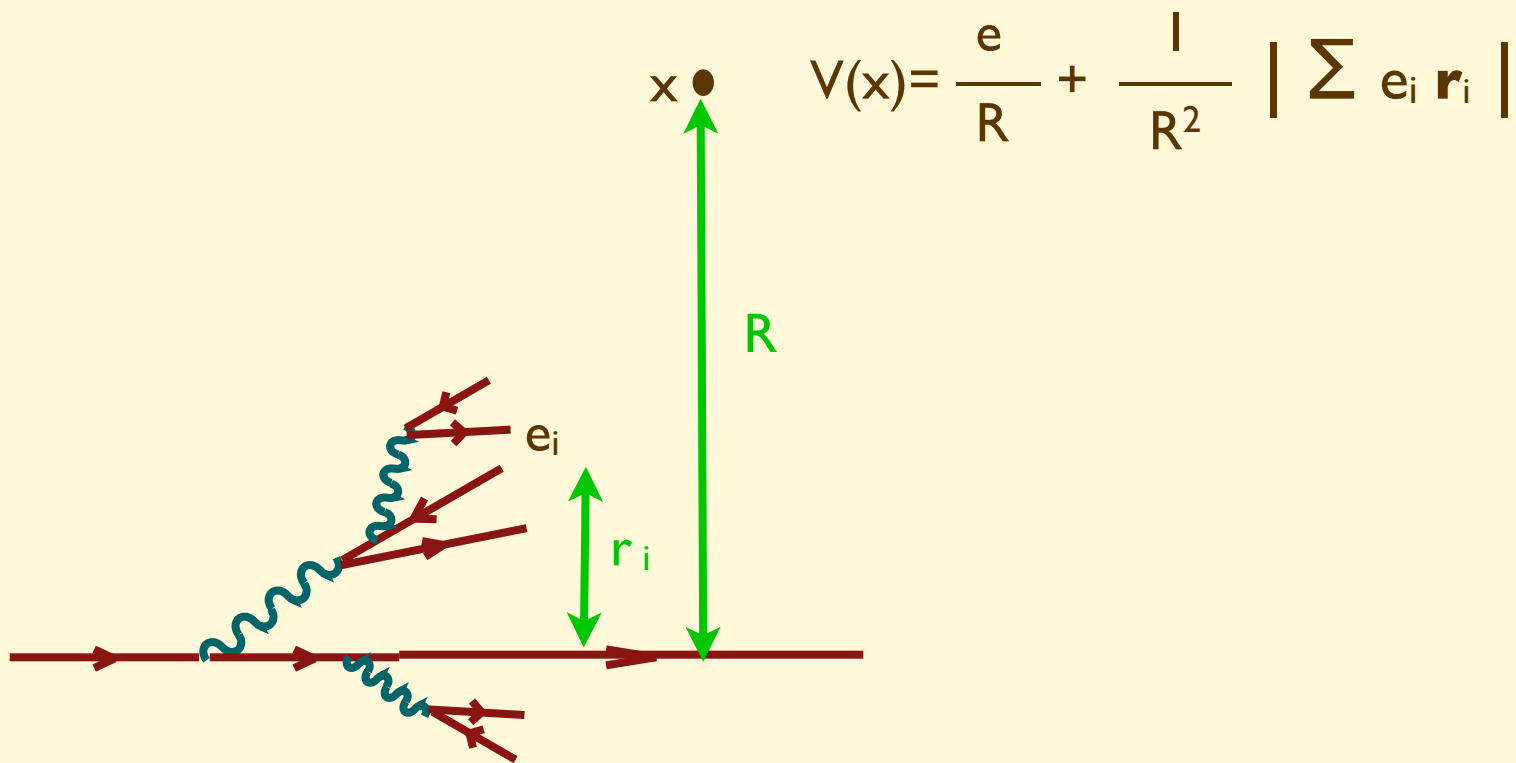
Further branchings will obey angular ordering relative to the new angles. As a result emission angles get smaller and smaller, squeezing the jet

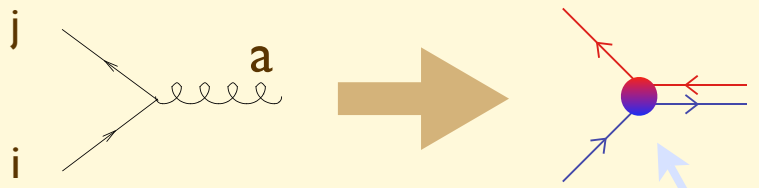


The construction can be iterated to the next emission, with the result that emission angles keep getting smaller and smaller => **jet structure**

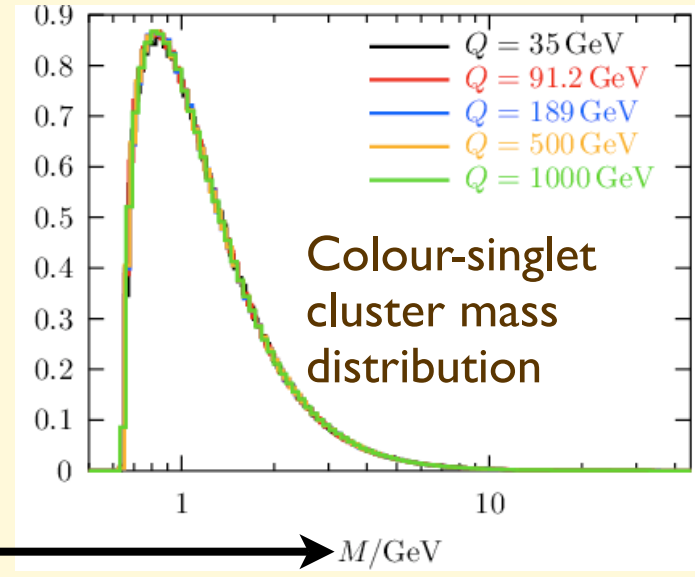
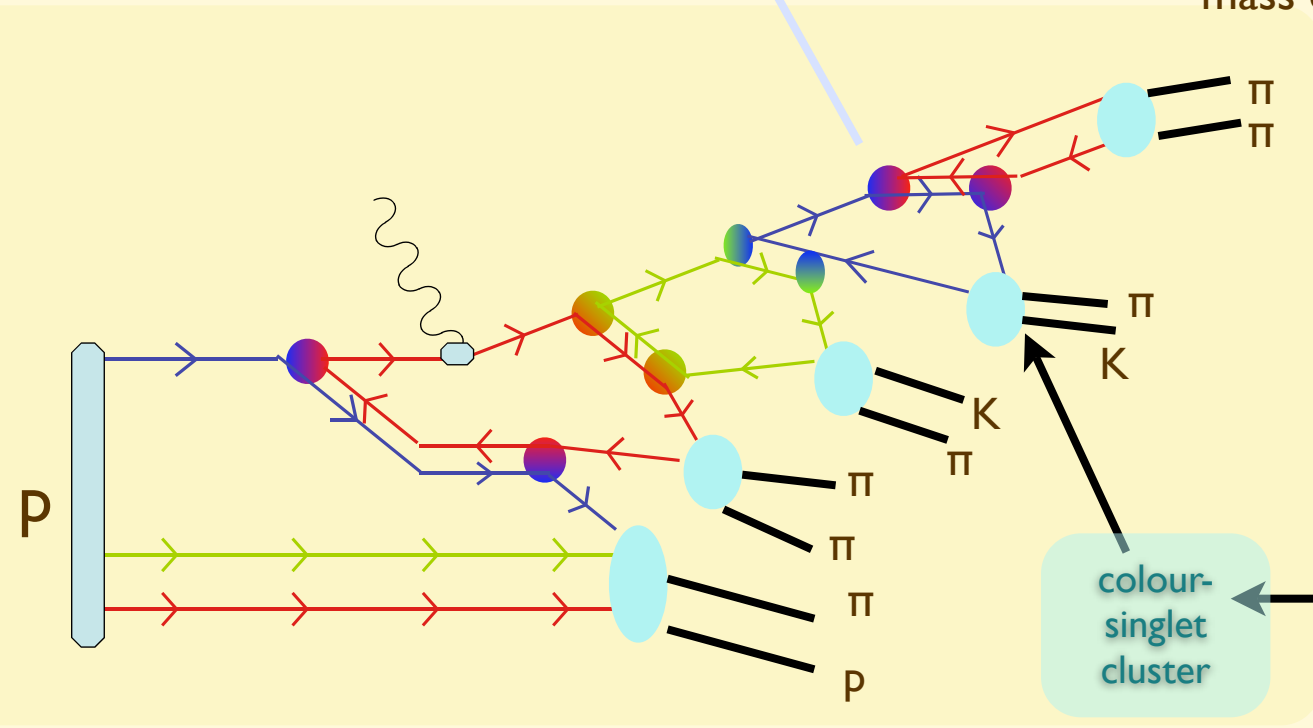


Total colour charge of the system is equal to the quark colour charge. Treating the system as the incoherent superposition of N gluons would lead to artificial growth of gluon multiplicity. Angular ordering enforces coherence, and leads to the proper evolution with energy of particle multiplicities.



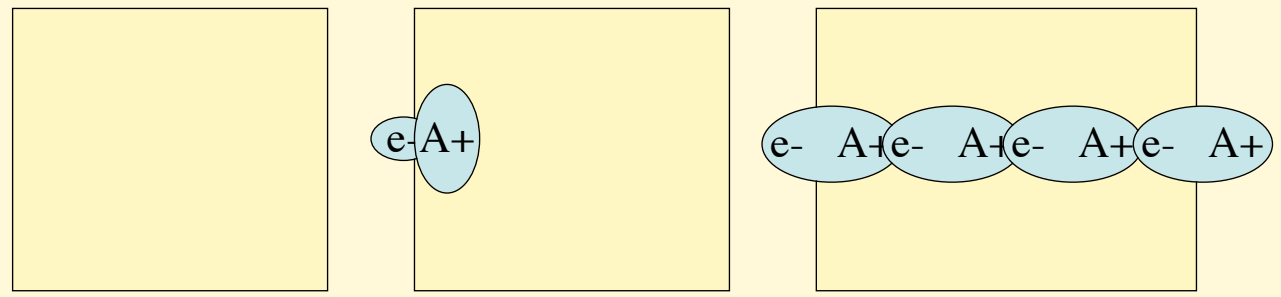


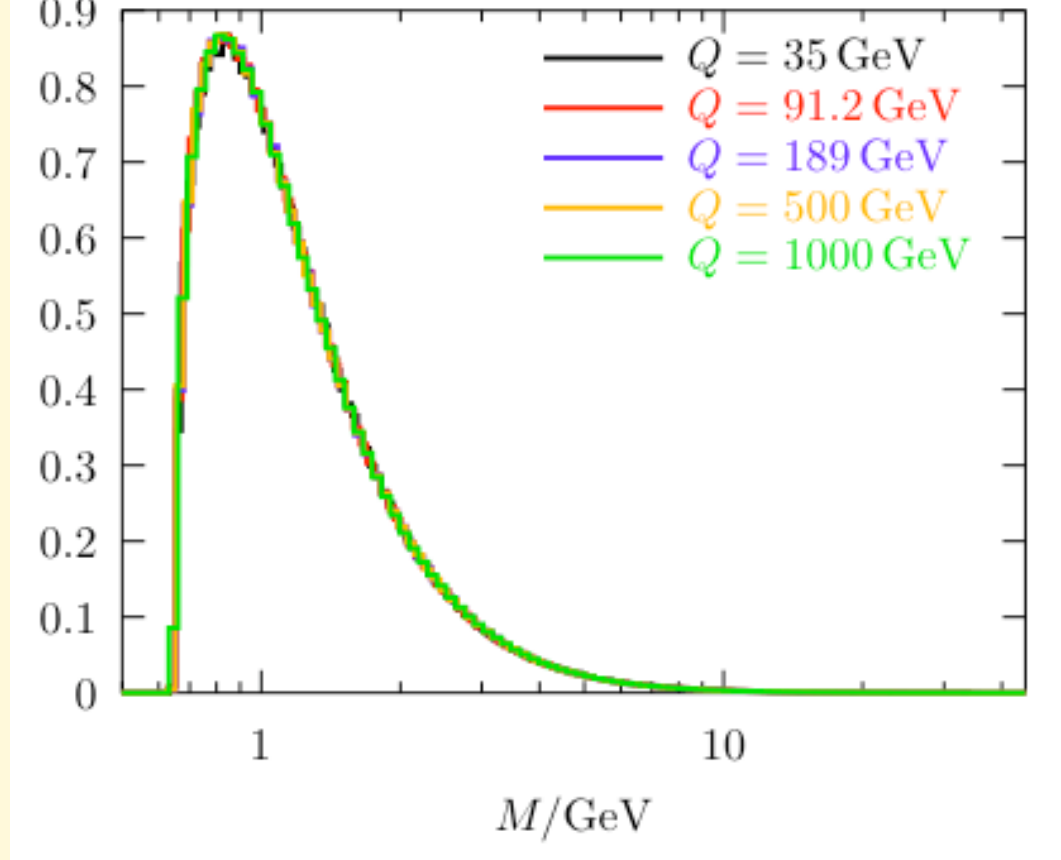
The structure of the perturbative evolution leads naturally to the clustering in phase-space of colour-singlet parton pairs ("preconfinement"). Long-range correlations are strongly suppressed. Hadronization will only act locally, on low-mass colour-singlet clusters.



colour-singlet cluster

Colour is left "behind" by the struck quark. The first soft gluon emitted at large angle will connect to the beam fragments, ensuring that the beam fragments can recombine to form hadrons, and will allow the struck quark to evolve without having to worry about what happens to the proton fragments.



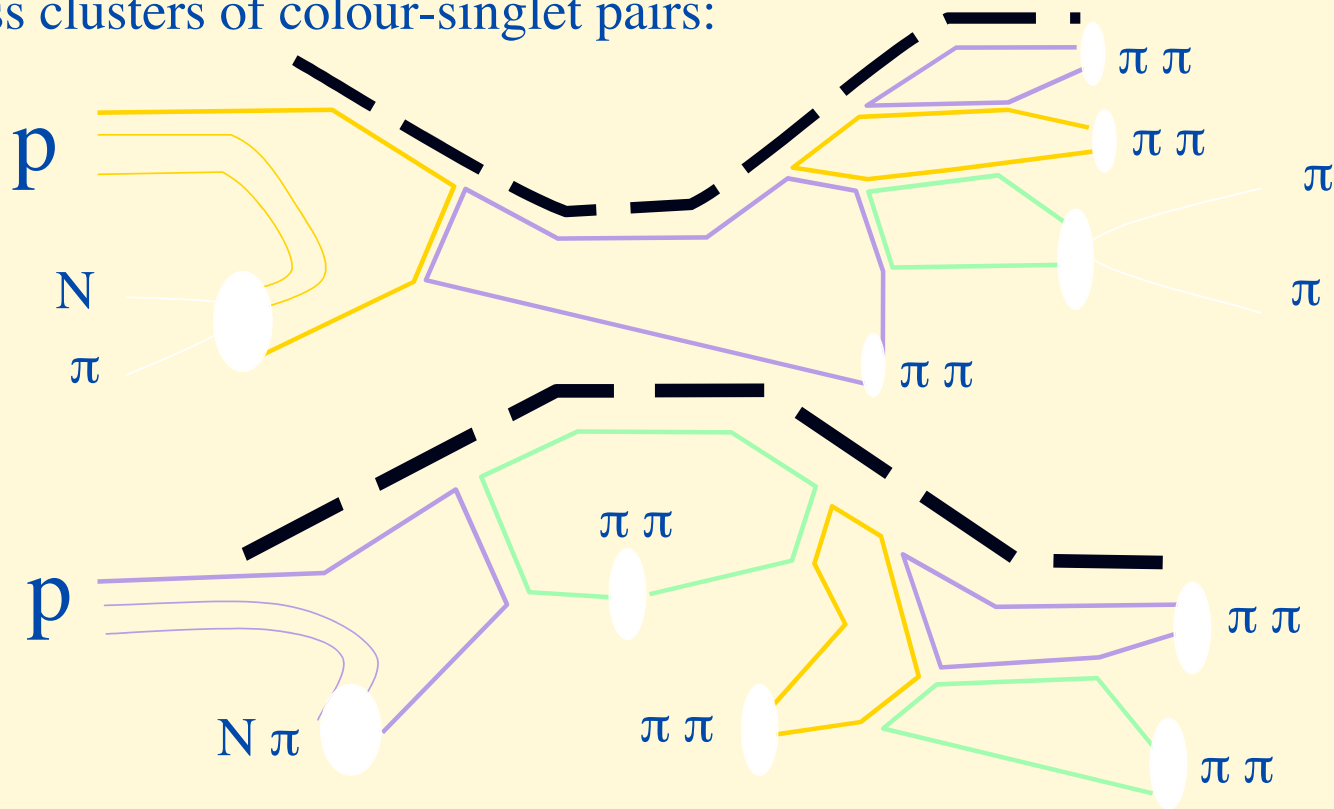


The existence of high-mass clusters, however rare, is unavoidable, due to IR cutoff which leads to a non-zero probability that no emission takes place. This is particularly true for evolution of massive quarks (as in, e.g. $Z \rightarrow bb$ or cc). Prescriptions have to be defined to deal with the “evolution” of these clusters. **This has an impact on the $z \rightarrow \mathbf{i}$ behaviour of fragmentation functions.**

Phenomenologically, this leads to uncertainties, for example, in the background rates for $H \rightarrow \gamma\gamma$ ($\text{jet} \rightarrow \gamma$).

Hadronization

At the end of the perturbative evolution, the final state consists of quarks and gluons, forming, as a result of angular-ordering, low-mass clusters of colour-singlet pairs:



Thanks to the cluster pre-confinement, hadronization is local and independent of the nature of the primary hard process, as well as of the details of how hadronization acts on different clusters. Among other things, one therefore expects:

$$\mathbf{N(\text{pions}) = C N(\text{gluons}),}$$
$$\mathbf{C = \text{constant} \sim 2}$$

Introduction to hadronic collisions: theoretical concepts and practical tools for the LHC

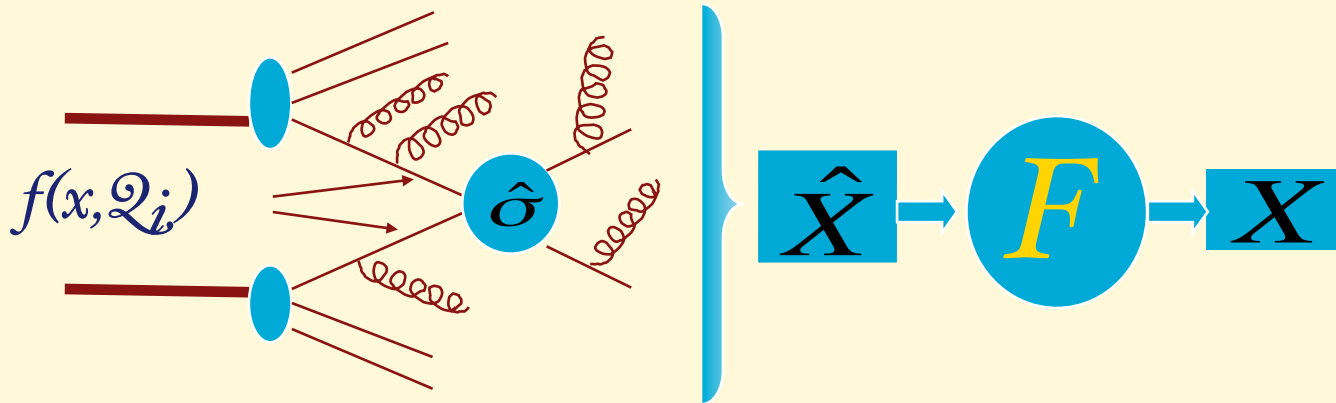
Lecture 3

Michelangelo L. Mangano

TH Unit, Physics Dept, CERN
michelangelo.mangano@cern.ch

Factorization Theorem

$$\frac{d\sigma}{dX} = \sum_{j,k} \int_{\hat{X}} f_j(x_1, Q_i) f_k(x_2, Q_i) \frac{d\hat{\sigma}_{jk}(Q_i, Q_f)}{d\hat{X}} F(\hat{X} \rightarrow X; Q_i, Q_f)$$



$f_j(x, Q)$ Parton distribution functions (PDF)

- sum over all initial state histories leading, at the scale Q , to:

$$\vec{p}_j = x \vec{P}_{proton}$$

$F(\hat{X} \rightarrow X; Q_i, Q_f)$

- transition from partonic final state to the hadronic observable (hadronization, fragm. function, jet definition, etc)
 - Sum over all histories with X in them

- The possible histories of initial and final state, and their relative probabilities, are in principle independent of the hard process (they only depend on the flavours of partons involved and on the scales Q)
- Once an algorithm is developed to describe initial (IS) and final (FS) state evolution, it can be applied to partonic IS and FS arising from the calculation of an arbitrary hard process
- Depending on the extent to which different possible FS and IS histories affect the value of the observable X , different realizations of the factorization theorem can be implemented, and 3 different tools developed:
 1. **Cross-section evaluators**
 2. **Parton-level Monte Carlos**
 3. **Shower Monte Carlos**

I: Cross-section evaluators

- Only some component of the final state is singled out for the measurement, all the rest being ignored (i.e. integrated over). E.g. $pp \rightarrow e^+ e^- + X$
- No 'events' are 'generated', only cross-sections are evaluated:

$$\sigma(pp \rightarrow Z^0), \quad \frac{d\sigma}{dM(e^+e^-) dy(e^+e^-)}, \quad \dots$$

Experimental selection criteria (e.g. jet definition or acceptance) are applied on parton-level quantities. Provided these are infrared/collinear finite, it therefore doesn't matter what **F(X)** is, as we assume (*fact. theorem*) that:

$$\sum_X F(\hat{X}, X) = 1 \quad \forall \hat{X}$$

- Thanks to the inclusiveness of the result, it is 'straightforward' to include higher-order corrections, as well as to resum classes of dominant and subdominant logs

State of the art

- NLO available for:
 - jet and heavy quarks production
 - prompt photon production
 - gauge boson pairs
 - most new physics processes (e.g. SUSY)
- NNLO available for:
 - $W/Z/DY$ production ($q\bar{q} \rightarrow W$)
 - Higgs production ($gg \rightarrow H$)

2: Parton-level (*aka* matrix-element) MC's

- Parton level configurations (i.e. sets of quarks and gluons) are generated, with probability proportional to the respective perturbative M.E.
- Transition function between a final-state parton and the observed object (jet, missing energy, lepton, etc) is unity
- No need to expand $f(x)$ or $F(X)$ in terms of histories, since they all lead to the same observable
- Experimentally, equivalent to assuming
 - perfect jet reconstruction ($\mathbf{P}_\mu^{parton} \rightarrow \mathbf{P}_\mu^{jet}$)
 - linear detector response

State of the art

- $W/Z/\gamma + N$ jets ($N \leq 6$)
- $W/Z/\gamma + Q \bar{Q} + N$ jets ($N \leq 4$)
- $Q \bar{Q} + N$ jets ($N \leq 4$)
- $Q \bar{Q} Q' \bar{Q}' + N$ jets ($N \leq 2$)
- $Q \bar{Q} H + N$ jets ($N \leq 3$)
- $nW + mZ + kH + N$ jets ($n+m+k+N \leq 8, N \leq 2$)
- N jets ($N \leq 8$)

ALPGEN: MLM, Moretti,
Piccinini, Pittau, Polosa
MADGRAPH: Maltoni, Stelzer
CompHEP: Boos et al
VECBOS: Giele et al
NJETS: Giele et al
Kleiss, Papadopoulos
.....

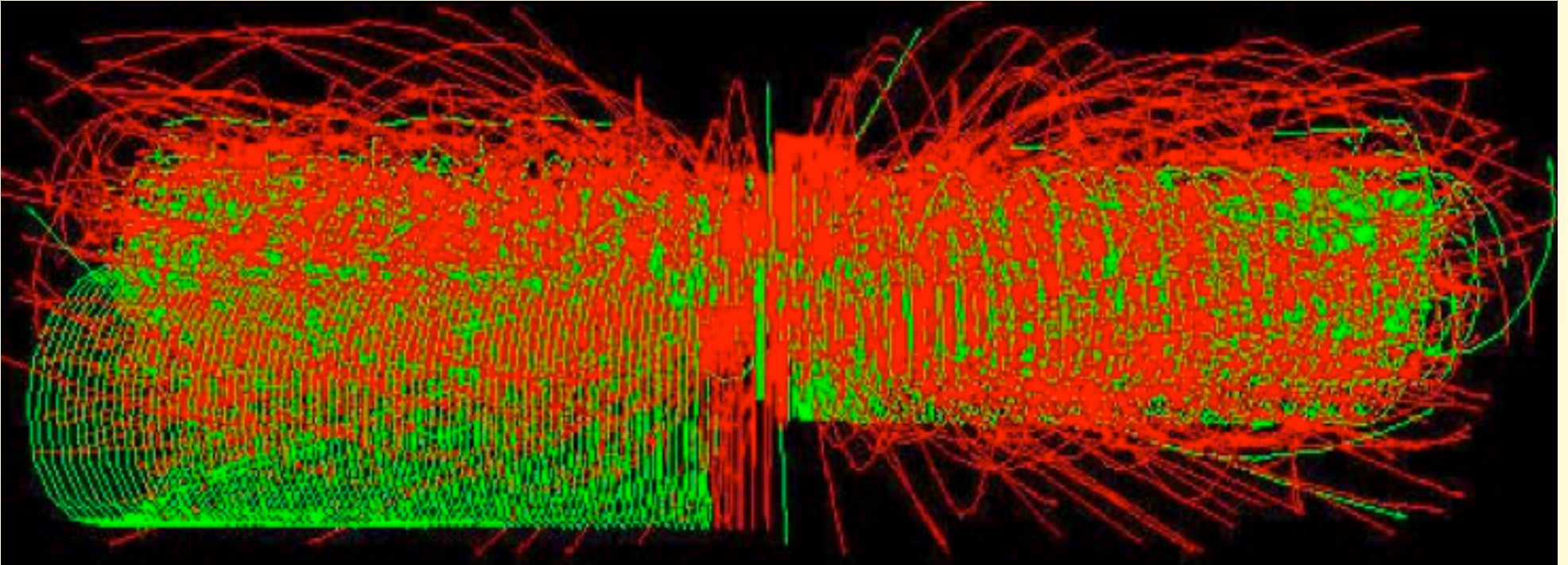
Example of complexity of the calculations, for $gg \rightarrow N$ gluons:

Njets	2	3	4	5	6	7	8
# diag's	4	25	220	2485	34300	5×10^5	10^7

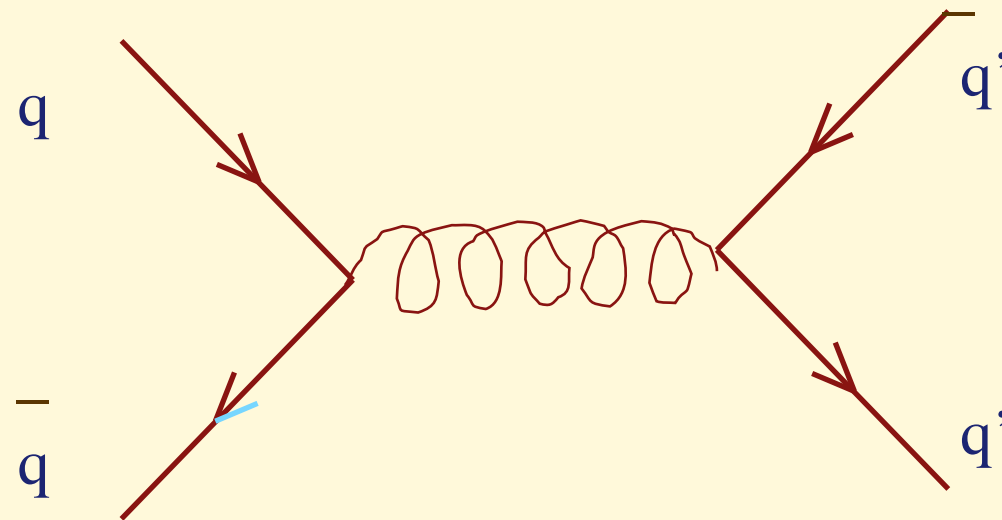
For each process, flavour state and colour flow (leading $1/N_c$) are calculated on an event-by-event basis, to allow QCD-coherent shower evolution

3: Shower Monte Carlos

Goal: complete description of the event,
at the level of individual hadrons



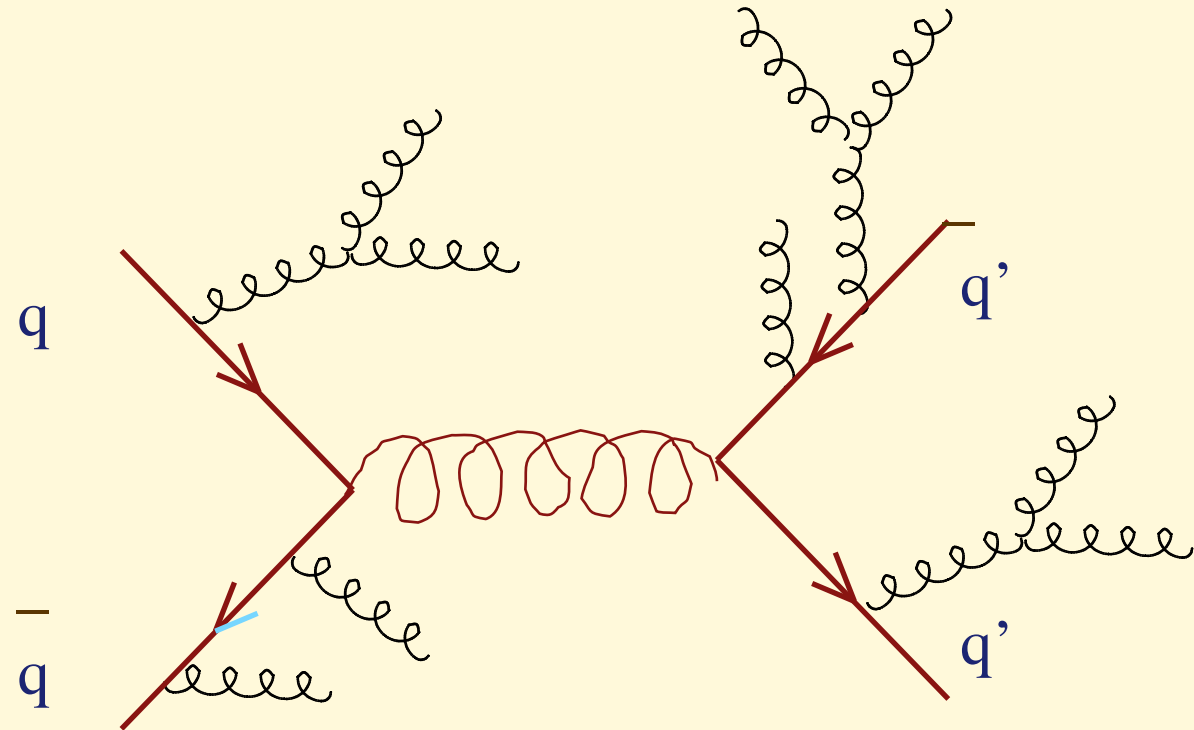
I: Generate the parton-level hard event



II: Develop the parton shower

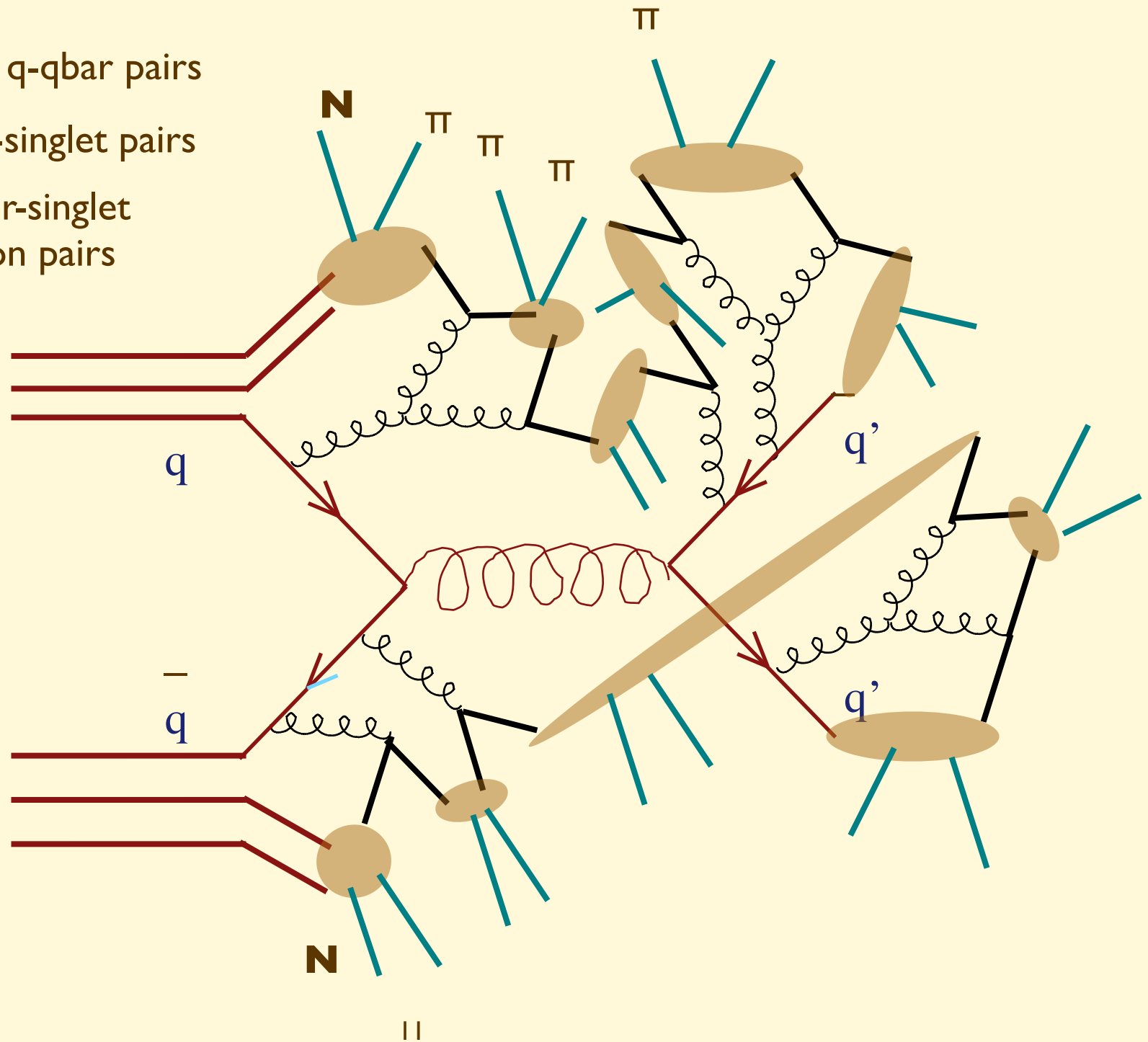
1. Final state

2. Initial state



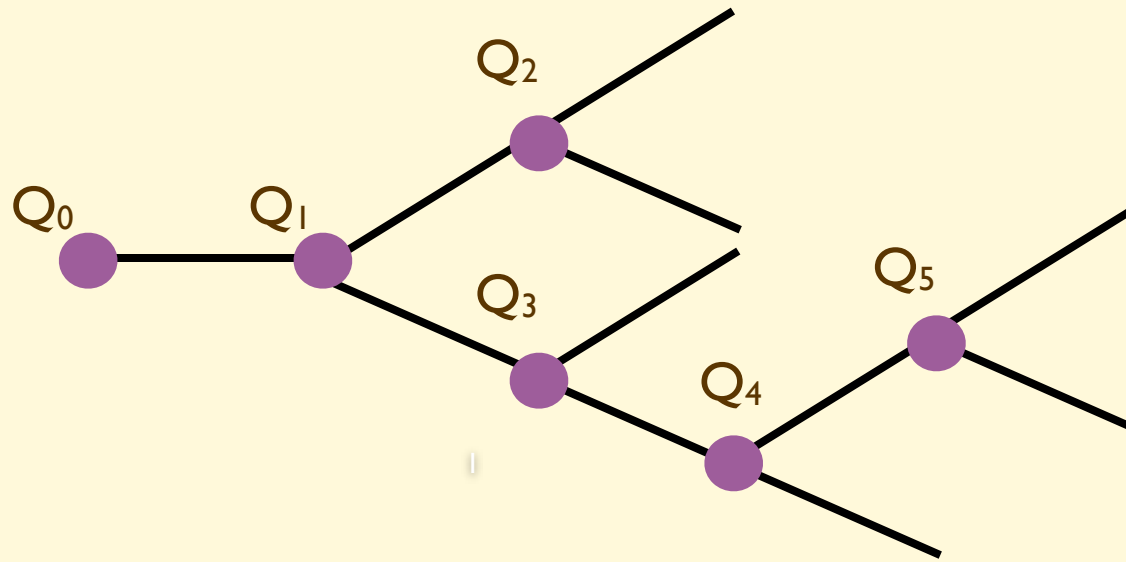
III: Hadronize partons

1. Split gluons into q - q bar pairs
2. Connect colour-singlet pairs
3. Decay the colour-singlet clusters into hadron pairs



The shower algorithm

Sequential probabilistic evolution (Markov chain)

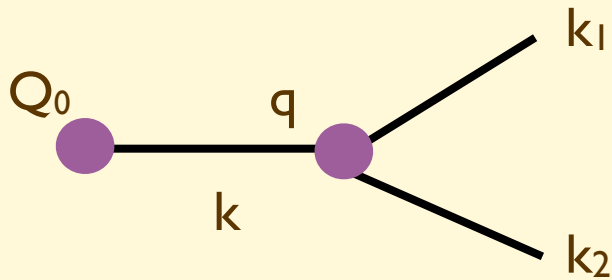


The probability of each emission only depends on the state of the splitting parton, and of the daughters. The QCD dynamics is encoded in these splitting probabilities.

The total probability of all possible evolutions is 1 (unitary evolution).

- The shower evolution does not change the event rate inherited from the parton level, matrix element computation.
- No K-factors from the shower, even though the shower describes higher-order corrections to the leading-order process

Single emission



$$\frac{d\text{Prob}(Q_0 \rightarrow q^2)}{dq^2 dz d\phi} = P_0 \frac{\alpha_s(\mu)}{2\pi} \frac{1}{q^2} P(z)$$

$$P_0 \Rightarrow \int d\text{Prob} = 1$$

$q^2 \approx$ virtuality scale of the branching:

$z = \mathbf{P}(\mathbf{k}_2) / \mathbf{P}(\mathbf{k}) \approx$ energy/momentum fraction carried by one of the two partons after splitting

- $(\mathbf{k}_1 + \mathbf{k}_2)^2$
- $\mathbf{k}_1 \cdot \mathbf{k}_2$
- \mathbf{k}_\perp^2
-

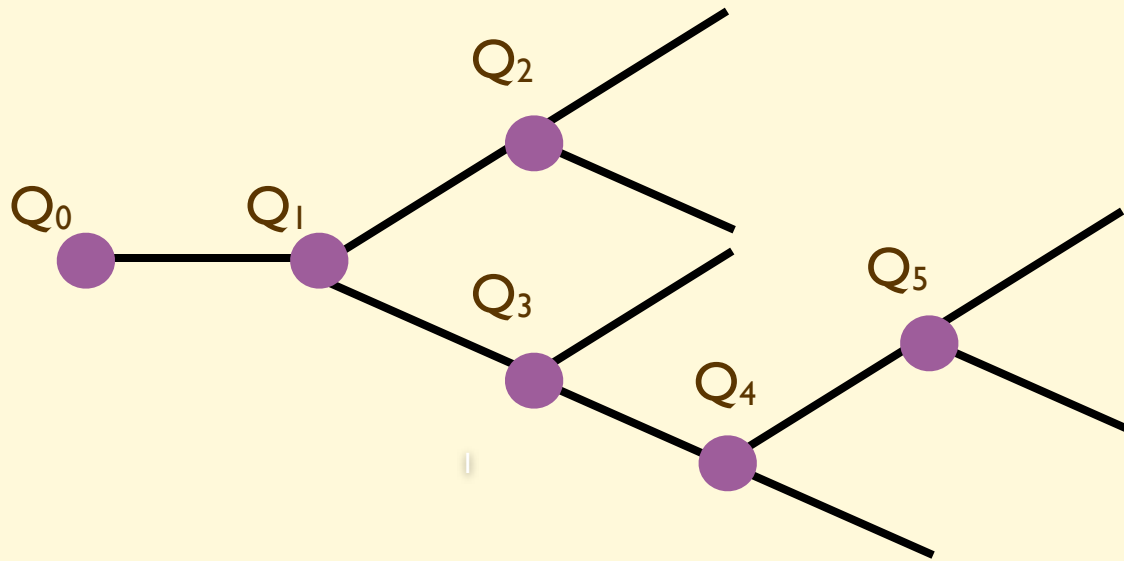
$\phi =$ azimuth

- $\mathbf{P} = \mathbf{k}^0$
- $\mathbf{P} = \mathbf{k} //$
- $\mathbf{P} = \mathbf{k} // + \mathbf{k}^0$
- ...

$\mu = f(\mathbf{z}, \mathbf{q})$

While at leading-logarithmic order (LL) all choices of evolution variables and of scale for α_s are equivalent, specific choices can lead to improved description of NLL effects and allow a more accurate and easy-to-implement inclusion of angular-ordering constraints and mass effects, as well as to a better merging of multijet ME's with the shower

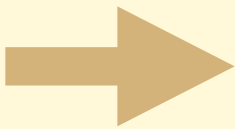
Multiple emission



$$\text{Prob}(Q_0 \rightarrow Q_1) = P_0 \frac{\alpha_s}{2\pi} \int_{Q_1}^{Q_0} \frac{dq^2}{q^2} dz P(z) d\phi$$

$$\begin{aligned} \text{Prob}(Q_0 \rightarrow Q_1 \rightarrow Q_2) &= P_0 \frac{\alpha_s}{2\pi} \int_{Q_1}^{Q_0} \frac{dq^2}{q^2} dz P(z) d\phi \frac{\alpha_s}{2\pi} \int_{Q_2}^{Q_1} \frac{dq^2}{q^2} dz P(z) d\phi \\ &\sim P_0 \frac{1}{2!} \left[\frac{\alpha_s}{2\pi} \int_{Q_2}^{Q_0} \frac{dq^2}{q^2} dz P(z) d\phi \right]^2 \end{aligned}$$

$$\text{Prob}(Q_0 \rightarrow X) = P_0 \times \sum \frac{1}{n!} \left[\frac{\alpha_s}{2\pi} \int_{\Lambda}^{Q_0} \frac{dq^2}{q^2} dz P(z) d\phi \right]^n = 1 \quad \Lambda = \text{infrared cutoff}$$



$$P_0 = \exp \left\{ - \frac{\alpha_s}{2\pi} \int_{\Lambda}^{Q_0} \frac{dq^2}{q^2} dz P(z) d\phi \right\}$$

P_0 = Sudakov form factor
 \sim probability of no emission
 between the scale Q_0 and Λ

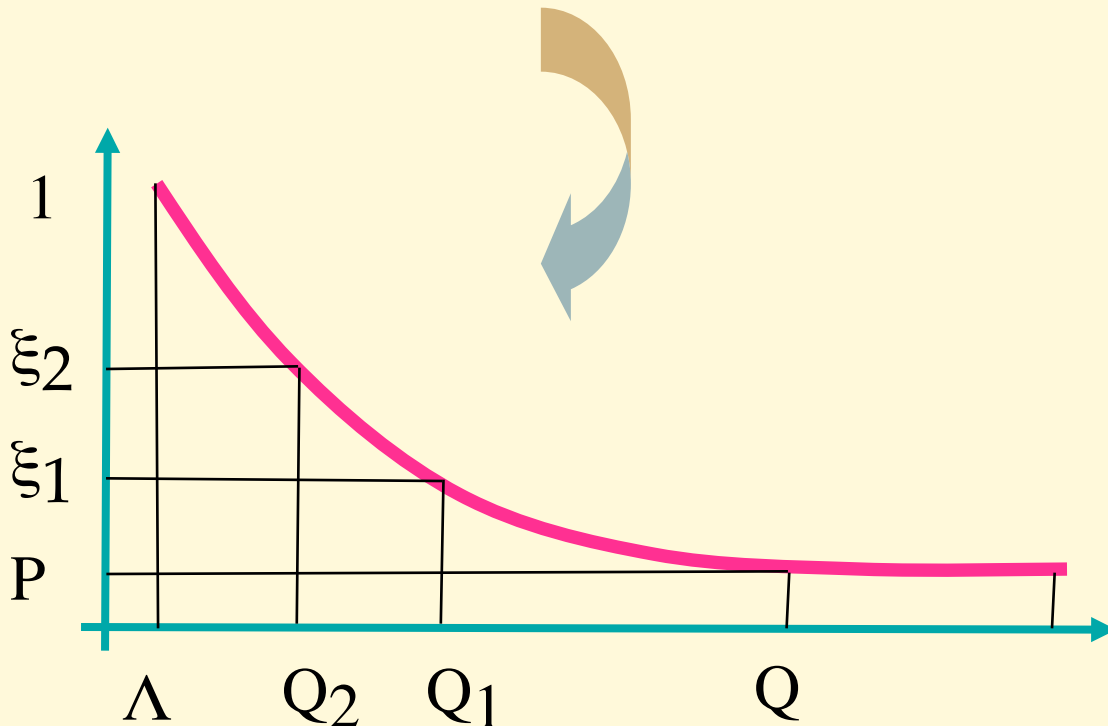
Generation of splittings

1. Generate $0 < \xi_1 < 1$
2. If $\xi_1 < P(Q, \Lambda) \Rightarrow$ no radiation, q' goes directly on-shell at scale $\Lambda \approx \text{GeV}$
3. Else
 1. calculate Q_1 such that $P(Q_1, \Lambda) = \xi_1$
 2. emission at scale Q_1 :

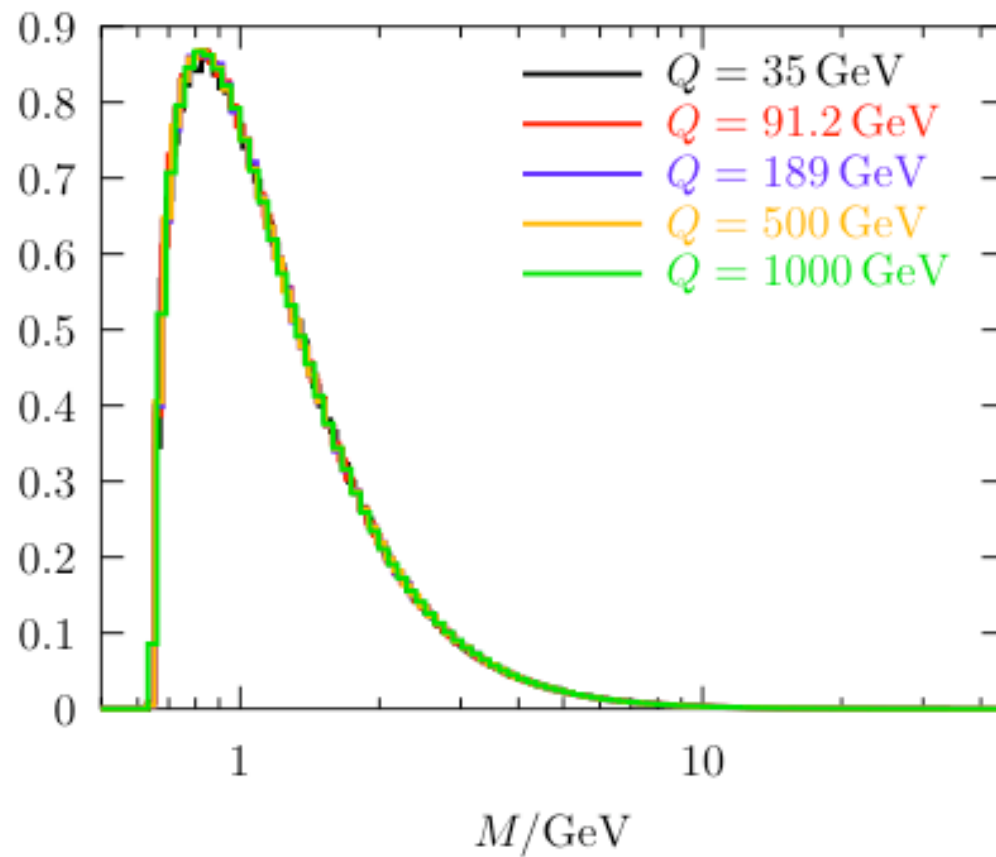
$$P(Q, \Lambda) = \exp \left[- \int_{\Lambda}^Q \frac{dq^2}{q^2} \frac{\alpha_s(q)}{2\pi} P(z) dz \right]$$



prob. of no radiation
between
 Q and Λ



4. Select z according to $P(z)$
5. Reconstruct the full kinematics of the splitting
6. Go back to 1) and reiterate, until shower stops in 2). At each step the probability of emission gets smaller and smaller



The existence of high-mass clusters, however rare, is unavoidable, due to IR cutoff which leads to a non-zero probability that no emission takes place. This is particularly true for evolution of massive quarks (as in, e.g. $Z \rightarrow bb$ or cc). Prescriptions have to be defined to deal with the “evolution” of these clusters. **This has an impact on the $z \rightarrow \mathbf{i}$ behaviour of fragmentation functions.**

Phenomenologically, this leads to uncertainties, for example, in the background rates for $H \rightarrow \gamma\gamma$ (jet $\rightarrow \gamma$).

This approach is extremely successful in describing the properties of hadronic final states!

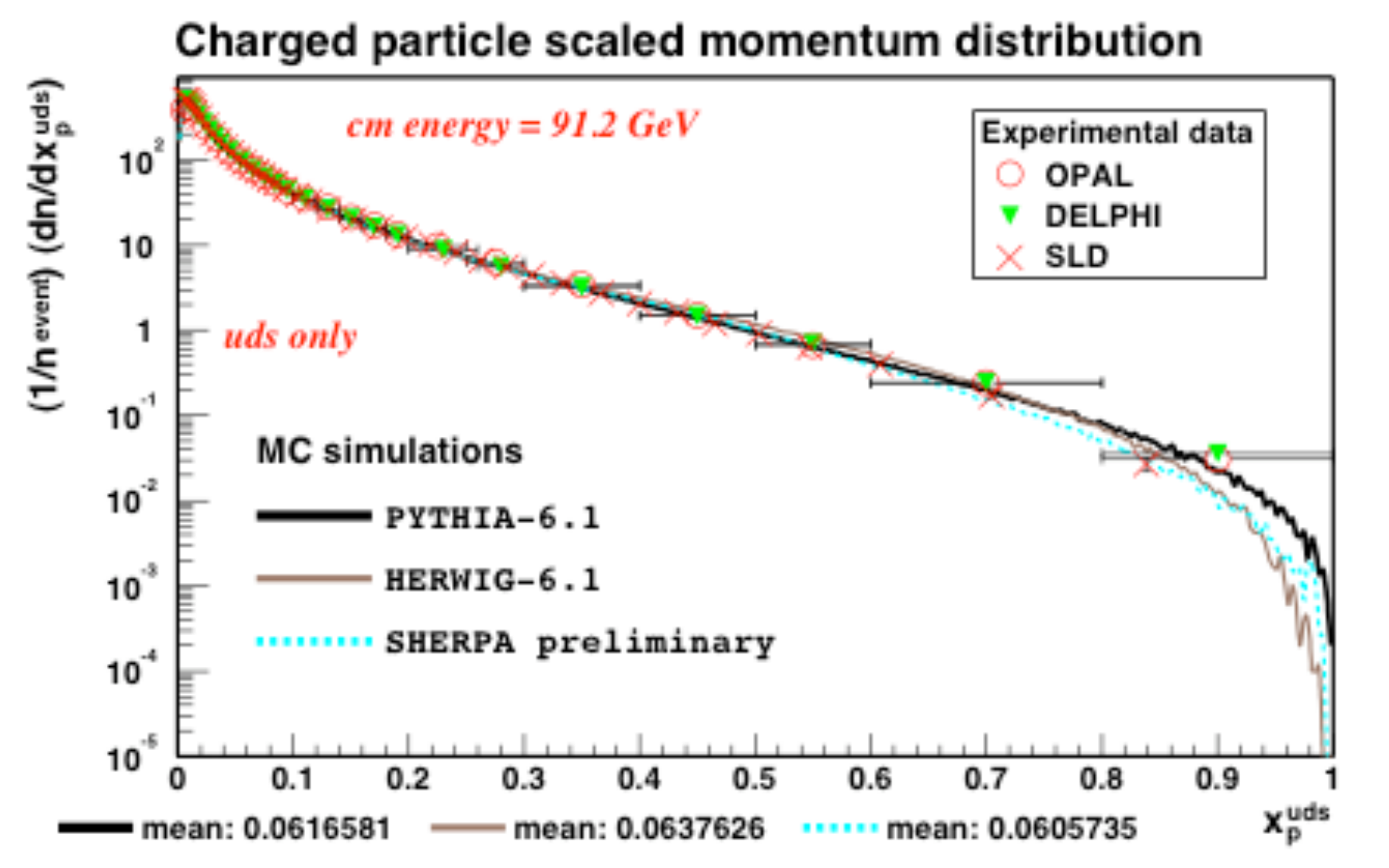
Ex: Particle multiplicities:

Particle	Experiment	Measured	Old Model	Herwig++	Fortran
All Charged	M,A,D,L,O	20.924 ± 0.117	20.22*	20.814	20.532*
γ	A,O	21.27 ± 0.6	23.03	22.67	20.74
π^0	A,D,L,O	9.59 ± 0.33	10.27	10.08	9.88
$\rho(770)^0$	A,D	1.295 ± 0.125	1.235	1.316	1.07
π^\pm	A,O	17.04 ± 0.25	16.30	16.95	16.74
$\rho(770)^\pm$	O	2.4 ± 0.43	1.99	2.14	2.06
η	A,L,O	0.956 ± 0.049	0.886	0.893	0.669*
$\omega(782)$	A,L,O	1.083 ± 0.088	0.859	0.916	1.044
$\eta'(958)$	A,L,O	0.152 ± 0.03	0.13	0.136	0.106
K^0	S,A,D,L,O	2.027 ± 0.025	2.121*	2.062	2.026
$K^*(892)^0$	A,D,O	0.761 ± 0.032	0.667	0.681	0.583*
$K^*(1430)^0$	D,O	0.106 ± 0.06	0.065	0.079	0.072
K^\pm	A,D,O	2.319 ± 0.079	2.335	2.286	2.250
$K^*(892)^\pm$	A,D,O	0.731 ± 0.058	0.637	0.657	0.578
$\phi(1020)$	A,D,O	0.097 ± 0.007	0.107	0.114	0.134*
p	A,D,O	0.991 ± 0.054	0.981	0.947	1.027
Δ^{++}	D,O	0.088 ± 0.034	0.185	0.092	0.209*
Σ^-	O	0.083 ± 0.011	0.063	0.071	0.071
Λ	A,D,L,O	0.373 ± 0.008	0.325*	0.384	0.347*
Λ^0	A,D,O	0.074 ± 0.009	0.078	0.091	0.063
Λ^+	O	0.099 ± 0.015	0.067	0.077	0.088
$\Lambda(1385)^\pm$	A,D,O	0.0471 ± 0.0046	0.057	0.0312*	0.061*
Λ^-	A,D,O	0.0262 ± 0.001	0.024	0.0286	0.029
$\Lambda(1530)^0$	A,D,O	0.0058 ± 0.001	0.026*	0.0288*	0.009*
Λ^0	A,D,O	0.00125 ± 0.00024	0.001	0.00144	0.0009
$f_2(1270)$	D,L,O	0.168 ± 0.021	0.113	0.150	0.173
$f_2'(1525)$	D	0.02 ± 0.008	0.003	0.012	0.012
D^\pm	A,D,O	0.184 ± 0.018	0.322*	0.319*	0.283*
$D^*(2010)^\pm$	A,D,O	0.182 ± 0.009	0.168	0.180	0.151*
D^0	A,D,O	0.473 ± 0.026	0.625*	0.570*	0.501
D_s^\pm	A,O	0.129 ± 0.013	0.218*	0.195*	0.127
$D_s^{*\pm}$	O	0.096 ± 0.046	0.082	0.066	0.043
J/Ψ	A,D,L,O	0.00544 ± 0.00029	0.006	0.00361*	0.002*
Λ_c^+	D,O	0.077 ± 0.016	0.006*	0.023*	0.001*
$\Psi'(3685)$	D,L,O	0.00229 ± 0.00041	0.001*	0.00178	0.0008*

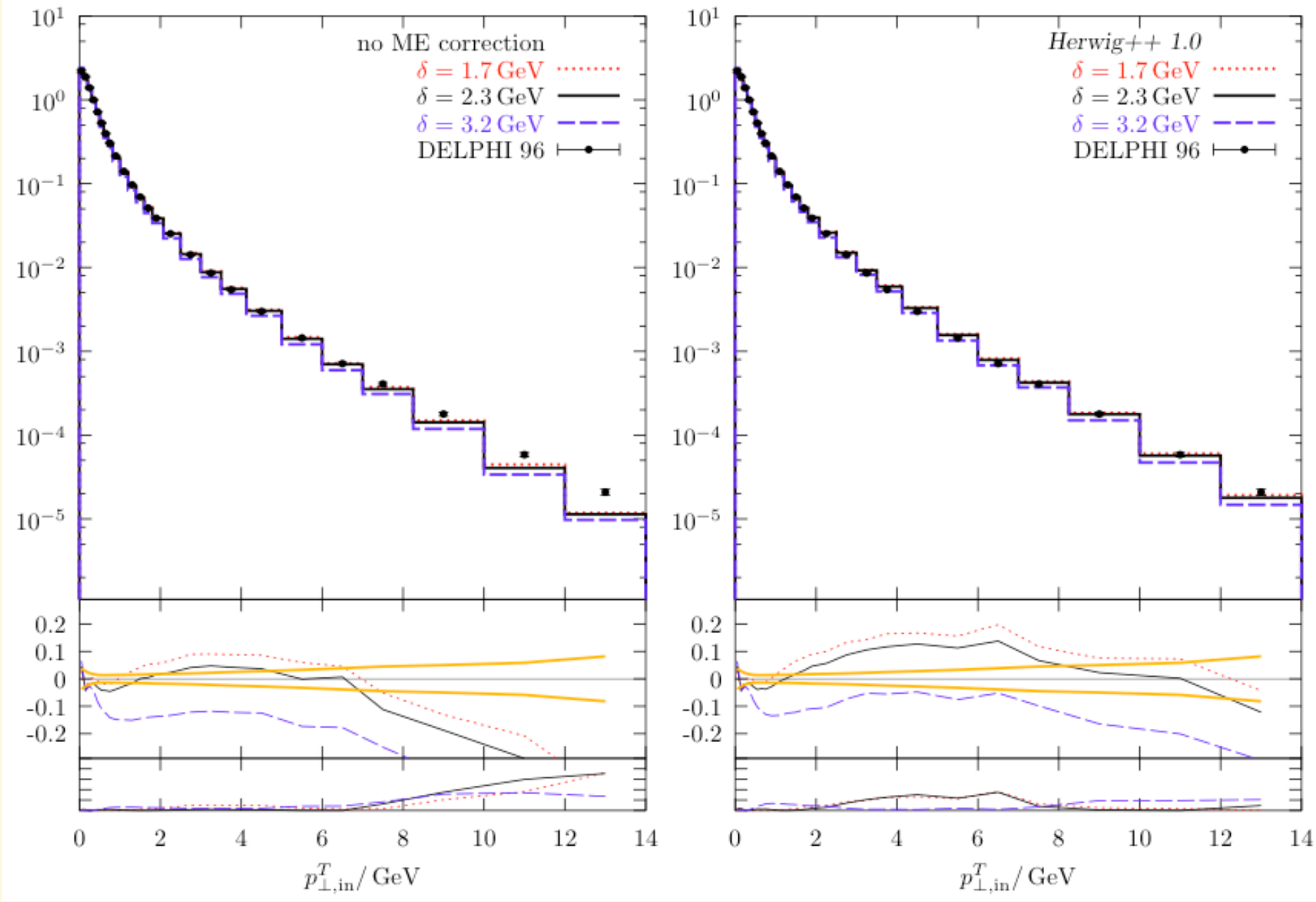
Table 2: Multiplicities per event at 91.2 GeV. We show results from Herwig++ with the implementation of the old cluster hadronization model (Old Model) and the new model (Herwig++), and from HERWIG 6.5 shower and hadronization (Fortran). Parameter values used are given in table 1. Experiments are Aleph(A), Delphi(D), L3(L), Opal(O), Mk2(M) and SLD(S). The * indicates a prediction that differs from the measured value by more than three standard deviations.

Ex: Energy distributions

(Winter, Krauss, Soff,
hep-ph/0311085)

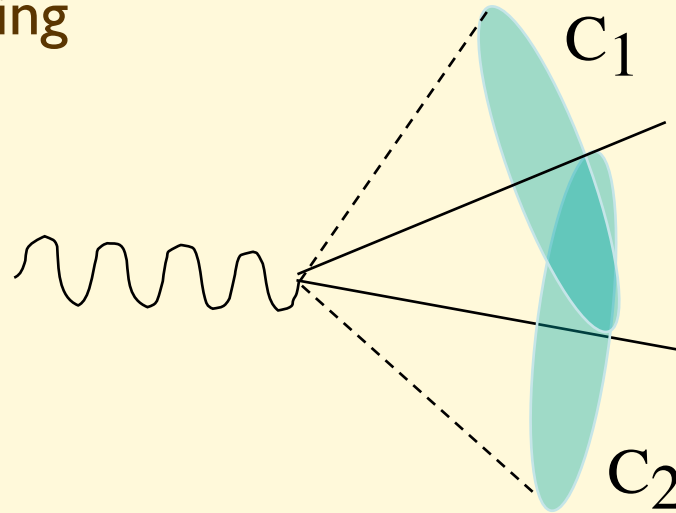


Ex: Transverse momenta w.r.t. thrust axis:



Main limitation of shower approach:

Because of angular ordering



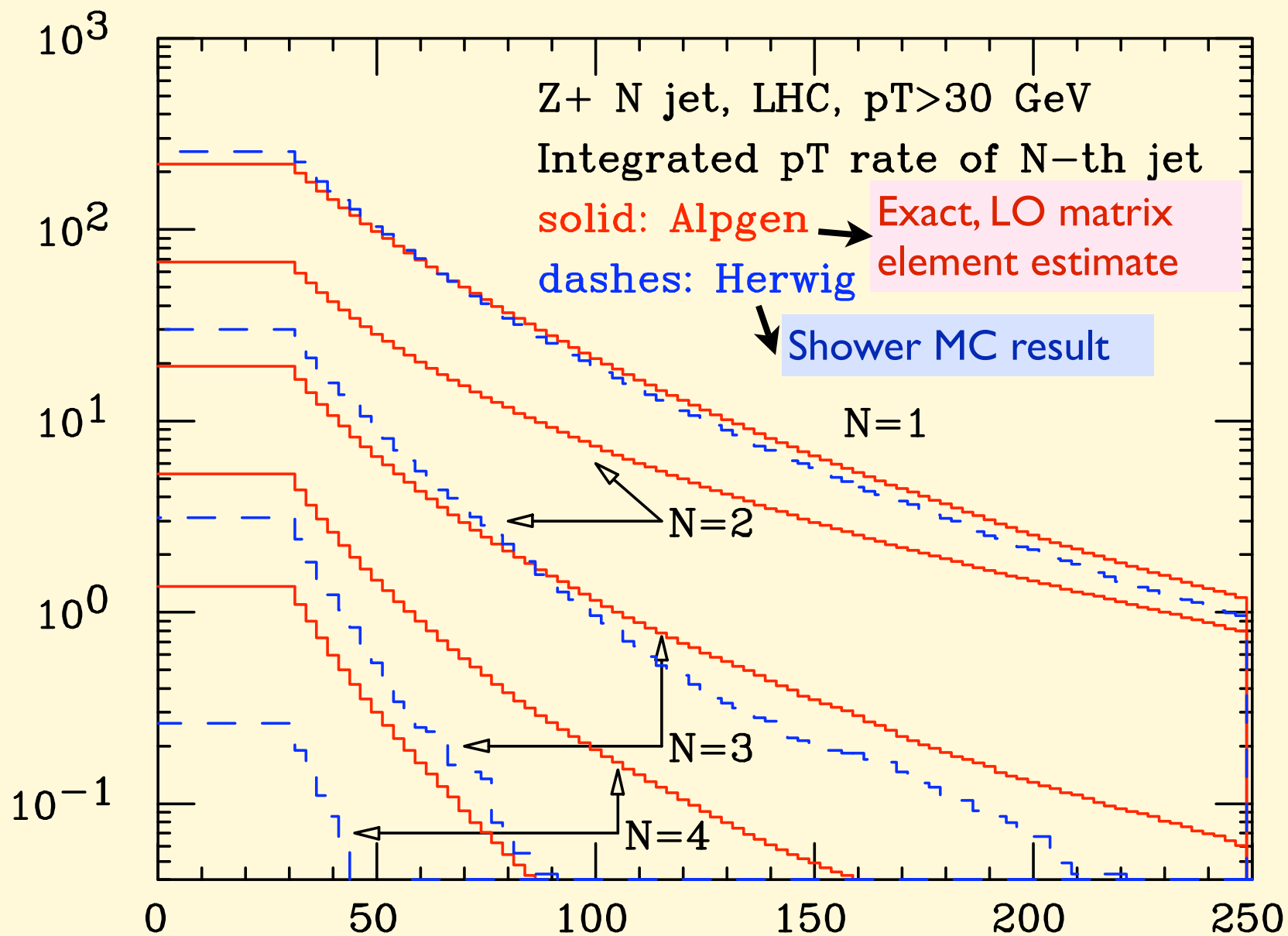
➔ **no emission outside $C_1 \oplus C_2$:**

- lack of hard, large-angle emission
- poor description of multijet events

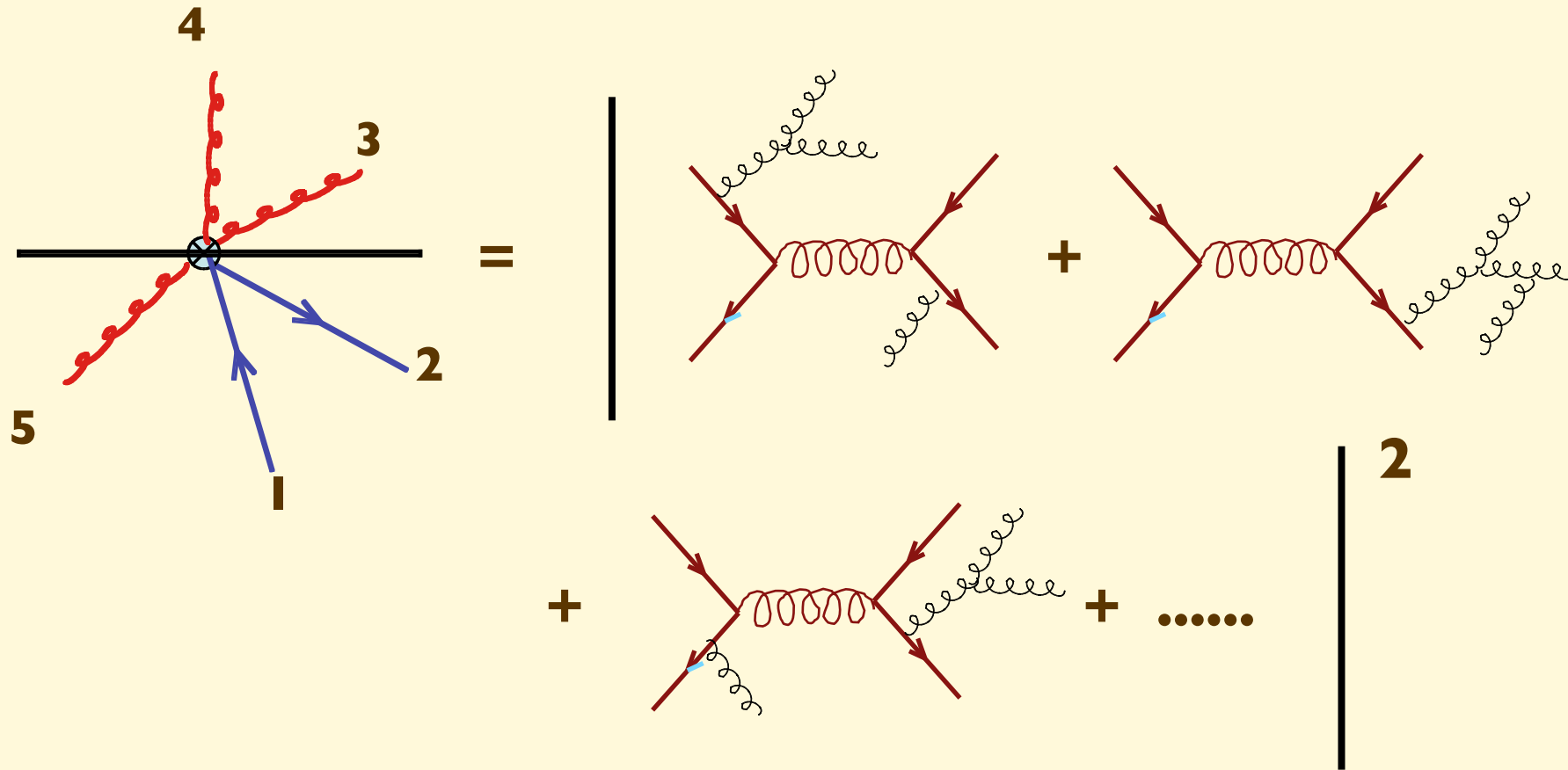
➔ **incoherent emission inside $C_1 \oplus C_2$:**

- loss of accuracy for intrajet radiation

Example

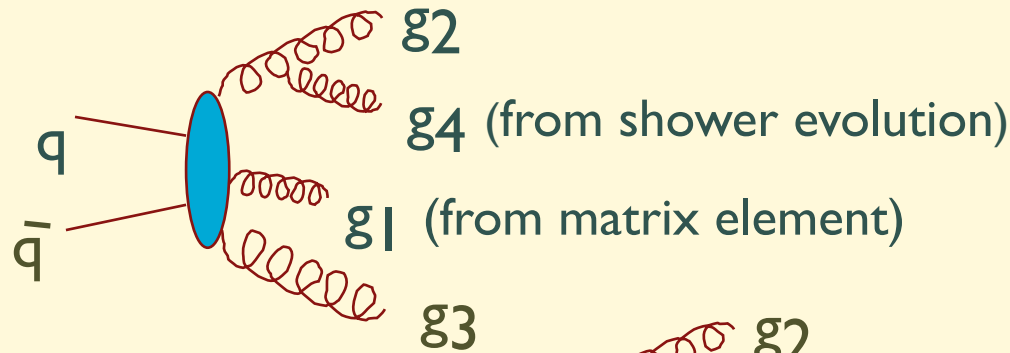


The obvious solution is to start the shower from a higher-order process calculated at the parton level with the exact LO matrix element:



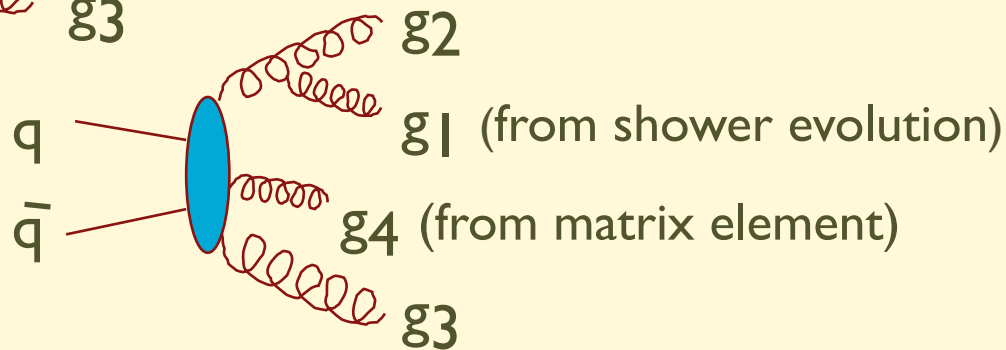
Each hard parton then undergoes the shower evolution according to the previous prescription.

This approach is also afflicted by difficulties:



with $p_{T1} \ll p_{T4} \ll p_{T2}, p_{T3}$

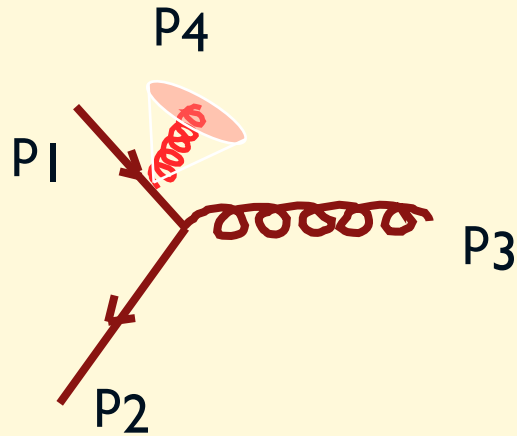
versus



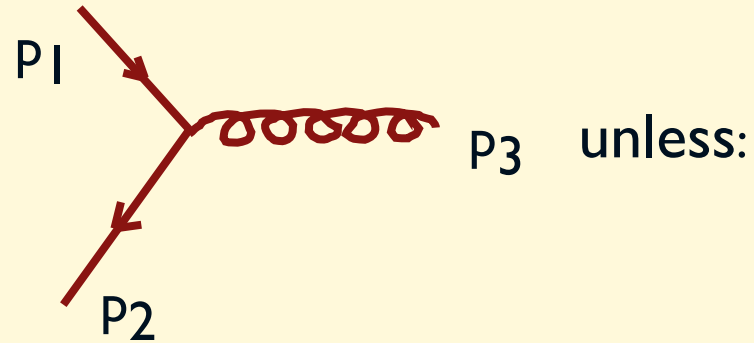
\Rightarrow **double counting of the same phase-space points**

Recent work started providing solutions to these problems, and new generations of MC codes successfully combine higher-order ME and shower evolution ("CKKW", "MLM matching")

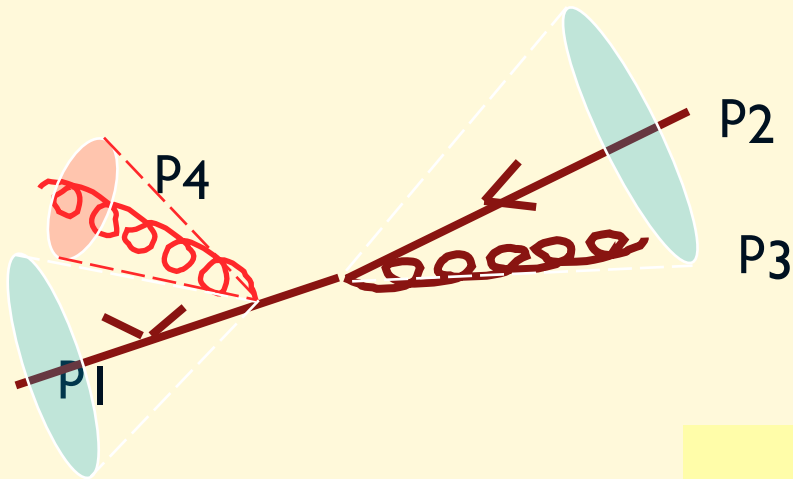
The problem: Leading vs subleading accuracy and double counting



is of $O(\alpha_s)$
relative to the
LO process



unless:



which gives a contribution
to $\sigma_{3\text{-jet}}$ of order

$$\alpha_s \log \frac{(p_2 + p_3)^2}{E_{T \text{ jet}}^2} \approx \alpha_s \left(\log \frac{p_T^{\max}}{p_T^{\min}} + \log \frac{1}{\Delta R} \right)$$



Double counting is sub-leading only if ΔR and $\frac{p_T^{\max}}{p_T^{\min}}$ are not too large

$$\frac{p_T^{\max}}{p_T^{\min}}$$

COMPLEMENTARITY OF THE 3 TOOLS

	ME MC's	X-sect evaluators	Shower MC's
Final state description	Hard partons → jets. Describes geometry, correlations, etc	Limited access to final state structure	Full information available at the hadron level
Higher order effects: loop corrections	Hard to implement, require introduction of negative probabilities	Straightforward to implement, when available	Included as vertex corrections (Sudakov FF's)
Higher order effects: hard emissions	Included, up to high orders (multijets)	Straightforward to implement, when available	Approximate, incomplete phase space at large angle

Recent progress:

MC@NLO for full 1-loop corrections

New algorithms to merge hard ME with showers

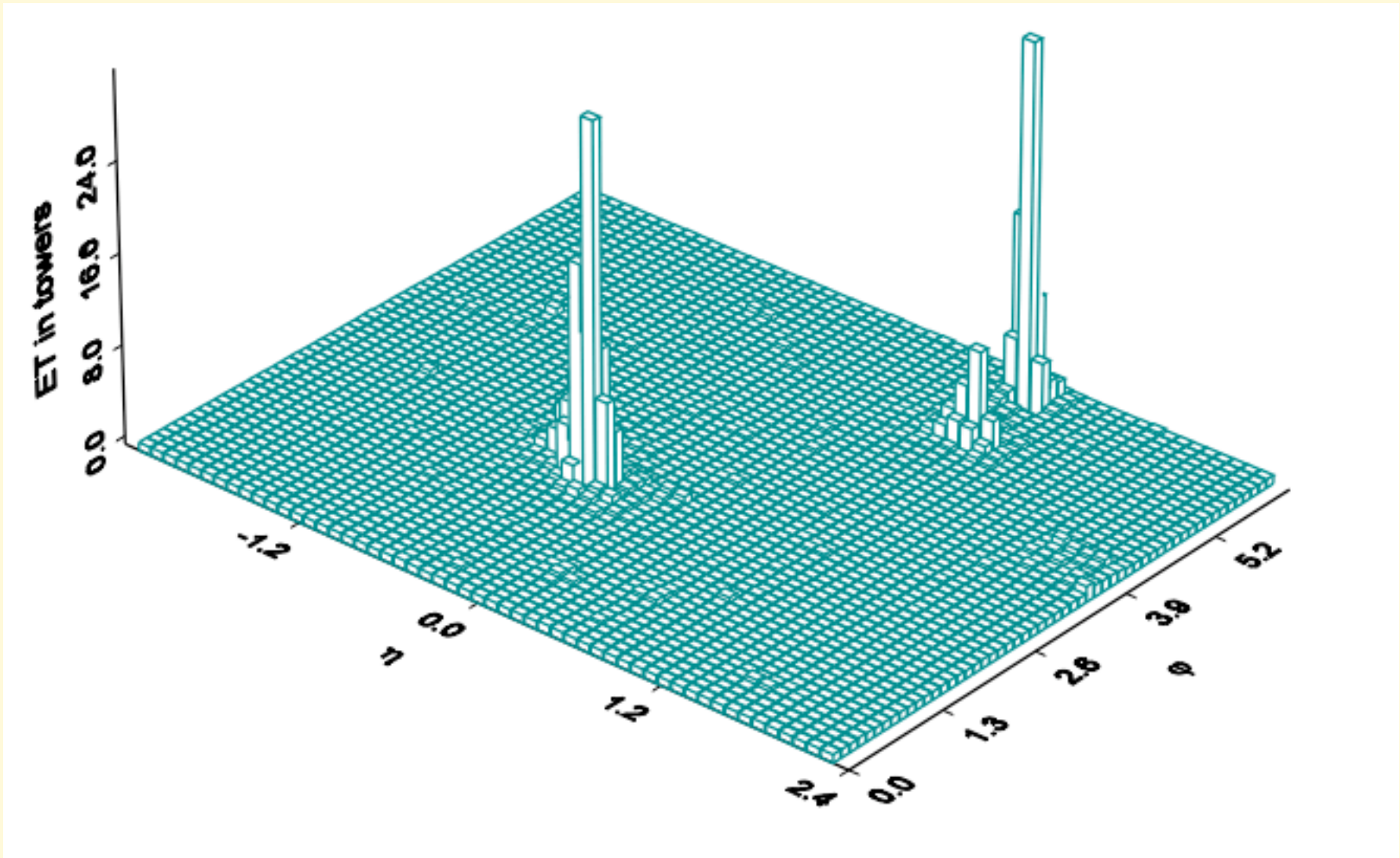
Introduction to hadronic collisions: theoretical concepts and practical tools for the LHC

Lecture 4

Michelangelo L. Mangano

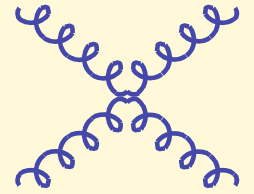
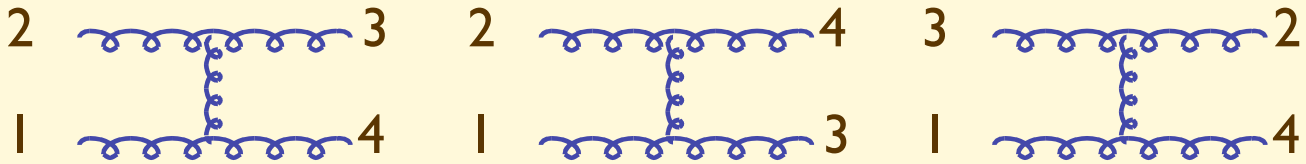
TH Unit, Physics Dept, CERN
michelangelo.mangano@cern.ch

Jets in hadronic collisions

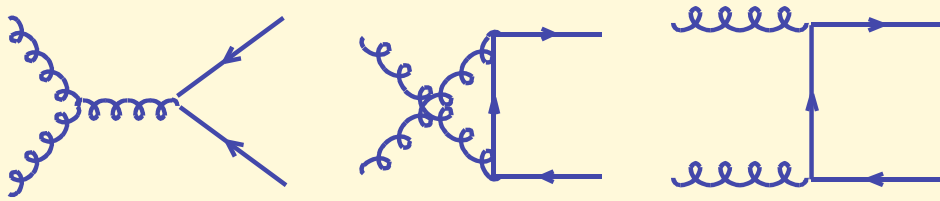


- Inclusive production of jets is the largest component of high- Q phenomena in hadronic collisions
- QCD predictions are known up to NLO accuracy
- Intrinsic theoretical uncertainty (at NLO) is approximately 10%
- Uncertainty due to knowledge of parton densities varies from 5-10% (at low transverse momentum, p_T to 100% (at very high p_T corresponding to high- x gluons)
- Jet are used as probes of the quark structure (possible substructure implies departures from point-like behaviour of cross-section), or as probes of new particles (peaks in the invariant mass distribution of jet pairs)

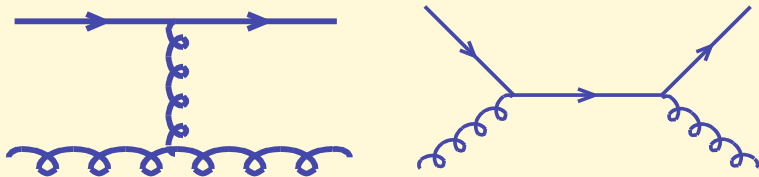
$gg \rightarrow gg$



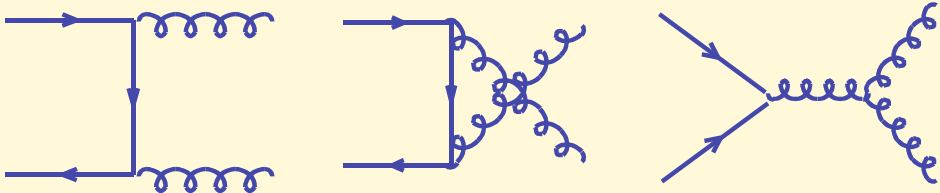
$gg \rightarrow q\bar{q}$



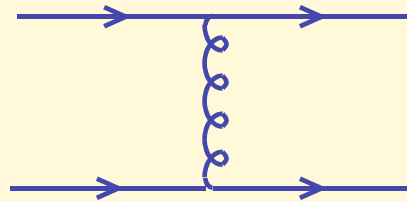
$qg \rightarrow qg$



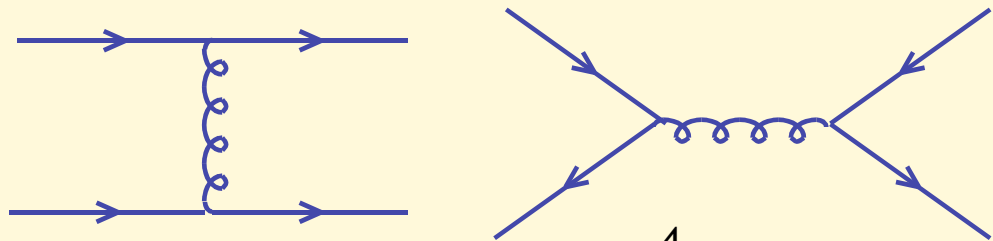
$q\bar{q} \rightarrow gg$



$q\bar{q}' \rightarrow q\bar{q}'$



$q\bar{q} \rightarrow q\bar{q}$

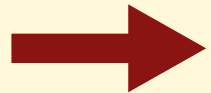


Phase space and cross-section for LO jet production

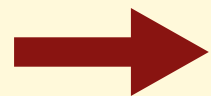
$$d[PS] = \frac{d^3 p_1}{(2\pi)^2 2p_1^0} \frac{d^3 p_2}{(2\pi)^2 2p_2^0} (2\pi)^4 \delta^4(P_{in} - P_{out}) dx_1 dx_2$$

$$(a) \quad \delta(E_{in} - E_{out}) \delta(P_{in}^z - P_{out}^z) dx_1 dx_2 = \frac{1}{2E_{beam}^2}$$

$$(b) \quad \frac{dp^z}{p^0} = dy \equiv d\eta$$



$$d[PS] = \frac{1}{4\pi S} p_T dp_T d\eta_1 d\eta_2$$



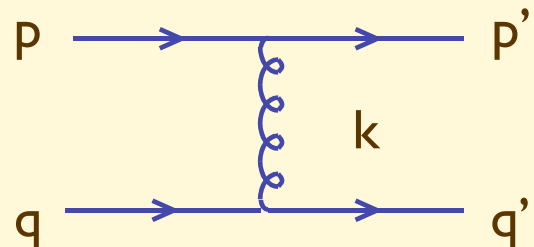
$$\frac{d^3 \sigma}{dp_T d\eta_1 d\eta_2} = \frac{p_T}{4\pi S} \sum_{i,j} f_i(x_1) f_j(x_2) \frac{1}{2\hat{s}} \sum_{kl} |M(ij \rightarrow kl)|^2$$

The measurement of p_T and rapidities for a dijet final state uniquely determines the parton momenta x_1 and x_2 . Knowledge of the partonic cross-section allows therefore the determination of partonic densities $f(x)$

Small-angle jet production, a useful approximation for the determination of the matrix elements and of the cross-section

At small scattering angle, $t = (p_1 - p_3)^2 \sim (1 - \cos \theta) \rightarrow 0$

and the $1/t^2$ propagators associated with t-channel gluon exchange dominate the matrix elements for all processes. In this limit it is easy to evaluate the matrix elements. For example:



$$\sim (\lambda^a)_{ij} (\lambda^a)_{kl} (2p_\mu) \frac{1}{t} (2q_\mu) = \frac{2s}{t} (\lambda^a)_{ij} (\lambda^a)_{kl}$$

where we used the fact that, for $k=p-p' \ll p$ (small angle scattering),

$$\bar{u}(p') \gamma_\mu u(p) \sim \bar{u}(p) \gamma_\mu u(p) = 2p_\mu$$

Using our colour algebra results, we then get: $\overline{\sum_{col,spin}} |M|^2 = \frac{1}{N_c^2} \frac{N_c^2 - 1}{4} \frac{4s^2}{t^2}$

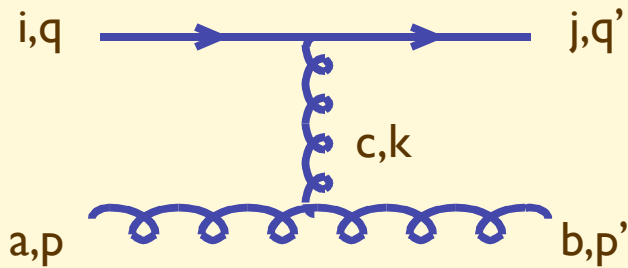
Noting that the result must be symmetric under $s \leftrightarrow u$ exchange, and setting

$N_c=3$, we finally obtain: $\overline{\sum_{col,spin}} |M|^2 = \frac{4}{9} \frac{s^2 + u^2}{t^2}$

which turns out to be the exact result!

Quark-gluon and gluon-gluon scattering

We repeat the exercise in the more complex case of qg scattering, assuming the dominance of the t-channel gluon-exchange diagram:



$$\sim f^{abc} \lambda_{ij}^c 2p_\mu \frac{1}{t} 2q_\mu = 2 \frac{s}{t} f^{abc} \lambda_{ij}^c$$

Using the colour algebra results, and enforcing the $s \leftrightarrow u$ symmetry, we get:

$$\overline{\sum_{col, spin}} |M|^2 = \frac{s^2 + u^2}{t^2}$$

which differs by only 20% from the exact result even in the large-angle region, at 90°

$$\overline{\sum_{col, spin}} |M|^2 = \frac{s^2 + u^2}{t^2} - \frac{4s^2 + u^2}{9us}$$

In a similar way we obtain for gg scattering (using the $t \leftrightarrow u$ symmetry):

$$\overline{\sum_{col, spin}} |M(gg \rightarrow gg)|^2 = \frac{9}{2} \left(\frac{s^2}{t^2} + \frac{s^2}{u^2} \right)$$

compared to the exact result

$$\overline{\sum_{col, spin}} |M(gg \rightarrow gg)|^2 = \frac{9}{2} \left(3 - \frac{ut}{s^2} - \frac{us}{t^2} - \frac{st}{u^2} \right)$$

with a 20% difference at 90°

Note that in the leading $1/t$ approximation we get the following result:

$$\hat{\sigma}_{gg} : \hat{\sigma}_{qg} : \hat{\sigma}_{qq} = \frac{9}{4} : 1 : \frac{4}{9}$$

where $4/9 = C_F / C_A = [(N^2-1)/2N] / N$ is the ratio of the squared colour charges of quarks and gluons

and therefore

$$d\sigma_{jet} = \int dx_1 dx_2 \sum_{ij} f_i(x_1) f_j(x_2) d\hat{\sigma}_{ij} = \int dx_1 dx_2 \sum_{ij} F(x_1) F(x_2) d\hat{\sigma}_{gg}$$

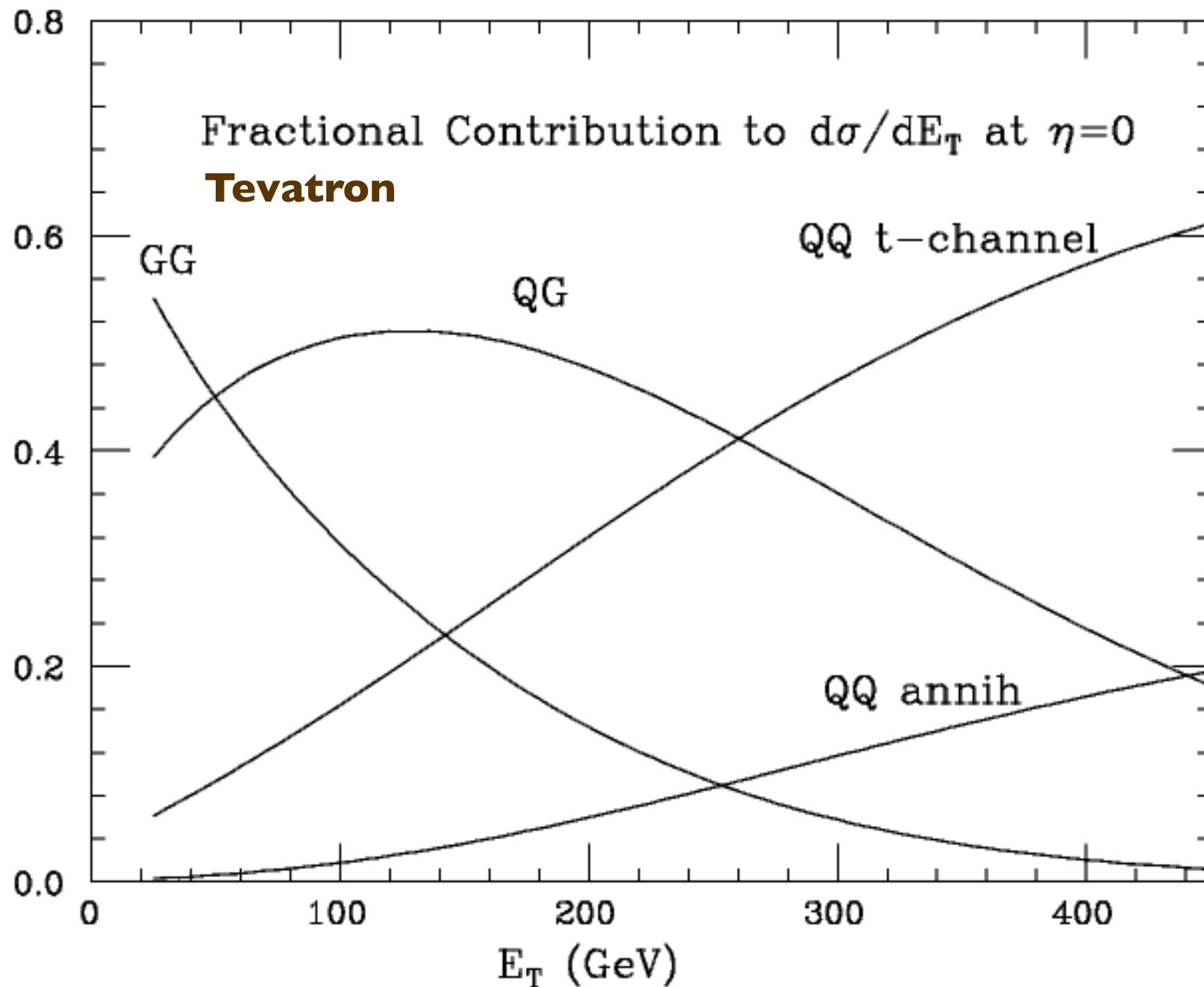
where we defined the 'effective parton density' $F(x)$:

$$F(x) = g(x) + \frac{4}{9} \sum_i [q_i(x) + \bar{q}_i(x)]$$

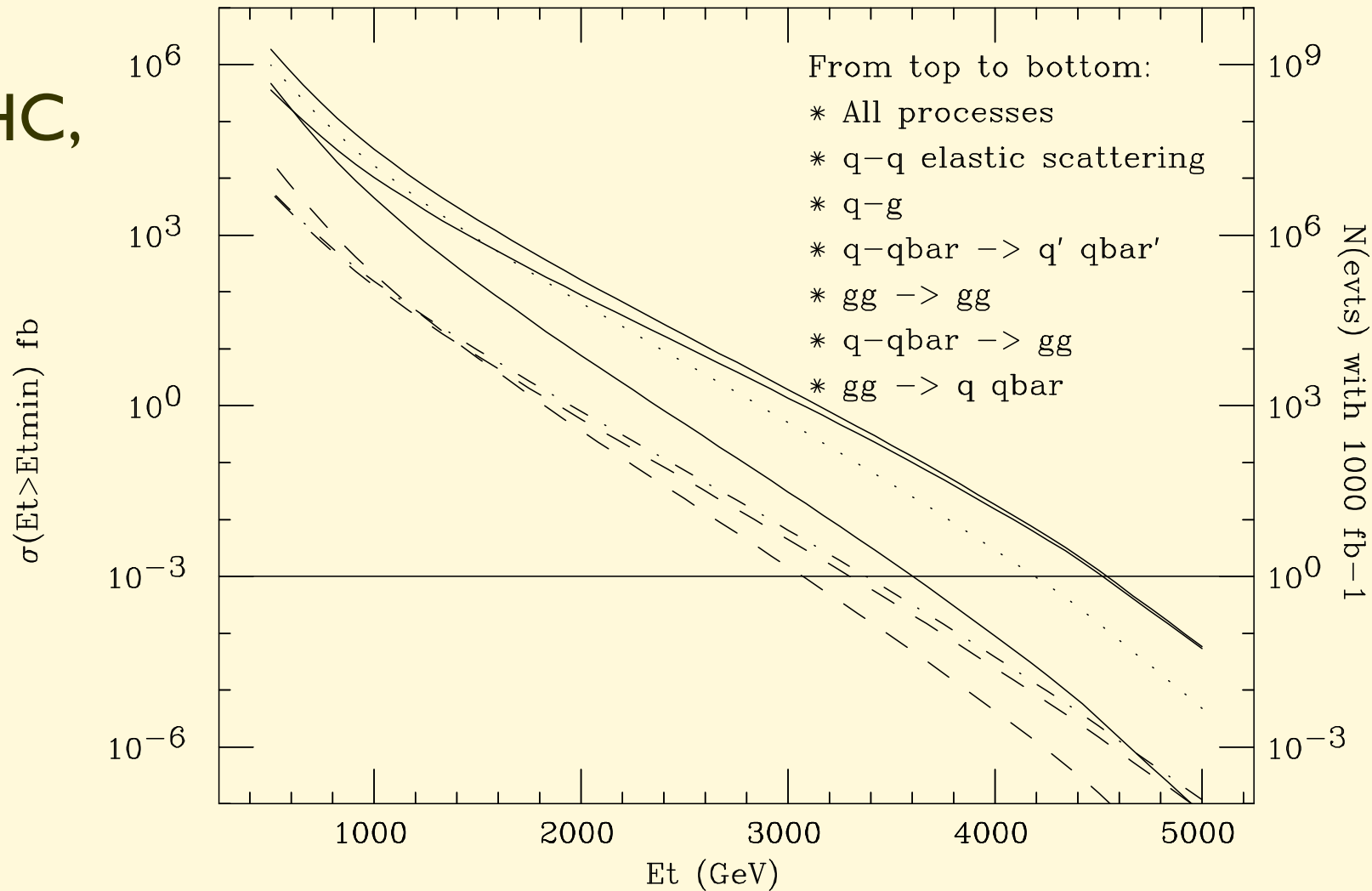
As a result jet data cannot be used to extract separately gluon and quark densities. On the other hand, assuming an accurate knowledge of the quark densities (say from HERA), jet data can help in the determination of the gluon density

Process	$\frac{d\hat{\sigma}}{d\Phi_2}$	at 90°
$qq' \rightarrow qq'$	$\frac{4}{9} \frac{\hat{s}^2 + \hat{u}^2}{\hat{t}^2}$	2.22
$qq \rightarrow qq$	$\left[\frac{4}{9} \left(\frac{\hat{s}^2 + \hat{u}^2}{\hat{t}^2} + \frac{\hat{s}^2 + \hat{t}^2}{\hat{u}^2} \right) - \frac{8}{27} \frac{\hat{s}^2}{\hat{u}\hat{t}} \right]$	3.26
$q\bar{q} \rightarrow q'\bar{q}'$	$\frac{4}{9} \frac{\hat{t}^2 + \hat{u}^2}{\hat{s}^2}$	0.22
$q\bar{q} \rightarrow q\bar{q}$	$\left[\frac{4}{9} \left(\frac{\hat{s}^2 + \hat{u}^2}{\hat{t}^2} + \frac{\hat{t}^2 + \hat{u}^2}{\hat{s}^2} \right) - \frac{8}{27} \frac{\hat{u}^2}{\hat{s}\hat{t}} \right]$	2.59
$q\bar{q} \rightarrow gg$	$\left[\frac{32}{27} \frac{\hat{t}^2 + \hat{u}^2}{\hat{t}\hat{u}} - \frac{8}{3} \frac{\hat{t}^2 + \hat{u}^2}{\hat{s}^2} \right]$	1.04
$gg \rightarrow q\bar{q}$	$\left[\frac{1}{6} \frac{\hat{t}^2 + \hat{u}^2}{\hat{t}\hat{u}} - \frac{3}{8} \frac{\hat{t}^2 + \hat{u}^2}{\hat{s}^2} \right]$	0.15
$gg \rightarrow qq$	$\left[-\frac{4}{9} \frac{\hat{s}^2 + \hat{u}^2}{\hat{s}\hat{u}} + \frac{\hat{u}^2 + \hat{s}^2}{\hat{t}^2} \right]$	6.11
$gg \rightarrow gg$	$\frac{9}{2} \left(3 - \frac{\hat{t}\hat{u}}{\hat{s}^2} - \frac{\hat{s}\hat{u}}{\hat{t}^2} - \frac{\hat{s}\hat{t}}{\hat{u}^2} \right)$	30.4

Quark/gluon composition



Jet production rates at the LHC, subprocess composition



The presence of a quark substructure would manifest itself via contact interactions (as in Fermi's theory of weak interactions). On one side these new interactions would lead to an increase in cross-section, on the other they would affect the jets' angular distributions. In the dijet CMF, QCD implies Rutherford law, and extra point-like interactions can then be isolated using a fit. With the anticipated statistics of 300 fb⁻¹, limits on the scale of the new interactions in excess of 40 TeV should be reached (to increase to 60 TeV with 3000 fb⁻¹)

Some more kinematics

Prove as an **exercise** that

$$x_{1,2} = \frac{p_T}{E_{beam}} \cosh y^* e^{\pm y_b}$$

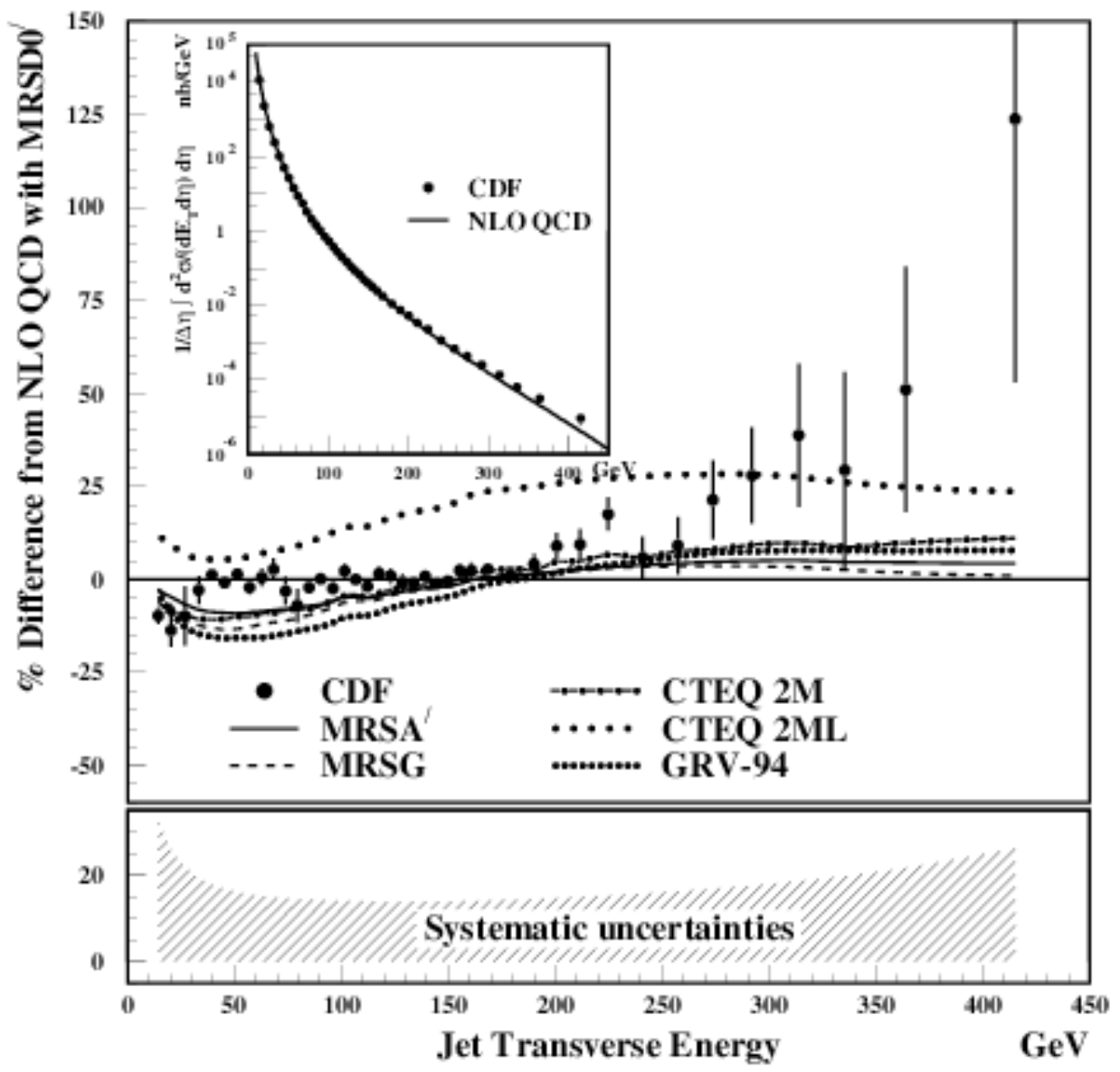
where

$$y^* = \frac{\eta_1 - \eta_2}{2}, \quad y_b = \frac{\eta_1 + \eta_2}{2}$$

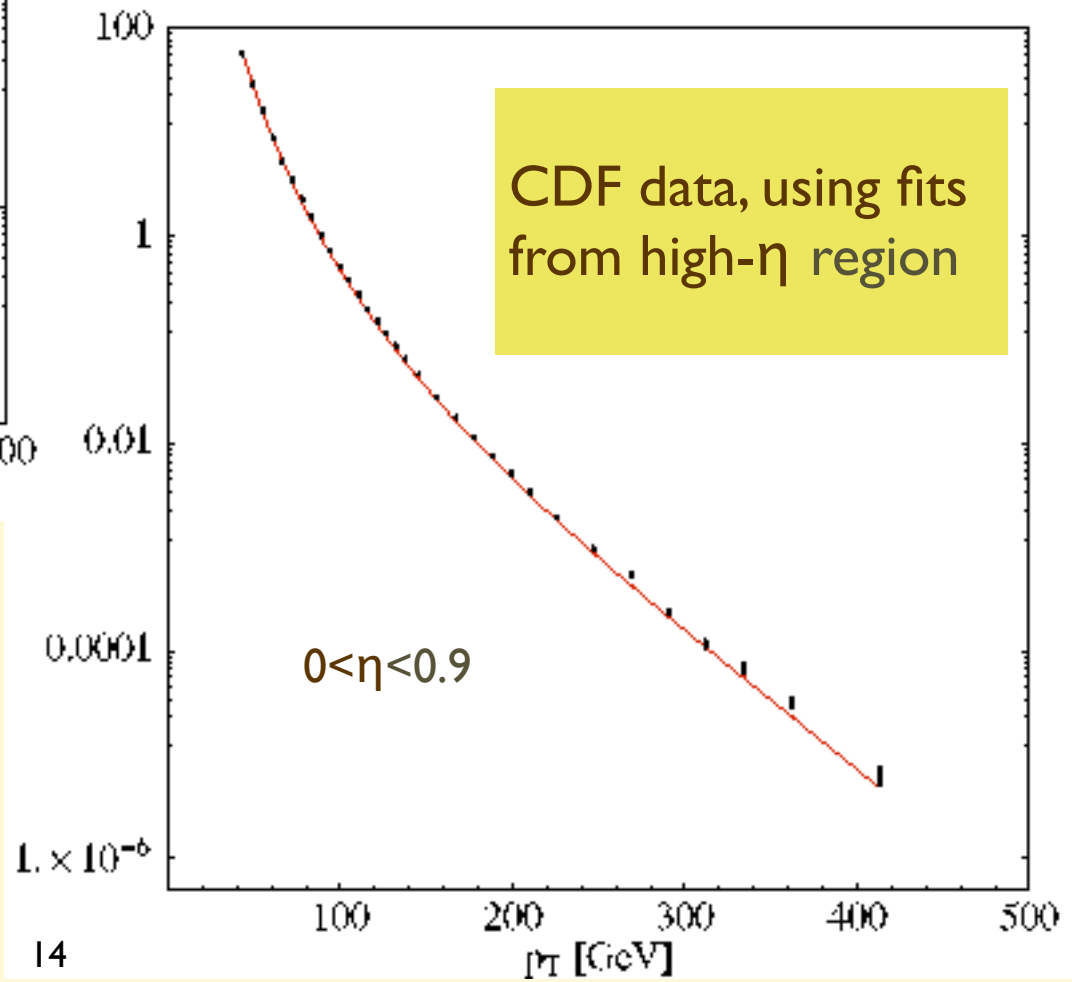
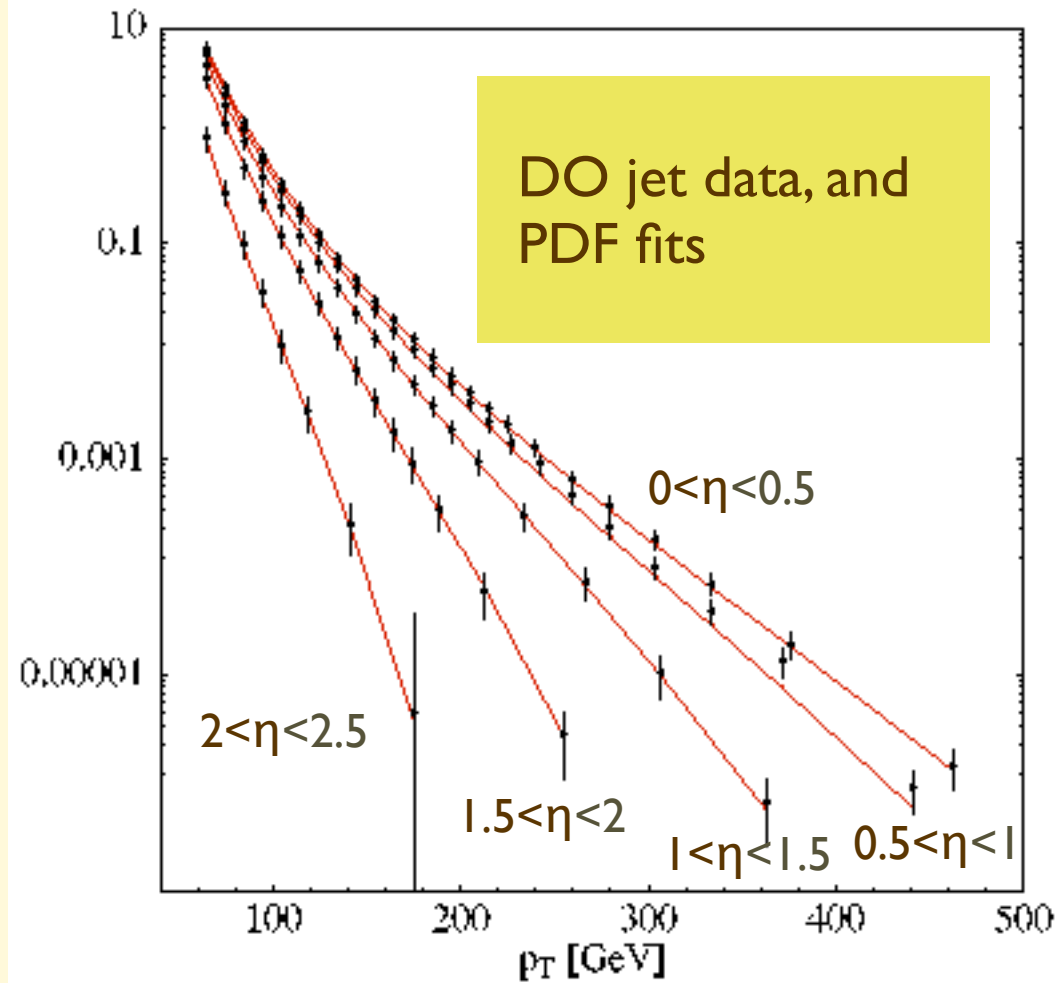
We can therefore reach large values of x either by selecting large invariant mass events:

$$\frac{p_T}{E_{beam}} \cosh y^* \equiv \sqrt{\tau} \rightarrow 1$$

or by selecting low-mass events, but with large boosts (y_b large) in either positive or negative directions. In this case, we probe large- x with events where possible new physics is absent, thus setting consistent constraints on the behaviour of the cross-section in the high-mass region, which could hide new phenomena.

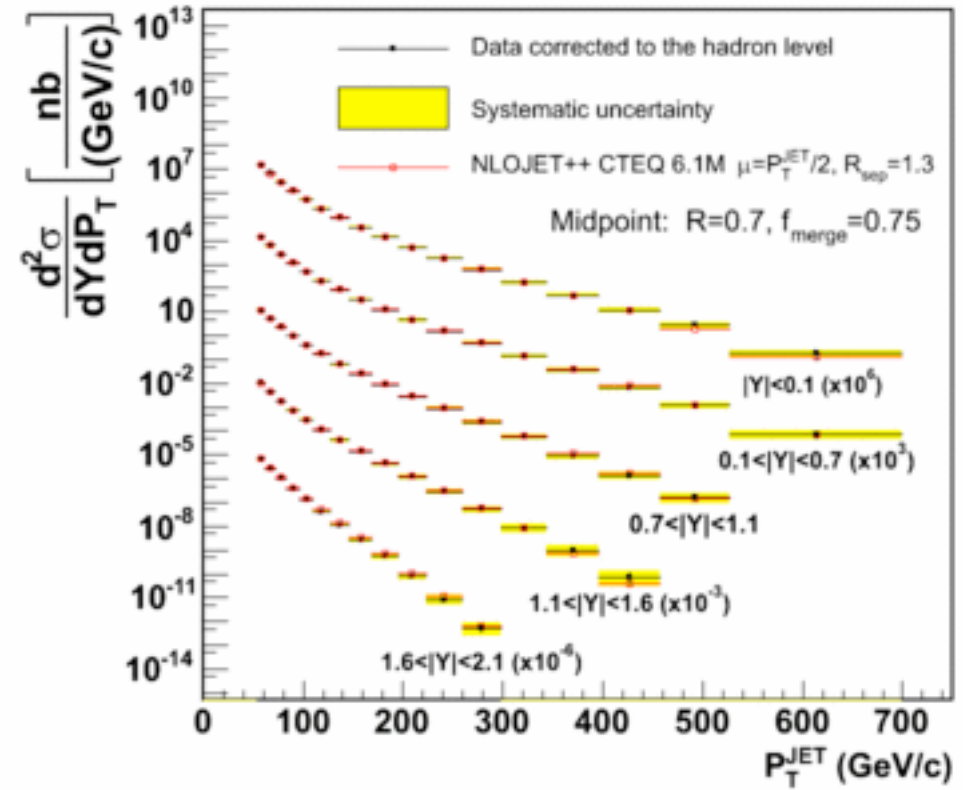


Example, at the Tevatron

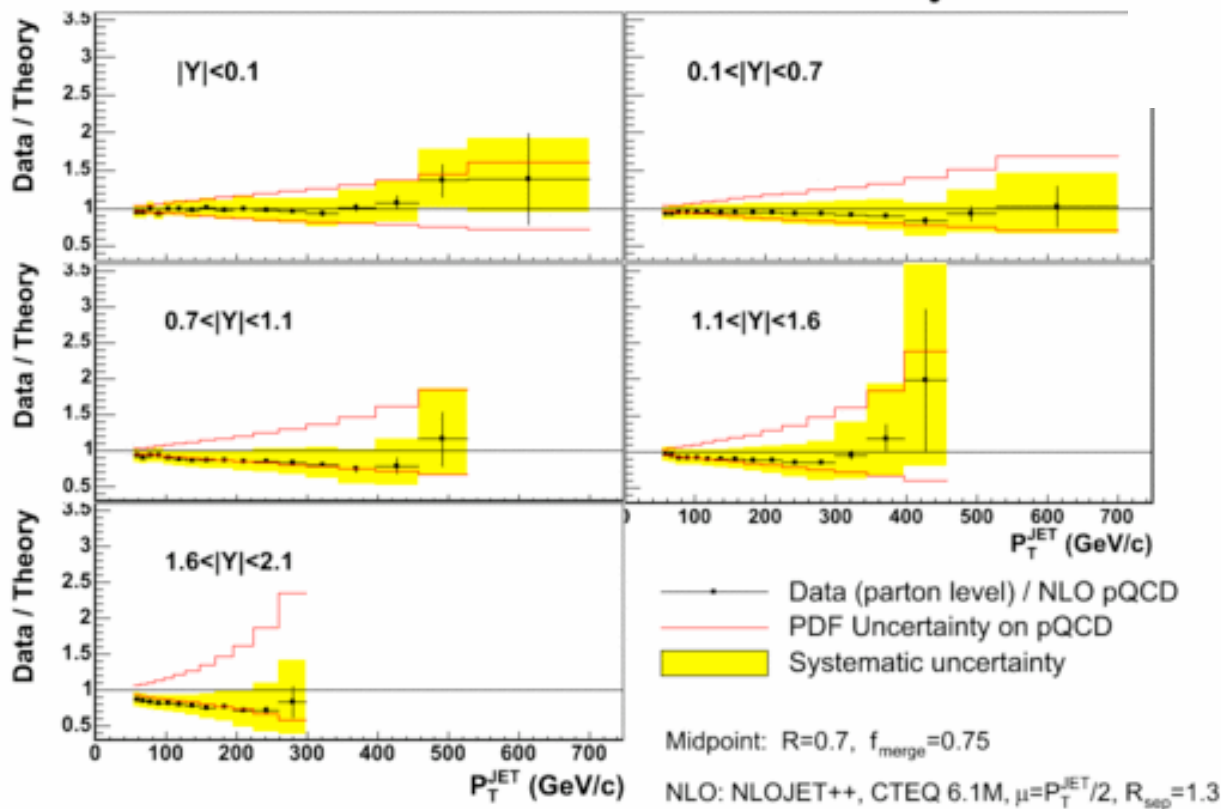


Tevatron, Run 2 results

CDF Run II Preliminary (L=1.13 fb⁻¹)



CDF Run II Preliminary $\int L=1.13 \text{ fb}^{-1}$



Leptons

Experimentally, electrons, muons and taus are entirely different objects. Their identification requires different components of the detector, different techniques, and is subject to different backgrounds.

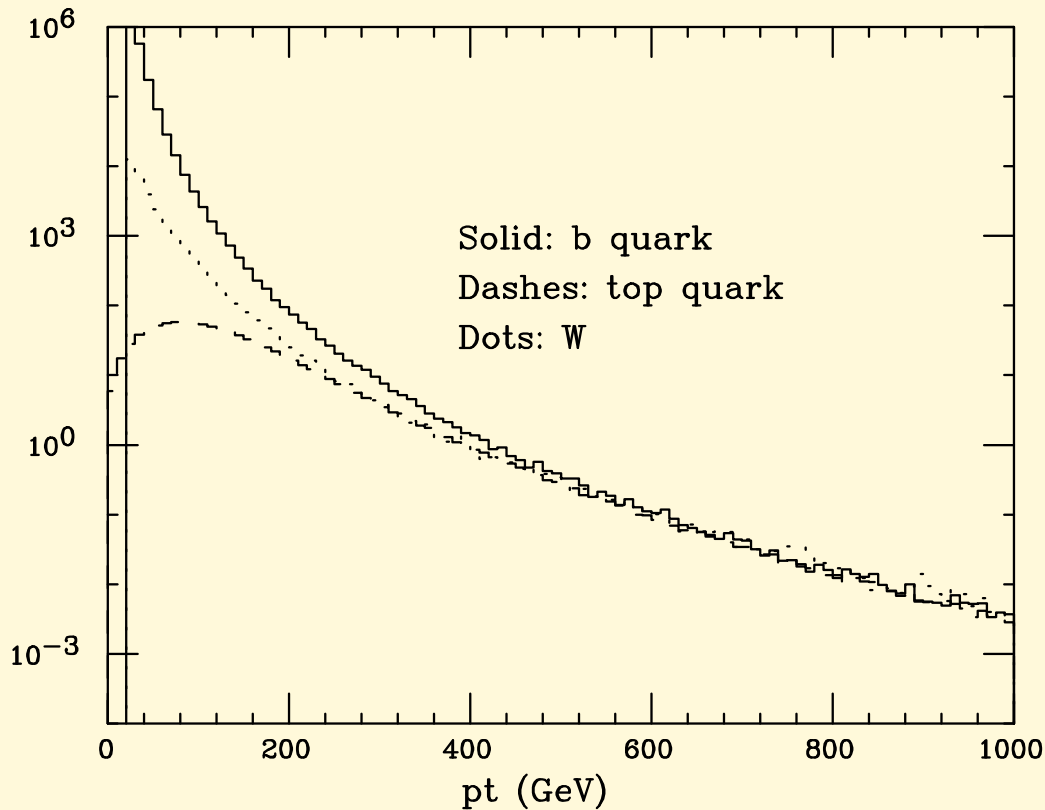
As seen from a theorist, all leptons are produced the same. Nevertheless there is a large variety of possible production mechanisms, each one of them leading to different overall properties of the final state. When considering leptons as a signal for new physics, it is important to have a clear picture of their irreducible SM sources

Single lepton

Sources of single high-pt leptons:

- $W \rightarrow e/\mu + \nu$
- $Z \rightarrow \tau\tau \rightarrow e/\mu + X$
- $b \rightarrow e/\mu + X$
- $t \rightarrow Wb \rightarrow e/\mu + \nu + b$

Differential Rates

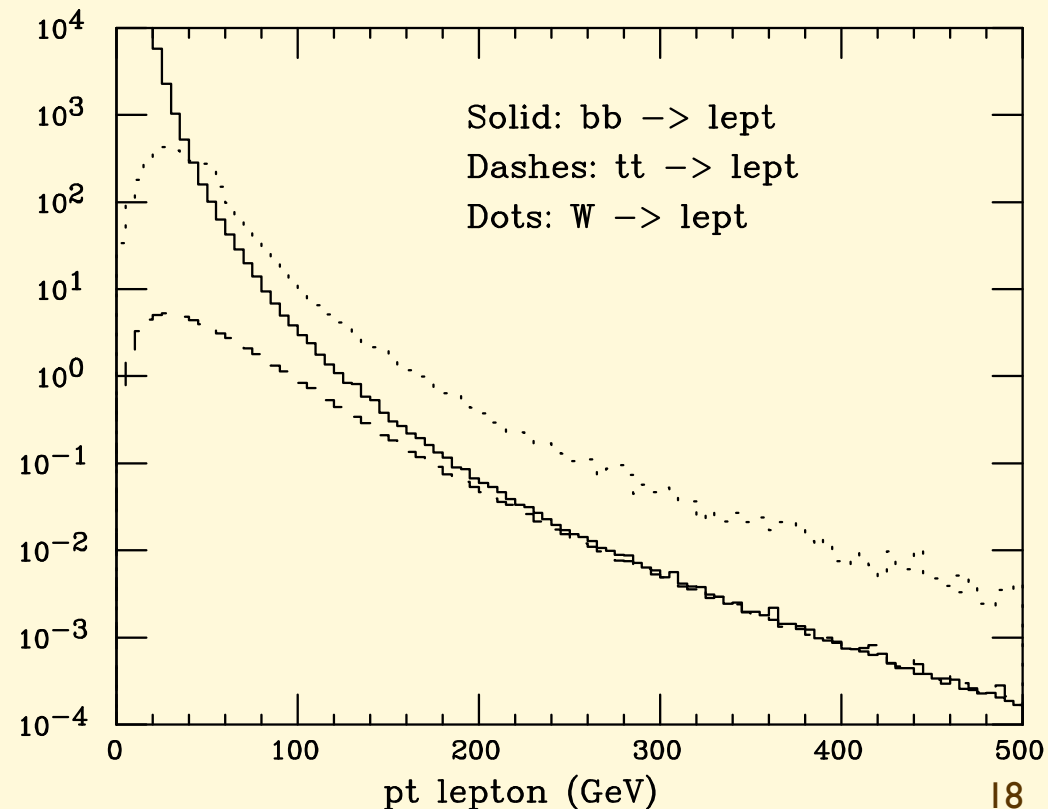


- At large pt b and t production \sim equal !
- At large pt , W and heavy quark production \sim equal!

*W \rightarrow lepton is a 2-body decay, b/t \rightarrow lepton is 3-body: lepton takes a larger fraction of momentum in W decay \Rightarrow harder spectrum, larger rate at higher pt in W production

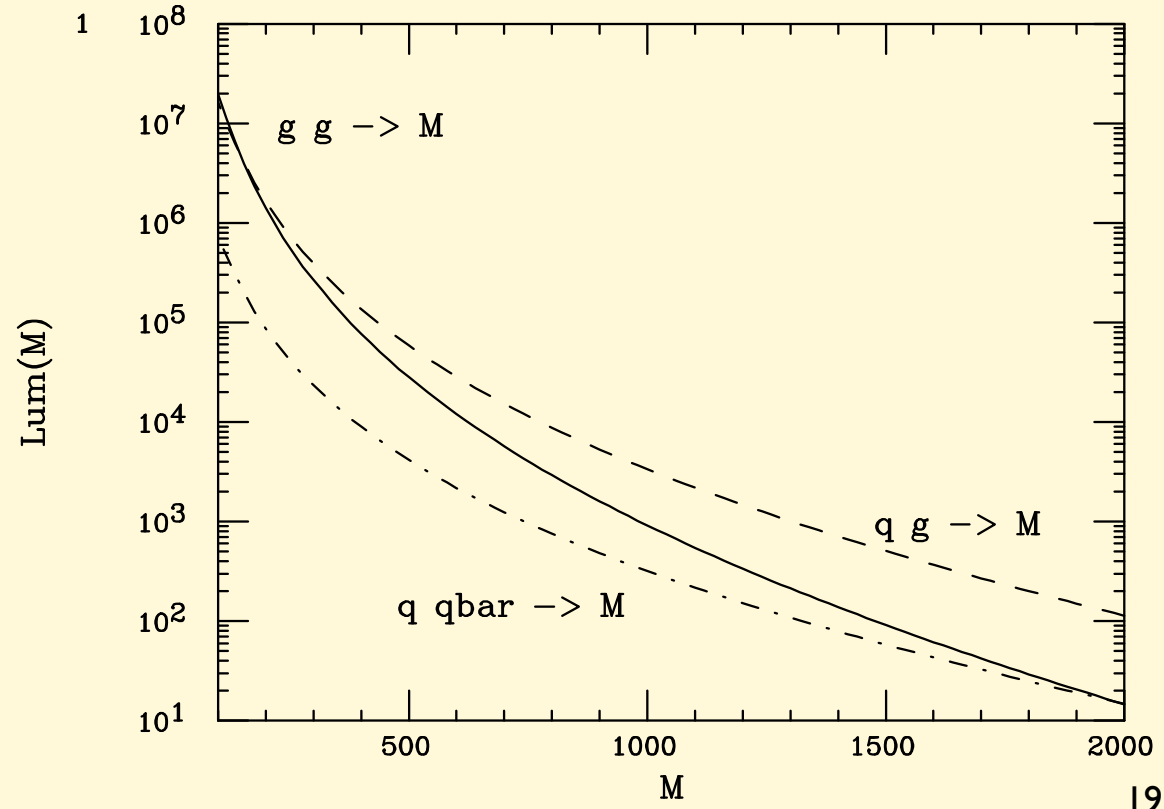
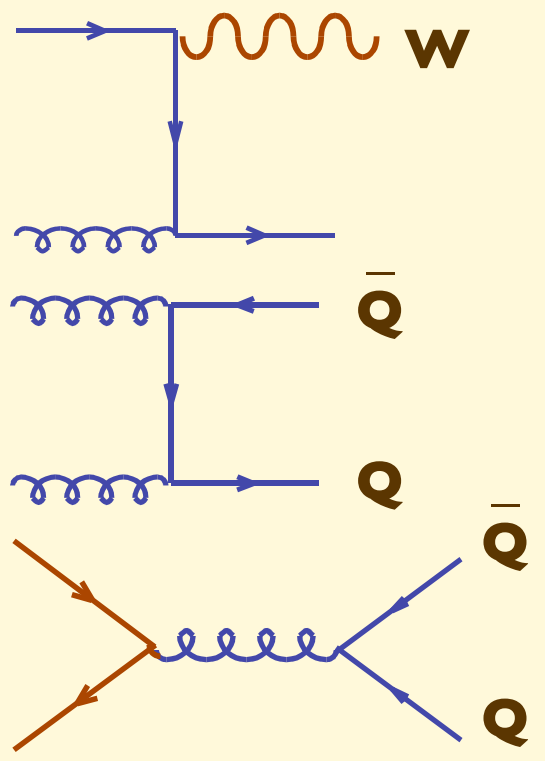
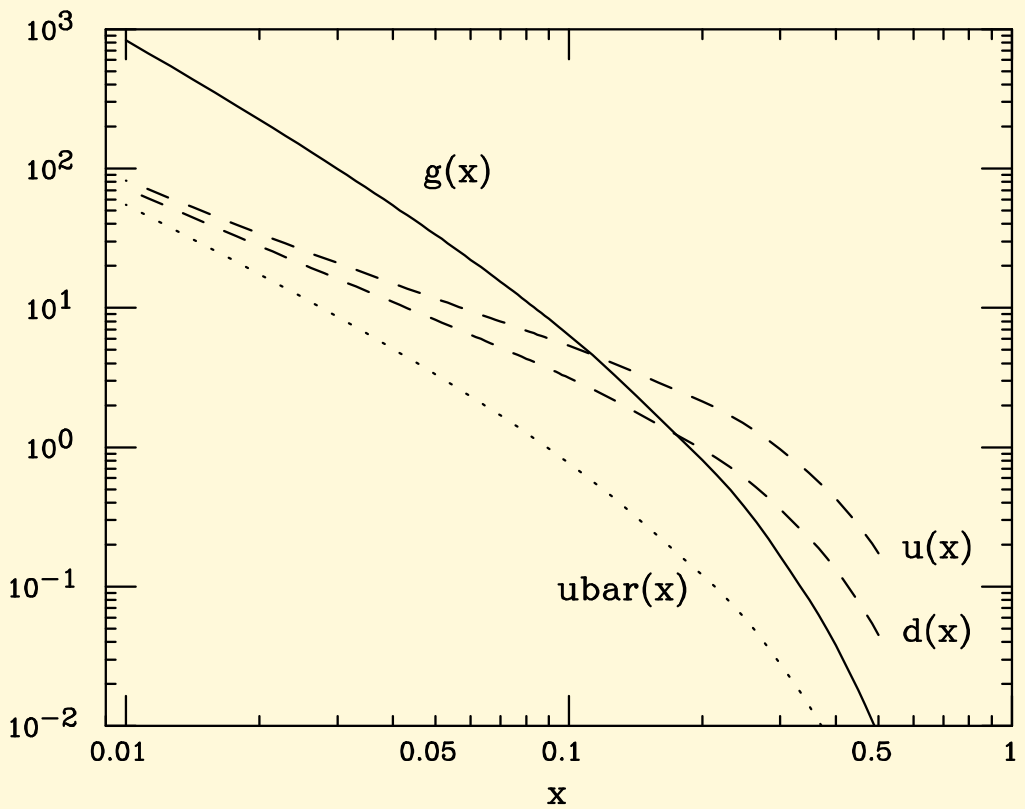
*The global features of the event accompanying the lepton will clearly be very different in each case. Which of the three processes will dominate in a given analysis, will therefore depend on the details

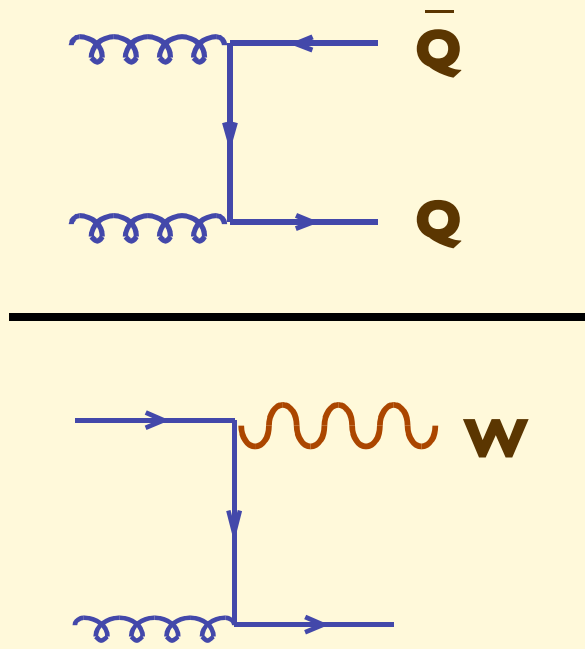
$d\sigma/dpt$ (pb/5 GeV)



How come Q and W spectra are comparable at large Et?

The LO processes for QQ production are weighted by the gg or qqbar luminosity, which drops at large mass much more rapidly than L(qg)





Quark colour charge

Initial state colour averages

$$= \frac{C_F \alpha_s}{1/2 \times \alpha_w} \times \left(\frac{N}{N^2 - 1} \right) \times \frac{1}{1/2} \times F(s \leftrightarrow u) \sim 1/3 \text{ at } 90^\circ$$

Quark weak charge

V-A, only L-handed quarks

$$\approx \frac{\alpha_s}{\alpha_w} \sim 3$$

Dileptons

One lepton W: 160 nb

WW	tt	Z
75pb	500pb	50nb
2l+MET, no jets	2l+MET, jets, b's	2l, m(l)=mZ, no MET, no jets

Dilepton production dominated by top pairs!

Trileptons

WWW	ttW	ZW
130fb	500fb	28pb

$ttW \sim 10^{-3} tt \Rightarrow$ trilepton contribution from tt, with 3rd lepton from $b \rightarrow l$ decay, important \Rightarrow require isolation!

Quadrileptons

WWWW	tttt	ZWWW
0.6fb	12fb	100fb

ZWWW=0.7fb

Ratios

W/Z	WW / WZ	WWW / WWZ	$WWWWW / WWWWZ$
3	2.5	1.3	1

Ratio determined by couplings to quarks, u/d asymmetry of proton

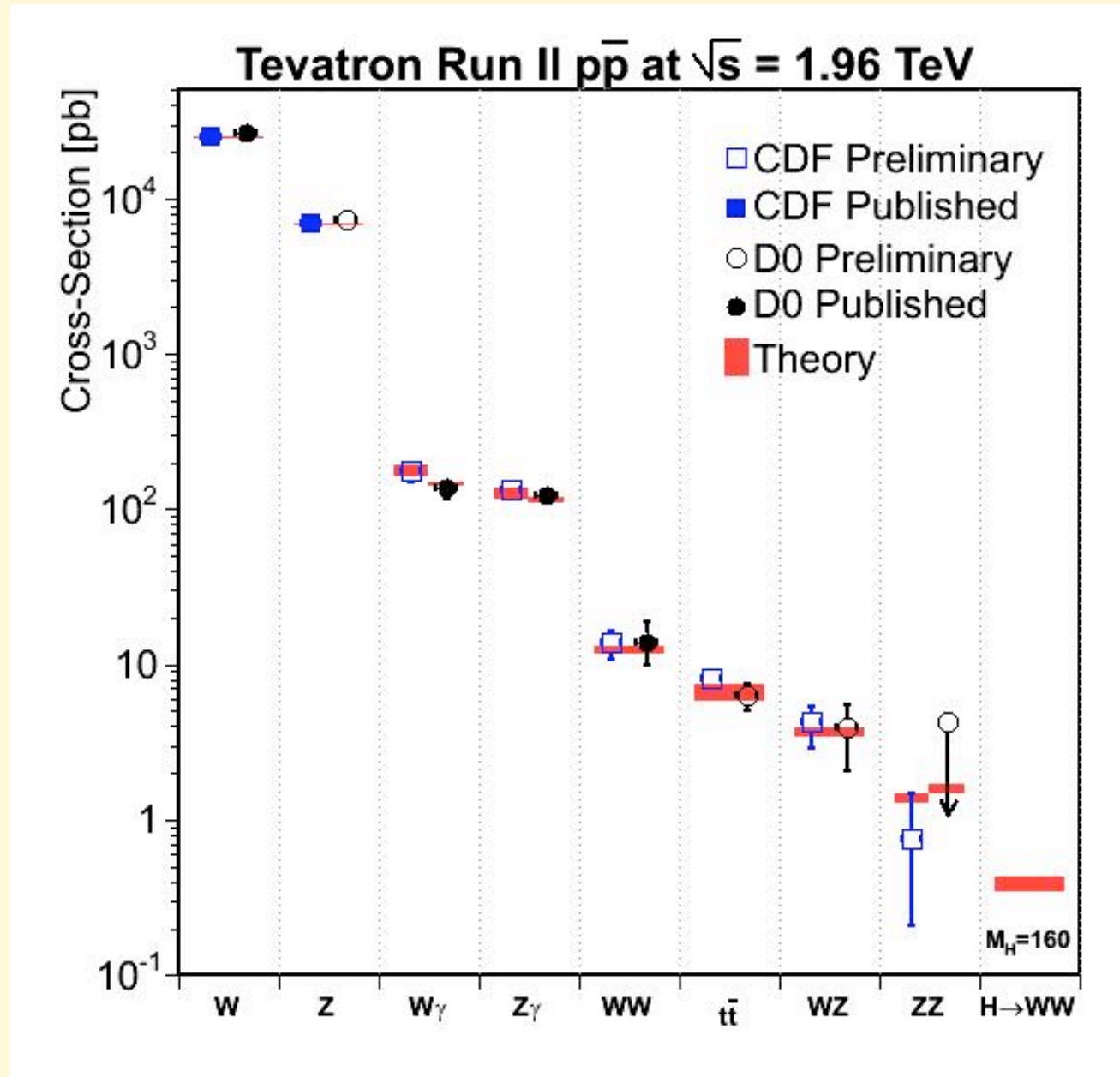


Ratio determined by couplings among W/Z, SU(2) invariance

WW/W	WWW / WW	$WWWWW / WWWW$
5.0E-04	2E-03	5E-03
ZW / W	ZWW / WW	$ZWWW / WWWW$
5.0E-04	4E-03	7E-03

$1W$
 $\sim 10^{-3}$

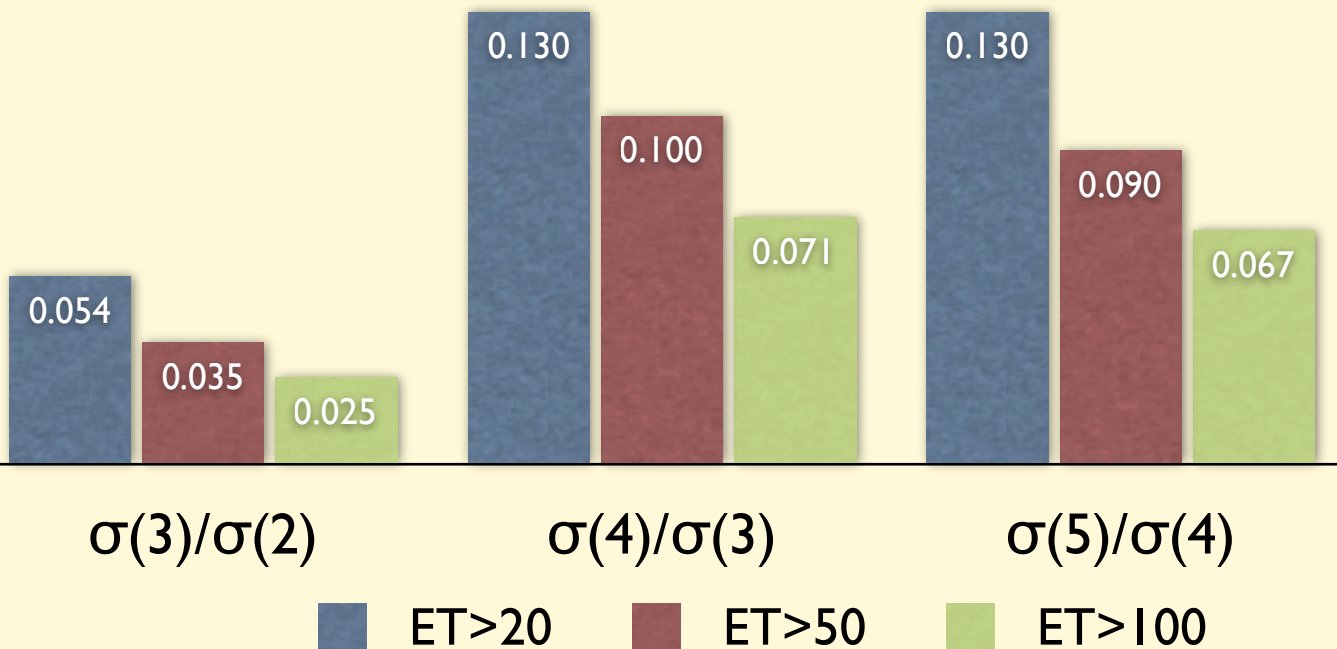
Current expl results on production of gauge bosons at the Tevatron



Some properties of rates for multijet final states

Multijet rates

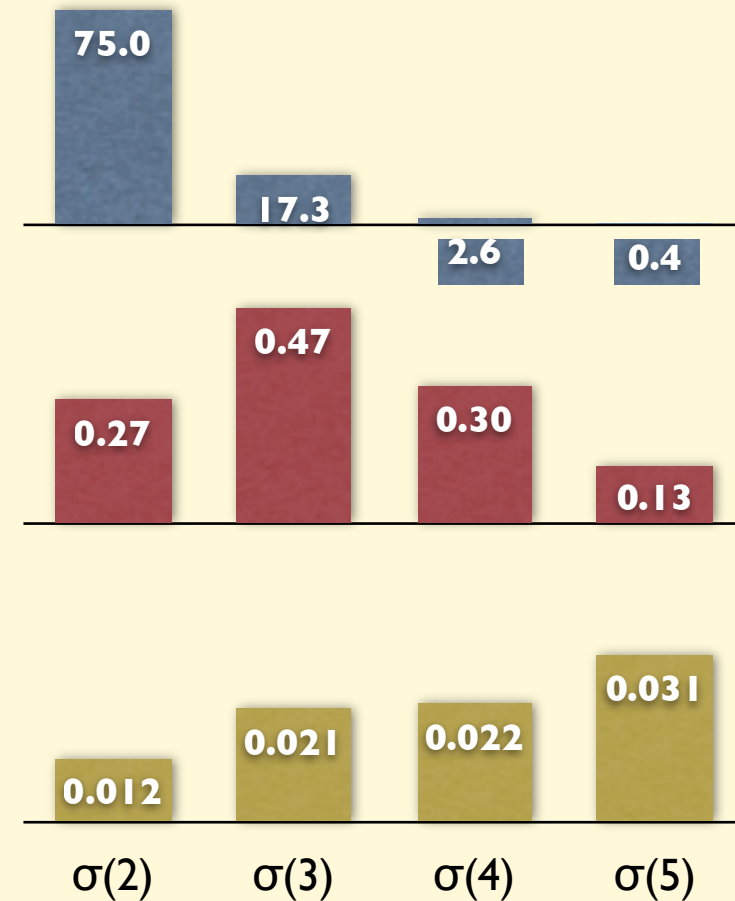
σ [μb]	N jet=2	N jet=3	N jet=4	N jet=5
$E_T^{\text{jet}} > 20 \text{ GeV}$	350	19	2.6	0.35
$E_T^{\text{jet}} > 50 \text{ GeV}$	12.7	0.45	0.045	0.004
$E_T^{\text{jet}} > 100 \text{ GeV}$	0.85	0.021	0.0015	0.0001



- The higher the jet E_T threshold, the harder to emit an extra jet
- When several jets are already present, however, emission of an additional one is less suppressed

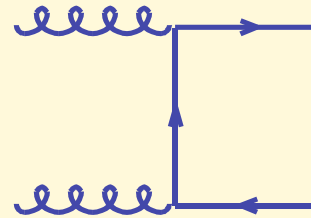
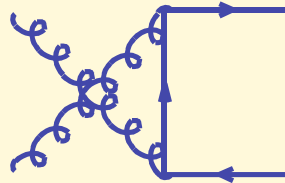
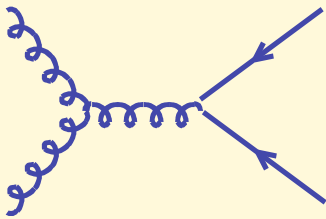
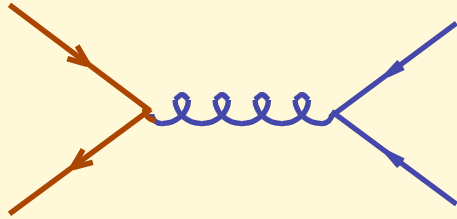
Multijet rates, vs \sqrt{s} , with $E_T^{\text{jet}} > 20 \text{ GeV}$

σ [μb]	N jet=2	N jet=3	N jet=4	N jet=5
$\sqrt{s} > 100 \text{ GeV}$	75	17.3	2.6	0.37
$\sqrt{s} > 500 \text{ GeV}$	0.27	0.47	0.30	0.13
$\sqrt{s} > 1000 \text{ GeV}$	0.012	0.021	0.022	0.031



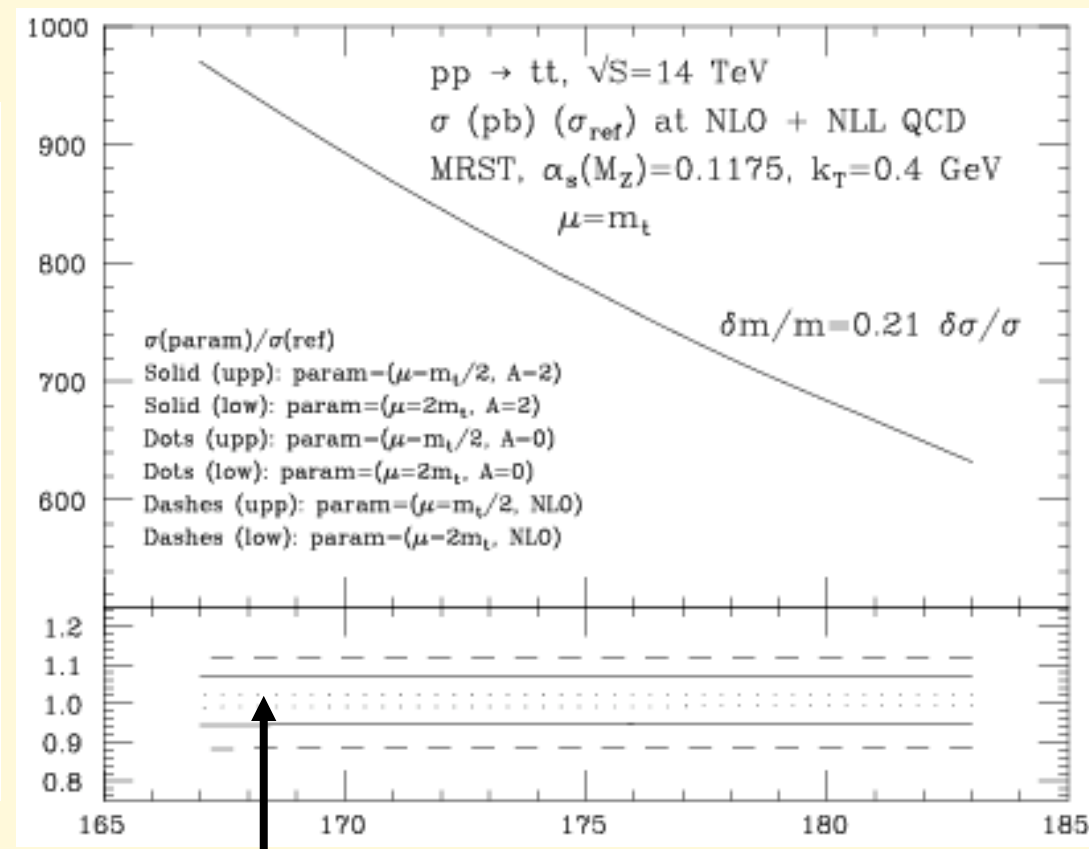
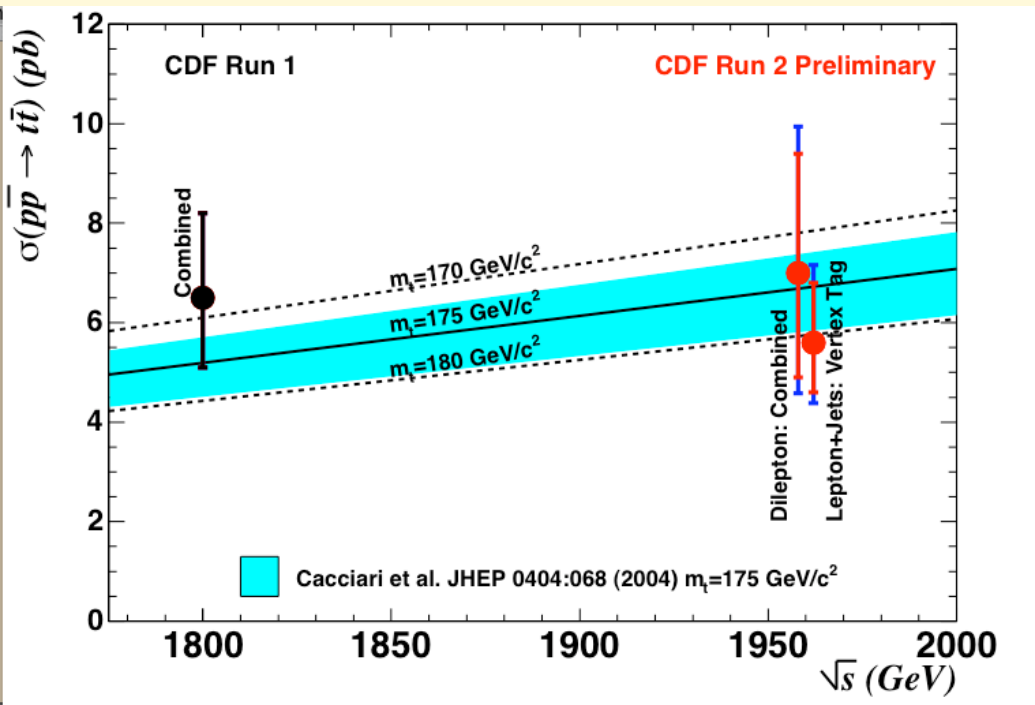
High mass final states are dominated by multijet configurations

Top production and bgs



	$\sigma(tt)$ [pb]	$\sigma(W+X)$	$\sigma(W+bbX)$ [ptb>20 GeV]	$\sigma(W+bbjj X)$ [ptb,ptj >20 GeV]
Tevatron	6	20×10^3	3	0.16
LHC	800	160×10^3	20	16
Increase	$\times 100$	$\times 10$	$\times 10$	$\times 100$

tt cross-section



$$\sigma_{tt}^{\text{FNAL}} = 6.5 \text{ pb } (1 \pm 5\%_{\text{scale}} \pm 7\%_{\text{PDF}})$$

$$\text{Scale unc: } \pm 12\%_{\text{NLO}} \Rightarrow \pm 5\%_{\text{NLO+NLL}}$$

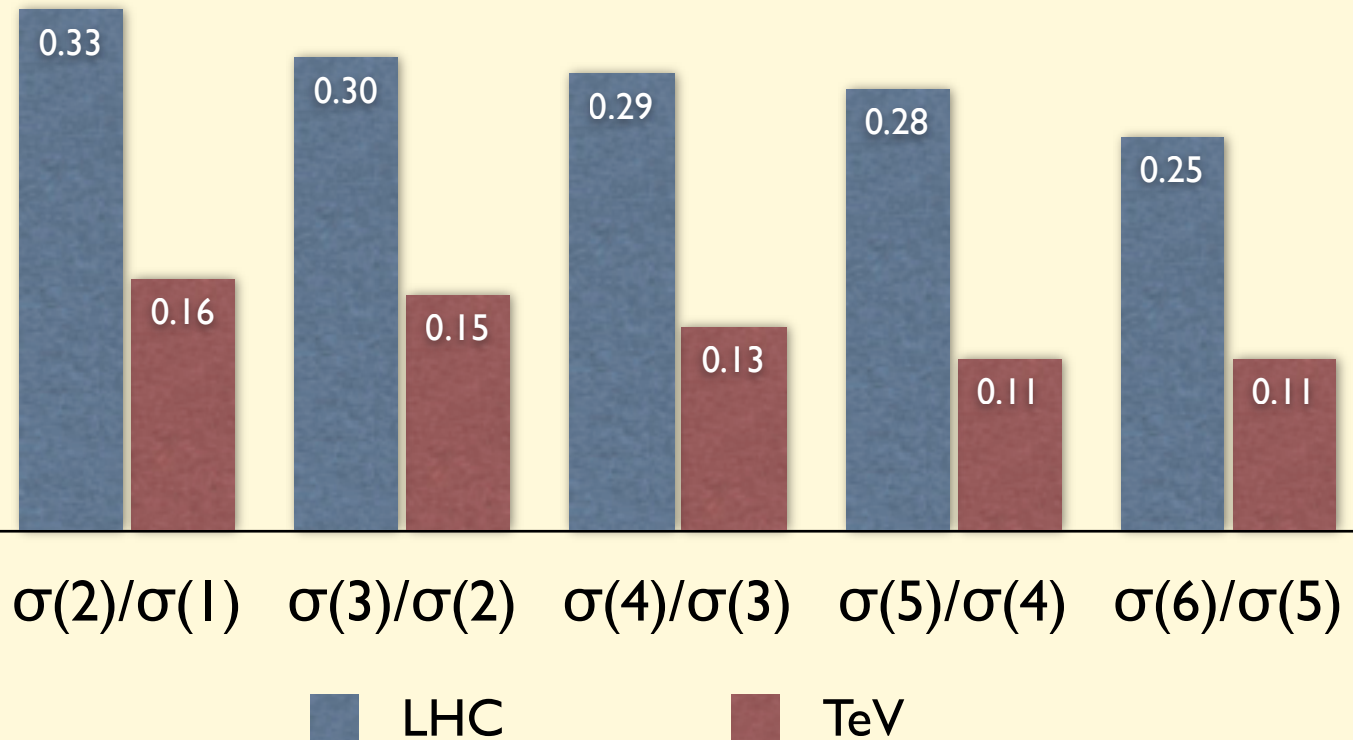
$$\Delta\sigma = \pm 6\% \Rightarrow \Delta m = \pm 2 \text{ GeV}$$

$$\sigma_{tt}^{\text{LHC}} = 840 \text{ pb } (1 \pm 5\%_{\text{scale}} \pm 3\%_{\text{PDF}})$$

W+Multijet rates

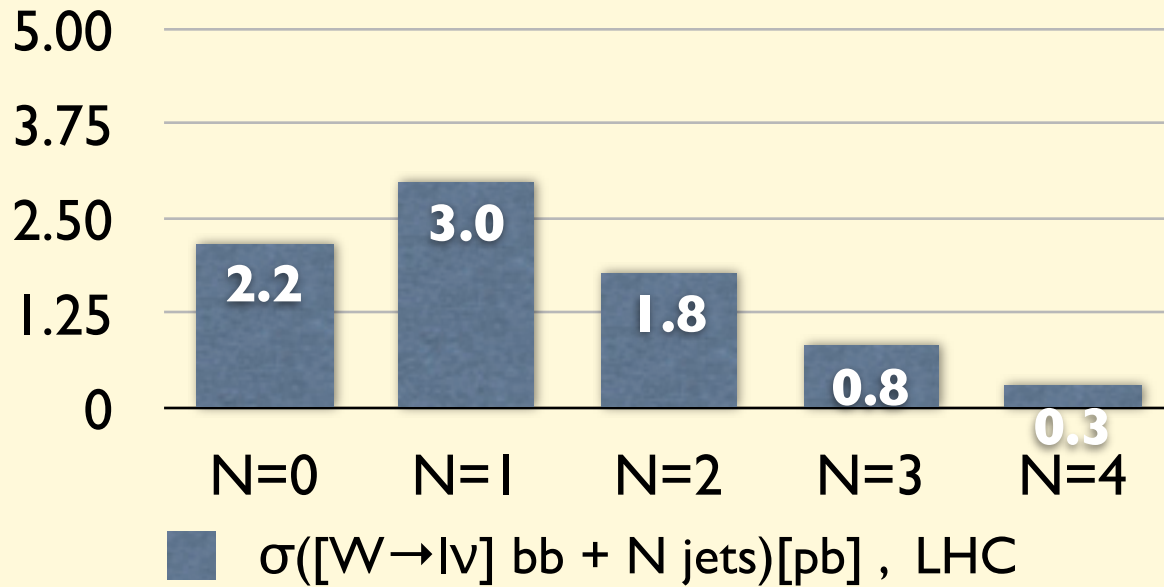
$\sigma \times B(W \rightarrow e\nu)$ [pb]	N jet=1	N jet=2	N jet=3	N jet=4	N jet=5	N jet=6
LHC	3400	1130	340	100	28	7
Tevatron	230	37	5.7	0.75	0.08	0.009

$E_T(\text{jets}) > 20 \text{ GeV}$, $|\eta| < 2.5$, $\Delta R > 0.7$



- Ratios almost constant over a large range of multiplicities
- $O(\alpha_s)$ at Tevatron, but much bigger at LHC

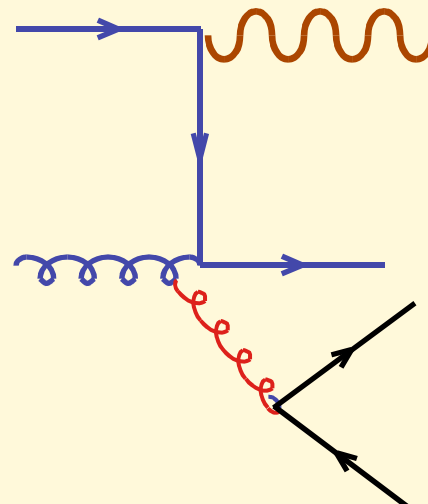
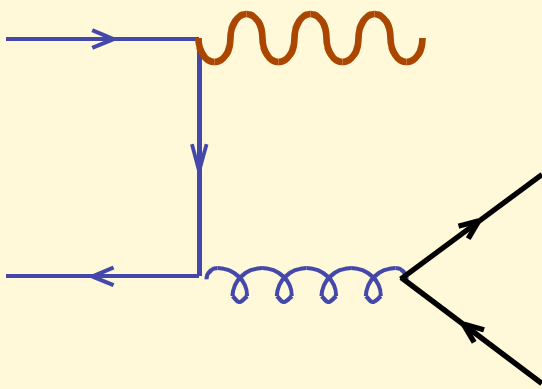
Wbb+jets rates



Pattern of multiplicity distribution very different than in W+jets!

In pp collisions (contrary to the Tevatron, p-pbar) :

$$N_{\text{jet}}=0 \propto \alpha_s^2 \times \text{Lum}(q \text{ qbar}) \approx N_{\text{jet}}=1 \propto \alpha_s^3 \times \text{Lum}(q \text{ g})$$



Beware of naive α_s power counting!!

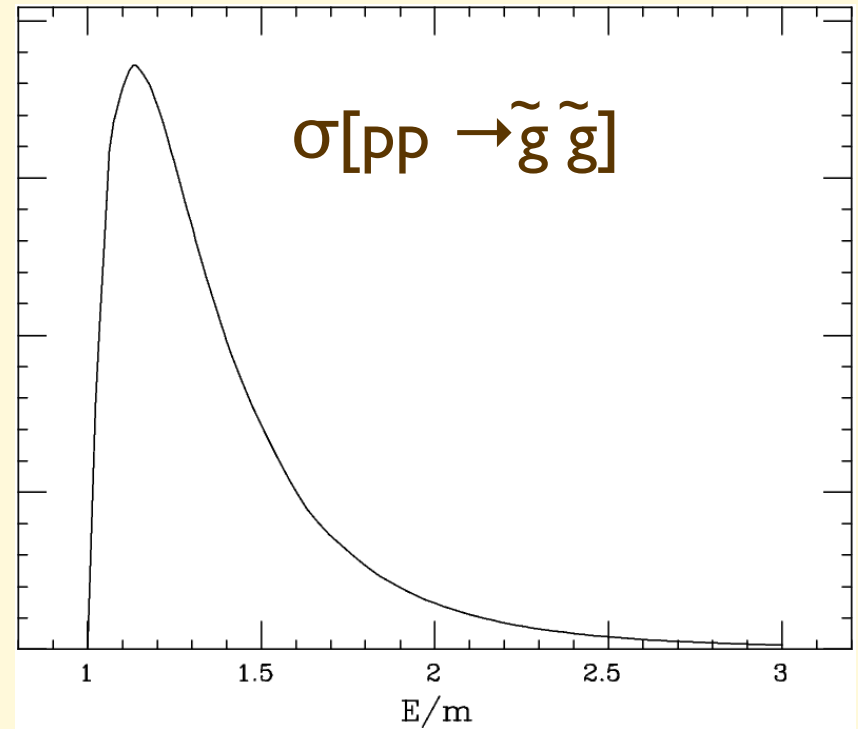
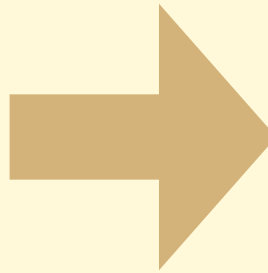
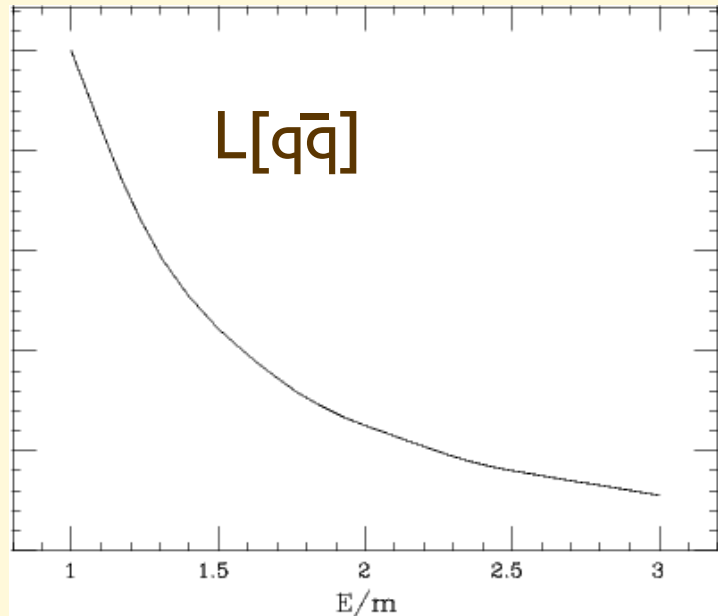
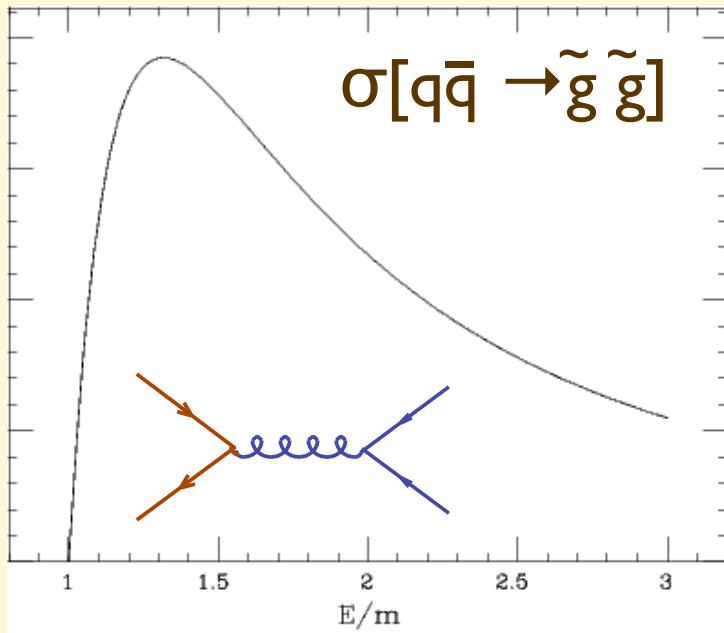
Introduction to hadronic collisions: theoretical concepts and practical tools for the LHC

Lecture 5

Michelangelo L. Mangano

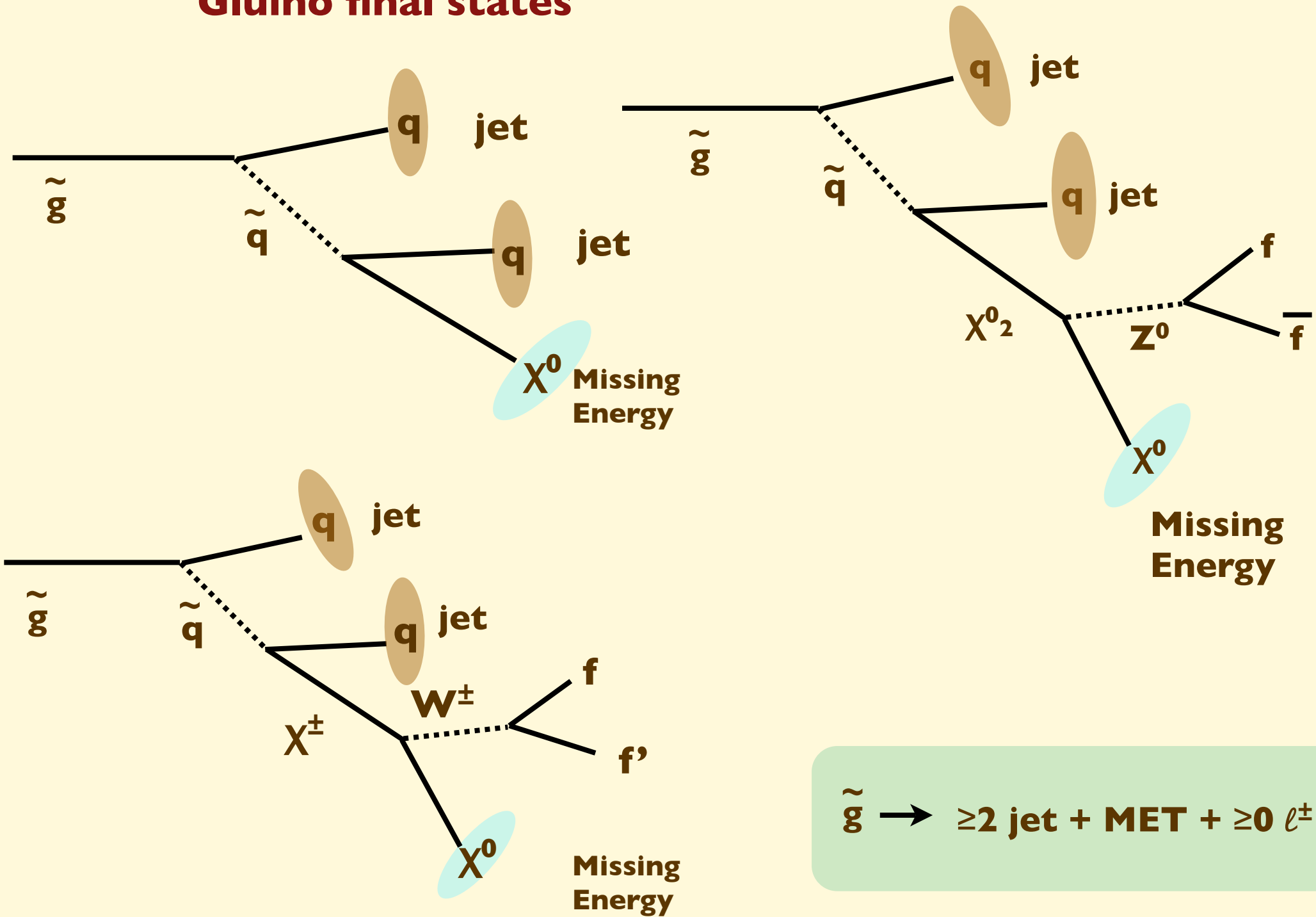
TH Unit, Physics Dept, CERN
michelangelo.mangano@cern.ch

Ex: Gluino pair production

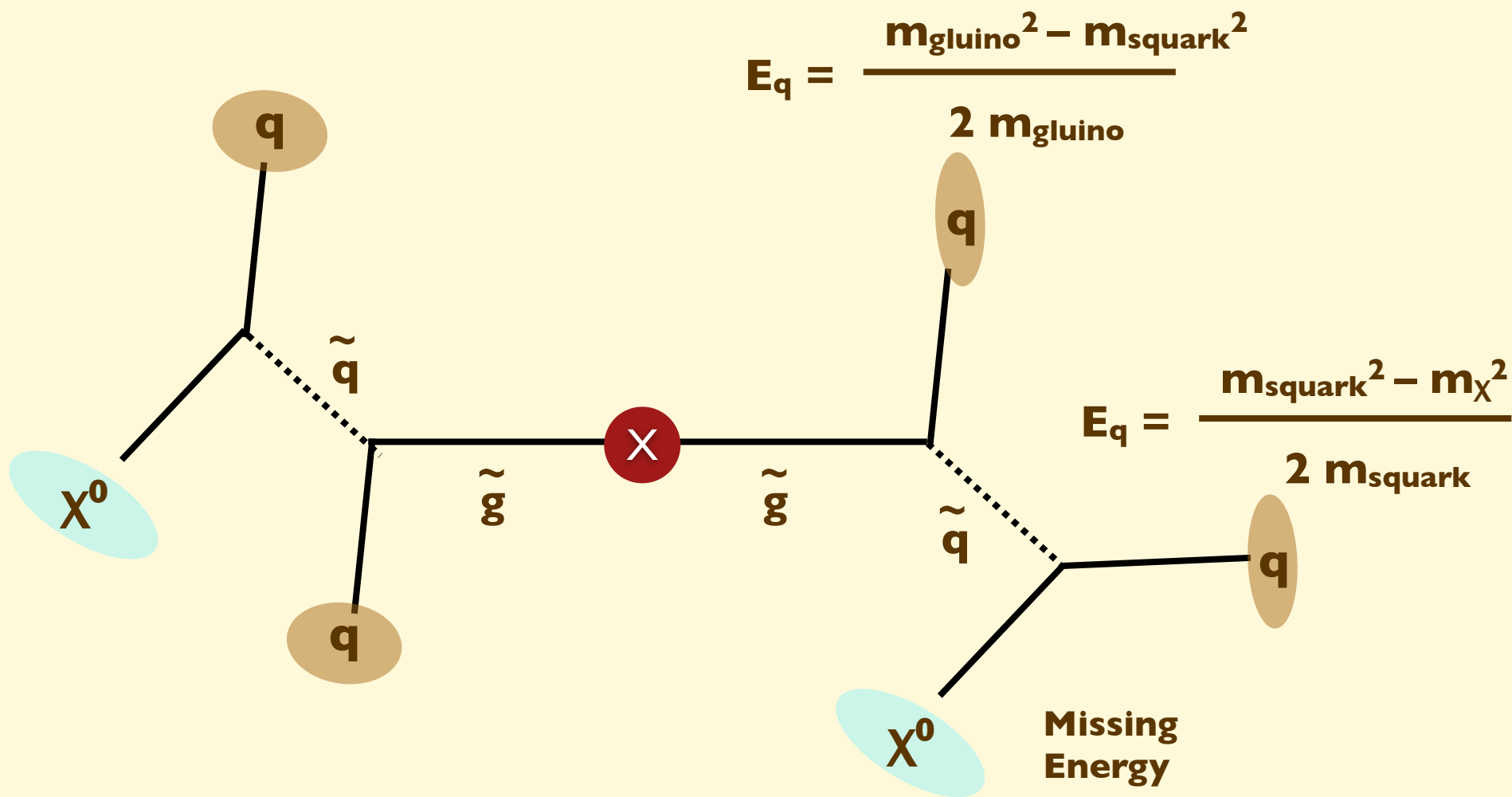


\Rightarrow slow gluinos, $\beta \sim 0.5$

Glauino final states



$\tilde{g} \tilde{g} \rightarrow 4 \text{ jet} + \text{MET}$



Widely-spaced jets, no significant hierarchy in transverse energies and missing E_T

Typical analysis cuts (ATLAS):

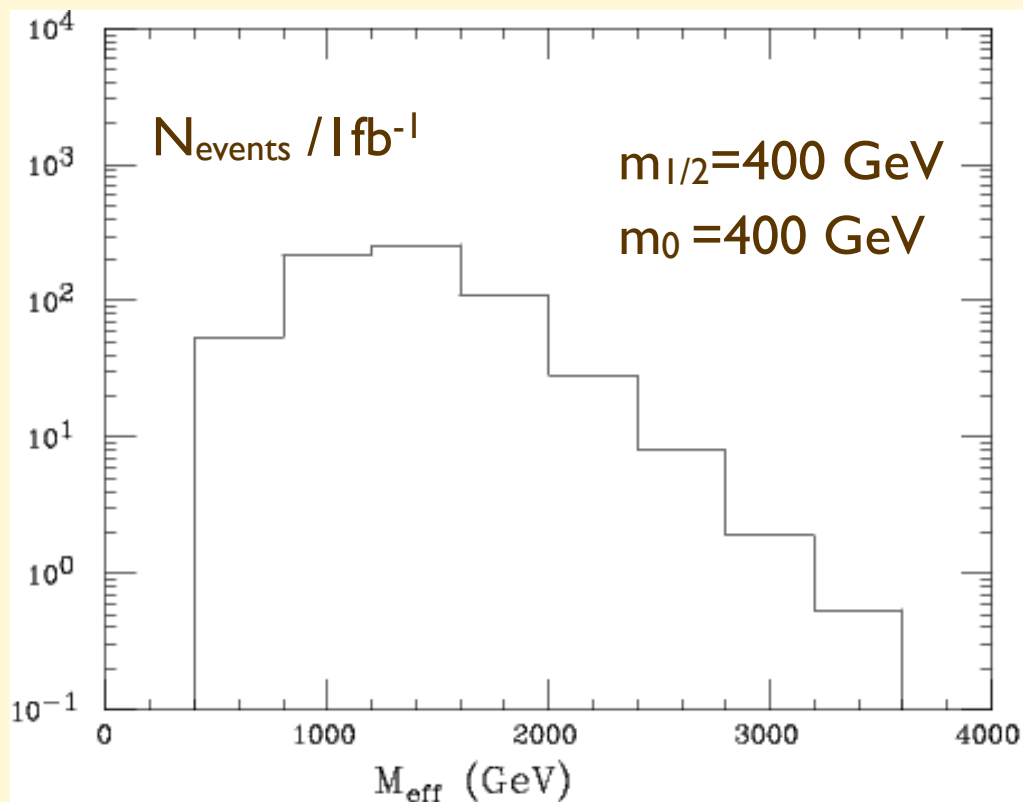
≥ 4 jets, $E_T > 50$ GeV leading jet $E_T > 100$ GeV

no lepton with $E_T > 20$ GeV

MissET > max(100, 0.2 M_{eff})

$$M_{\text{eff}} = \text{MET} + \sum_{i=1, \dots, 4} E_T^i$$

Transverse sphericity > 0.2



SM Backgrounds

Missing energy $\Rightarrow \nu_s \Rightarrow W/Z$ production

“Irreducible”: individual events cannot be distinguished from the signal

Z+4jets, Z $\rightarrow \nu\nu$

“Reducible”: individual events feature properties which distinguish them from the signal, but these can only be exploited with limited efficiency

W+3jets, W $\rightarrow \tau\nu$, $\tau \rightarrow$ hadrons (jet)

τ jet has low multiplicity, and originates from a displaced vertex, because of τ 's lifetime

W+4jets, W $\rightarrow e/\mu \nu$, lepton undetected

e/μ can be detected, but cannot be vetoed with 100% efficiency, else the signal would be killed as well (e/μ may come from π conversions or decays)

$t\bar{t} \rightarrow W$ +jets, with W \rightarrow leptons as above

In addition to the above, top decays have b's, but these cannot be detected and vetoed with 100% efficiency

“Instrumental”: individual events resemble the signal because of instrumental “effects” (namely instrumental deficiencies)

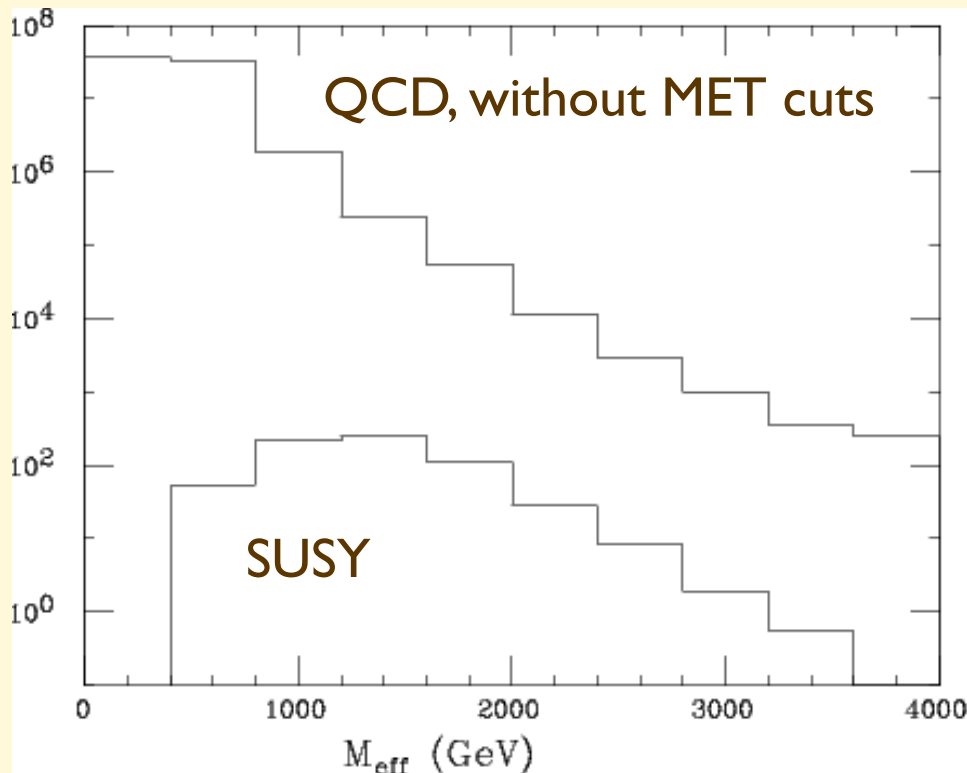
Multijets

The missing ET may originate from several sources:

Mismeasurement of the energy of individual jets

Incomplete coverage in rapidity (forward jets undetected)

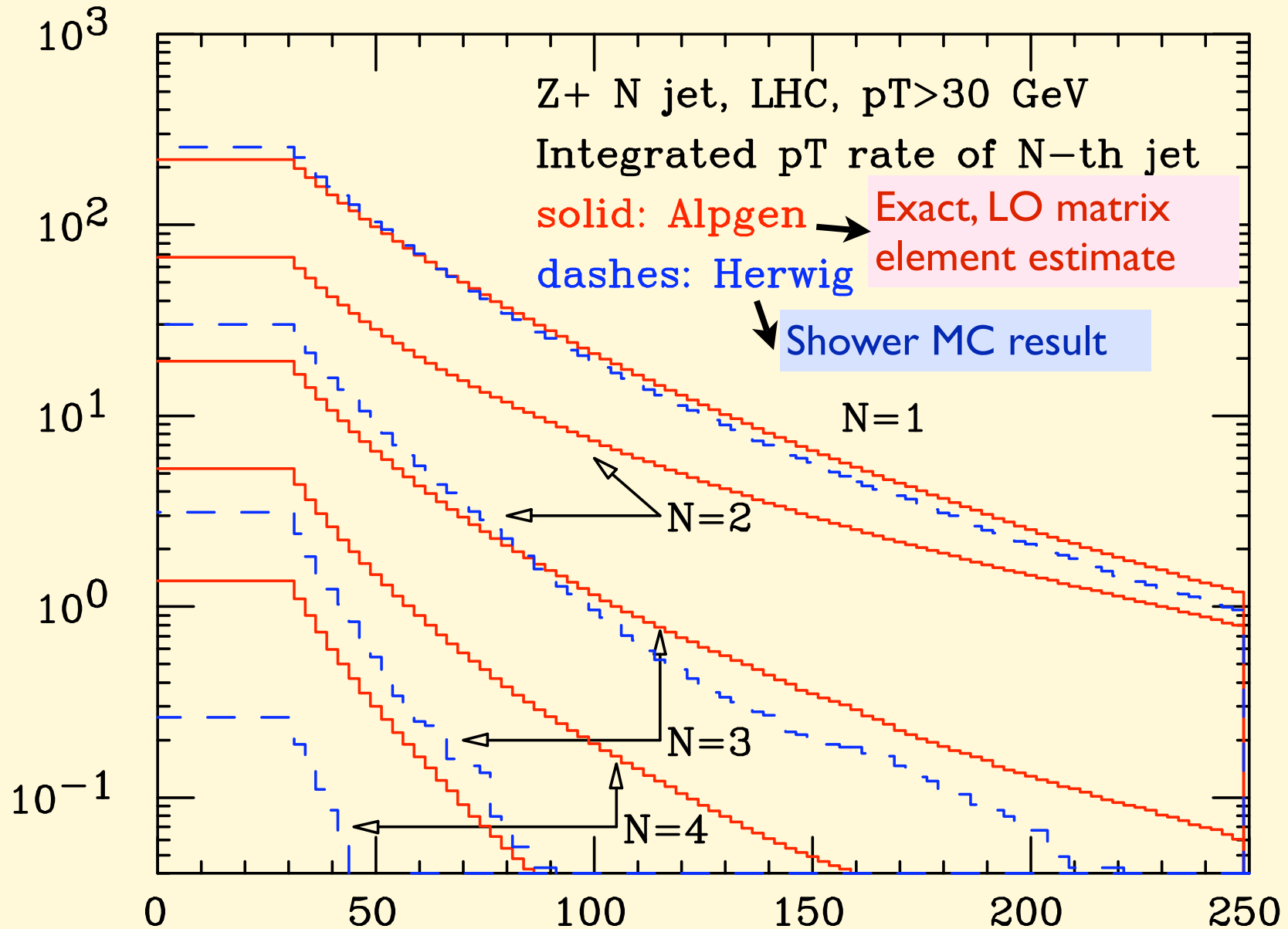
Accidental extra deposits of energy (cosmic rays on time, beam backgrounds, , electronic noise, etc.etc.etc.)



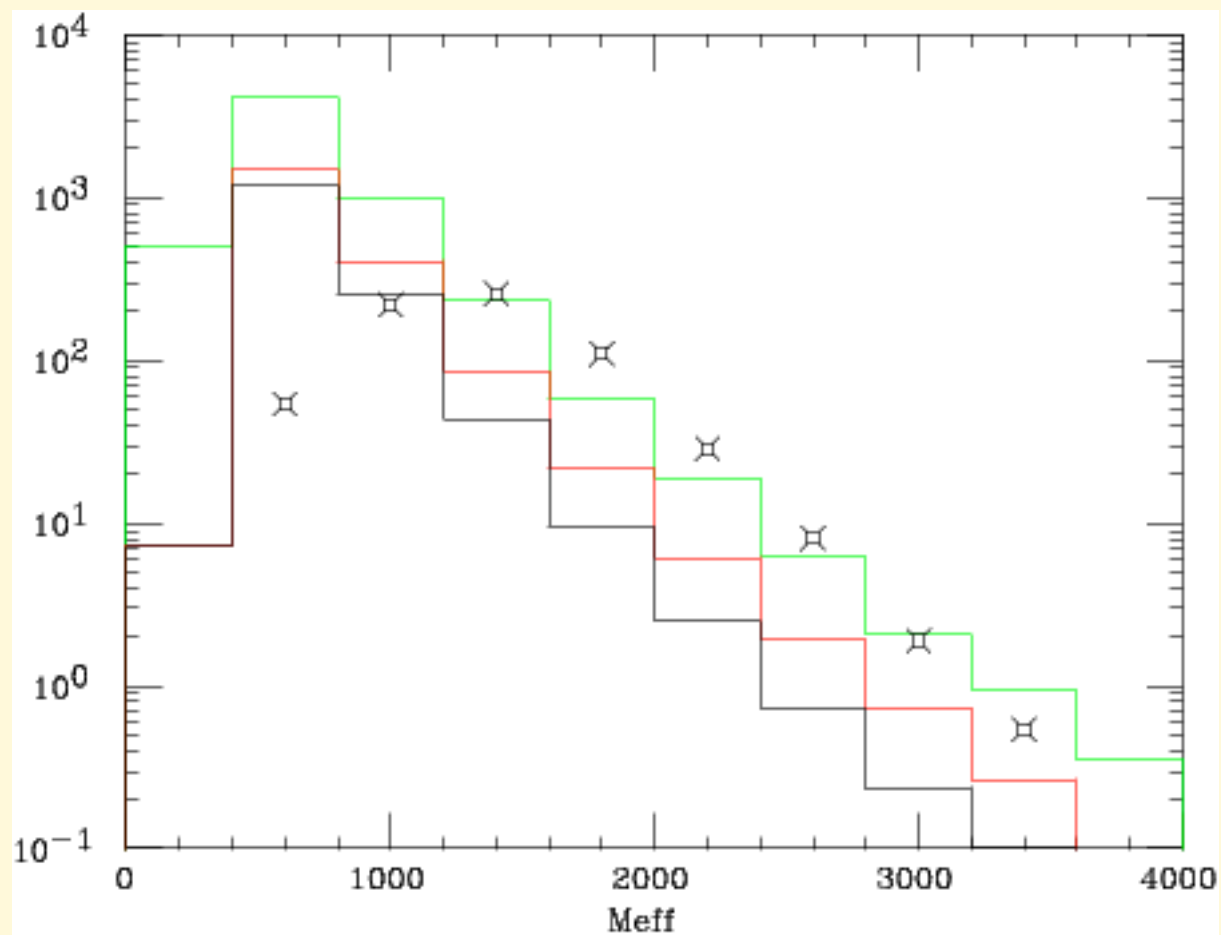
It is sufficient that these effects leave a permille fraction of the QCD rate for the signal to be washed away!

Z(\rightarrow vv) + jets

I. Shower MC vs Matrix element results



$Z(\rightarrow \nu\nu) + \text{jets}$



- Jet cuts only
- + MET cut
- + ST cut
- ⊗ SUSY

Normalizing the bg rate using data ...

Use $Z \rightarrow ee$ + multijets, apply same cuts as MET analysis but replace MET with $ET(e^+e^-)$

Extract $Z \rightarrow \nu\nu$ bg using, bin-by-bin:

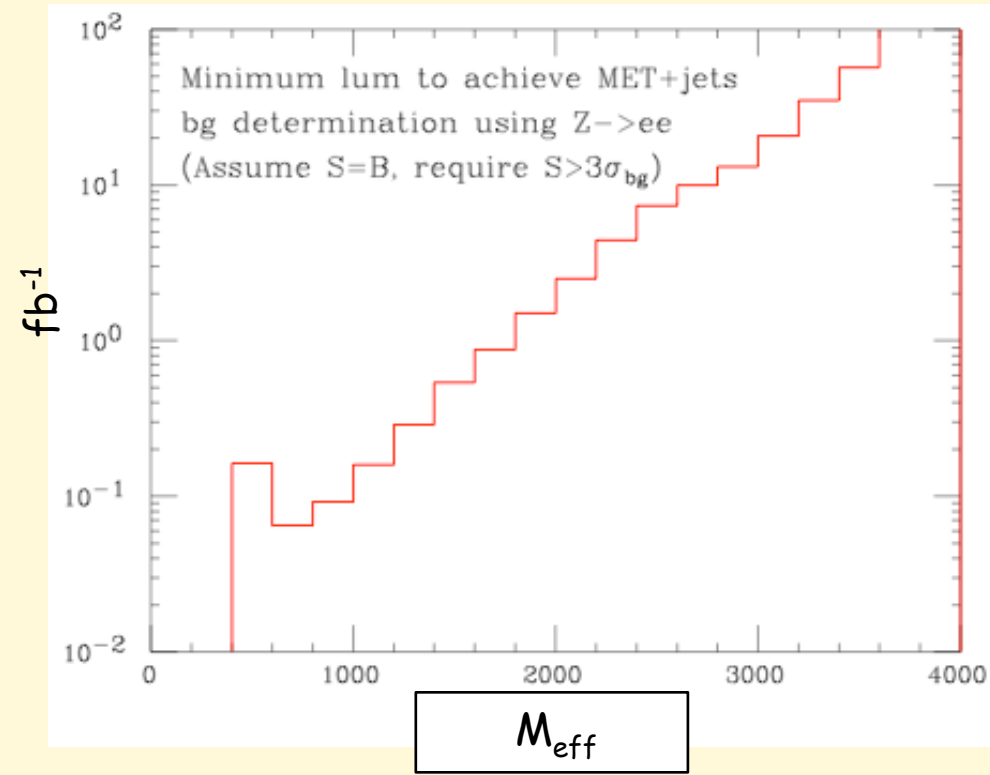
$$(Z \rightarrow \nu\nu) = (Z \rightarrow ee) B(Z \rightarrow \nu\nu)/B(Z \rightarrow ee)$$

Assume that the SUSY signal is of the same size as the bg, and evaluate the luminosity required to determine the $Z \rightarrow \nu\nu$ bg with an accuracy such that:

$$N_{\text{susy}} > 3 \text{ sigma}$$

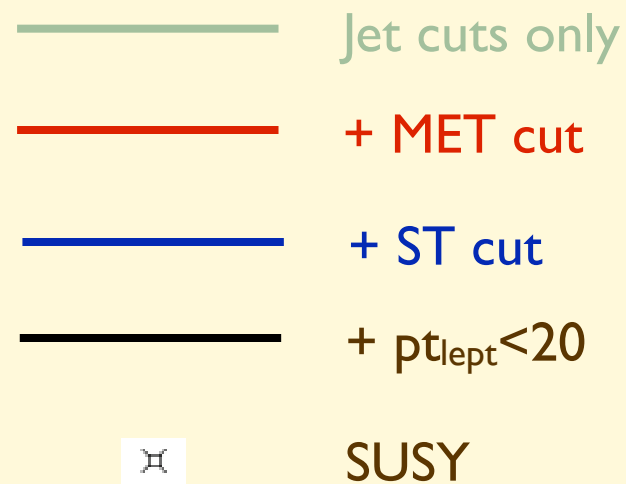
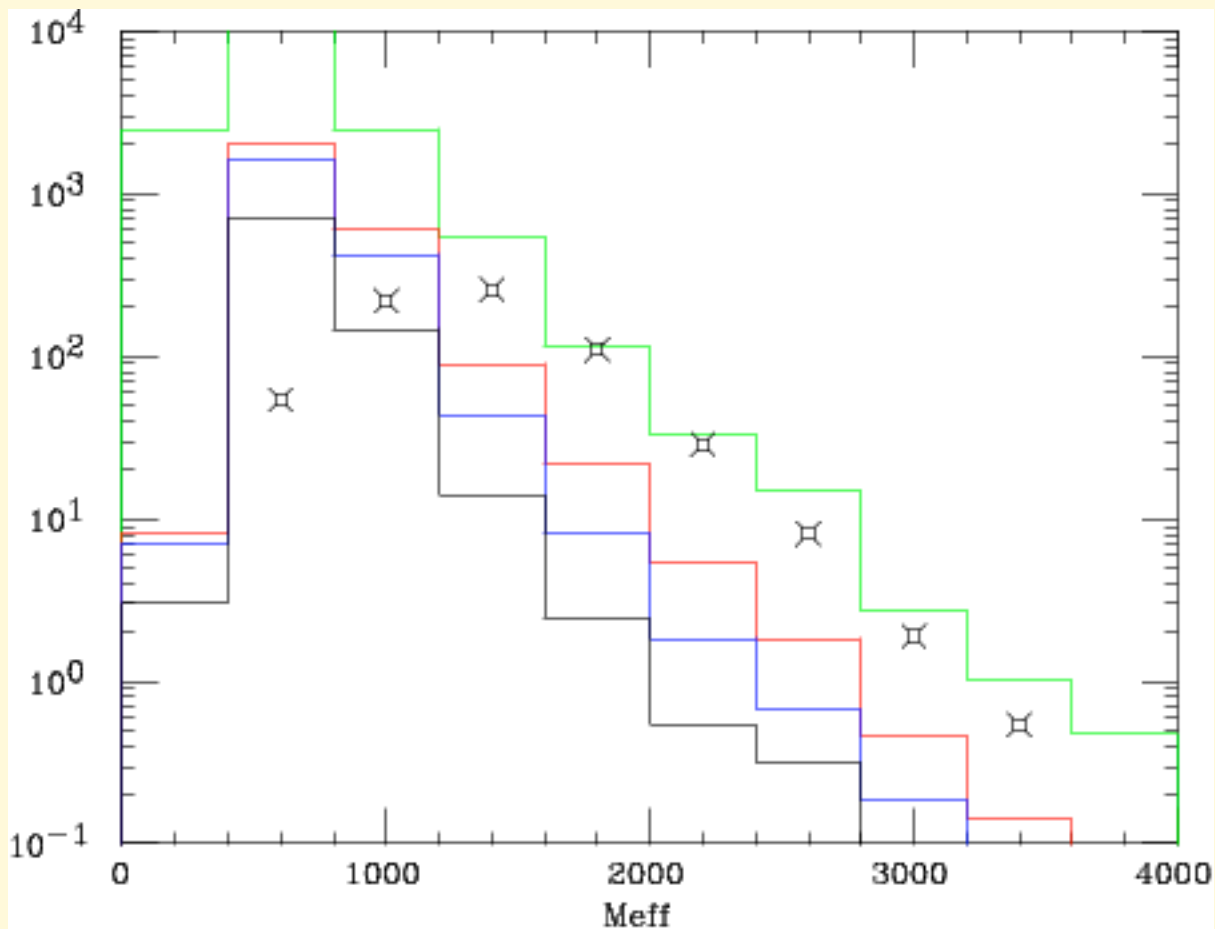
where

$$\text{sigma} = \sqrt{N(Z \rightarrow ee)} * B(Z \rightarrow \nu\nu)/B(Z \rightarrow ee)$$

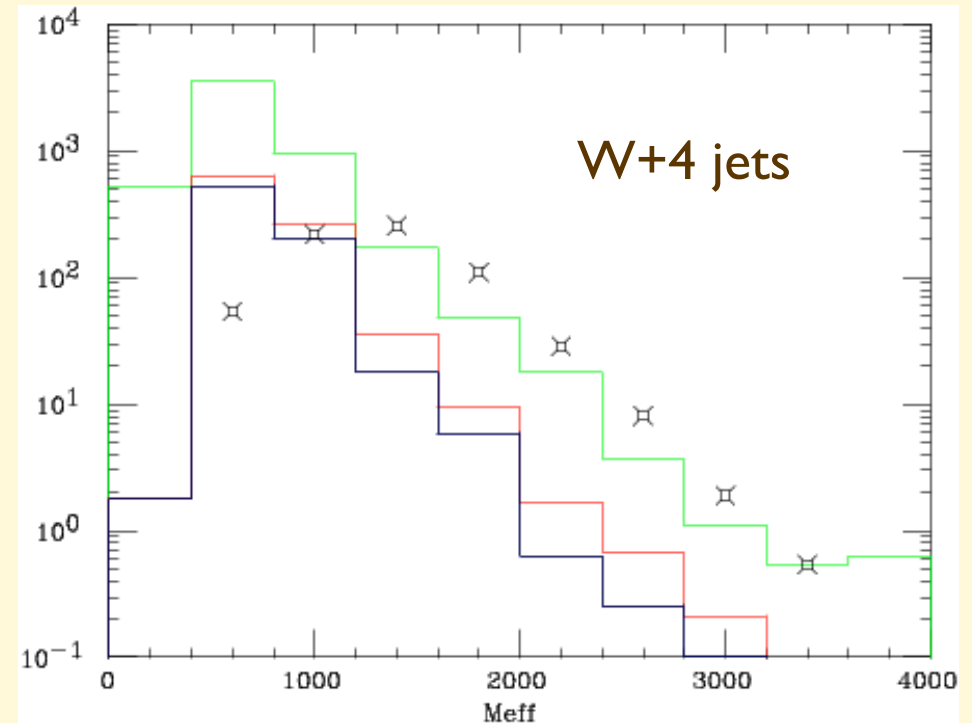
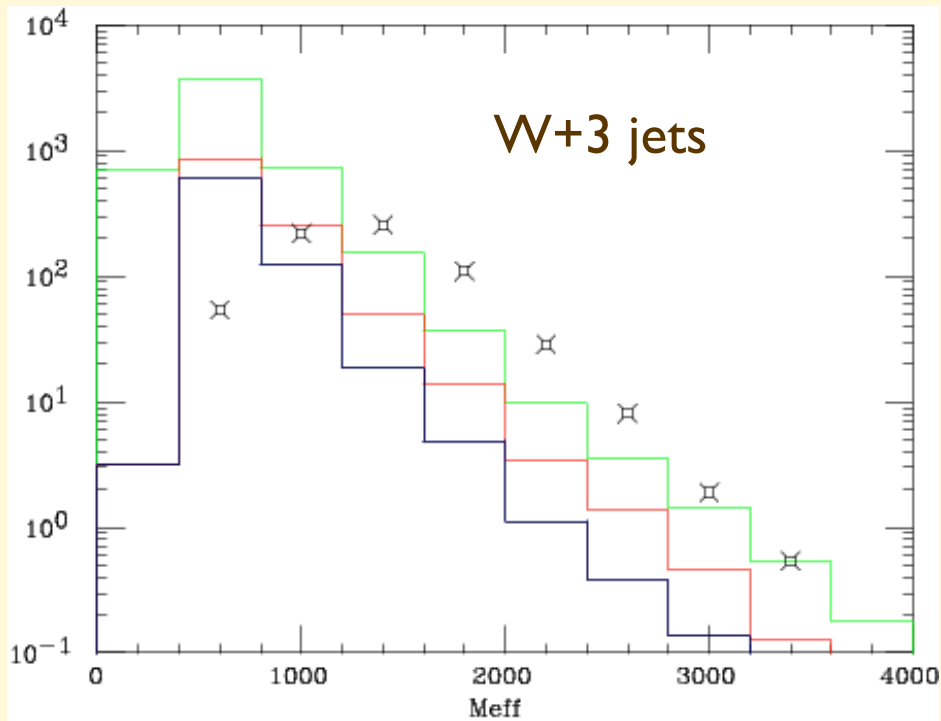







=> several hundred pb^{-1} are required. They are sufficient if we believe in the MC shape (and only need to fix the overall normalization). Much more is needed if we want to keep the search completely MC independent

$W(\rightarrow lv) + 4 \text{ jets}$

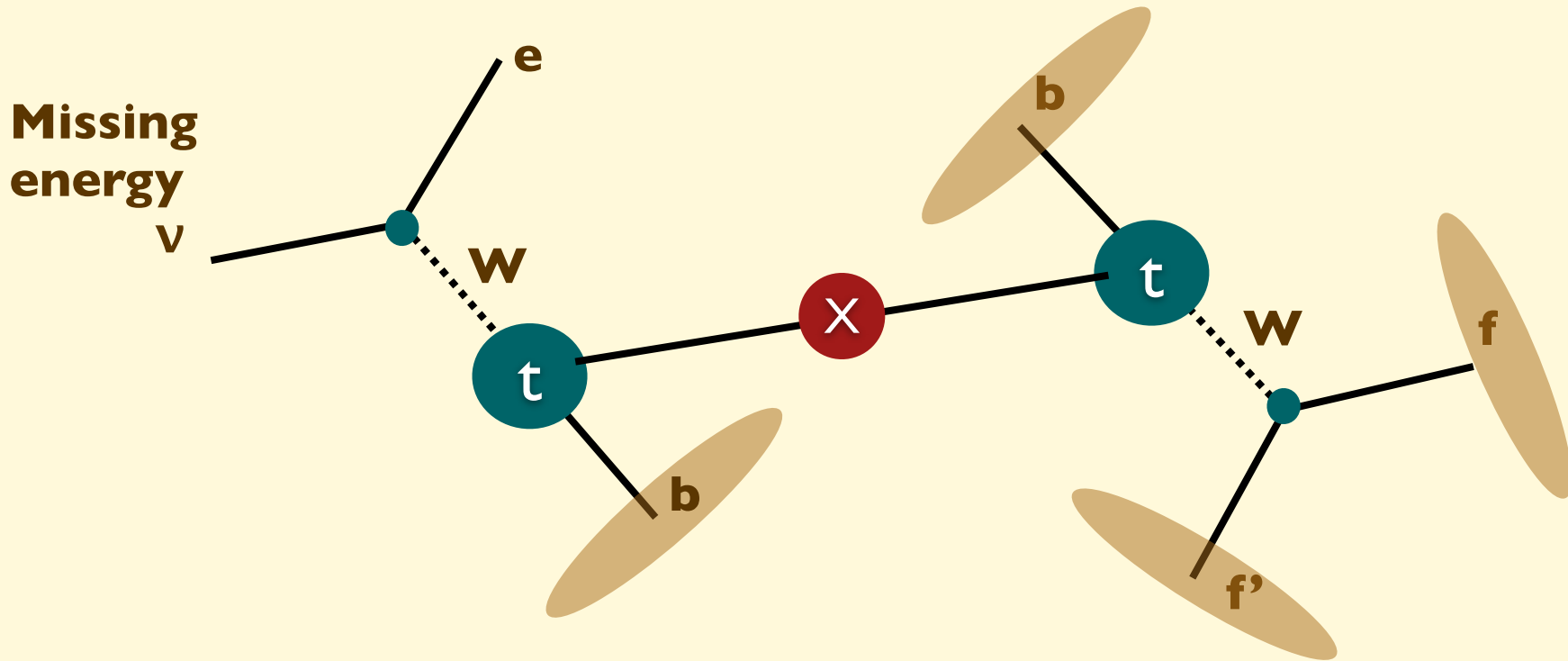


$W(\rightarrow \text{tau-jet } \nu) + \text{jets}$

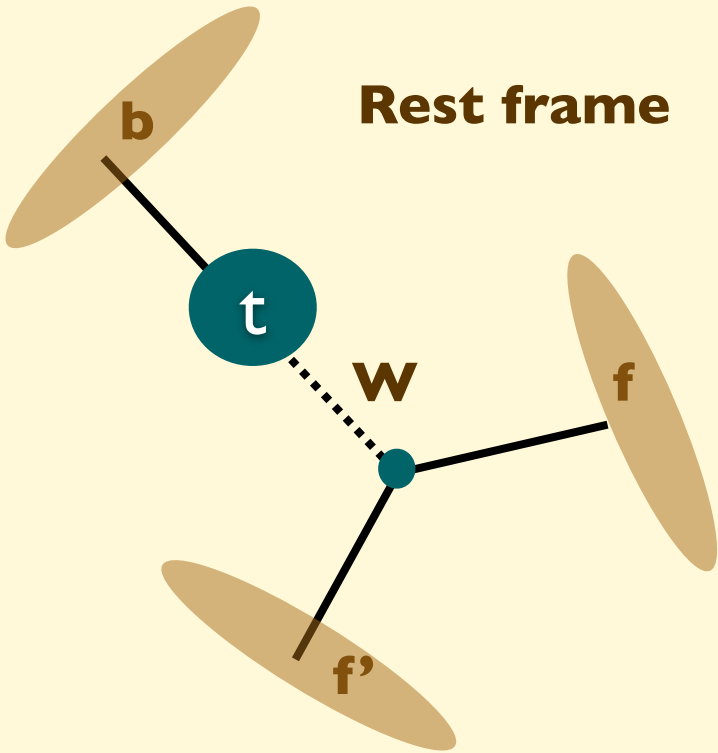


-  Jet cuts only
-  + MET cut
-  + ST cut
-  + $p_{T\text{lept}} < 20$
-  SUSY

Top final states



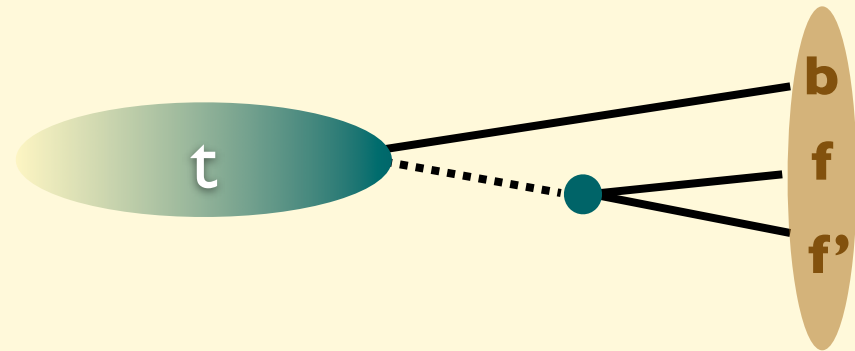
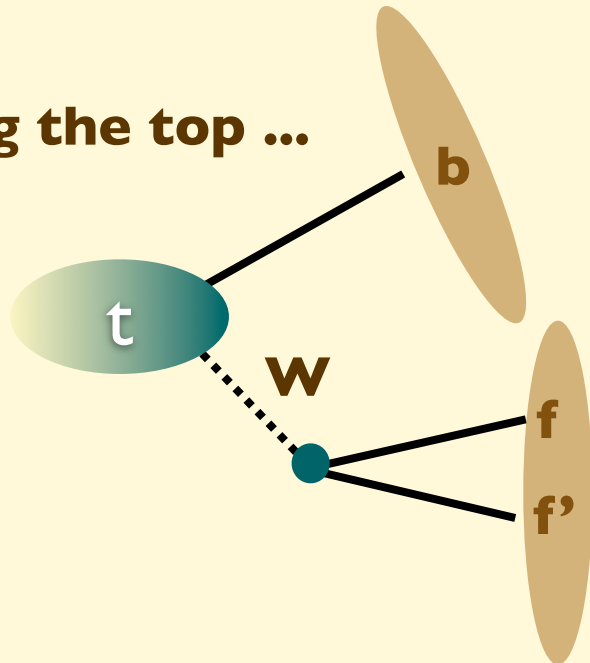
Top final states



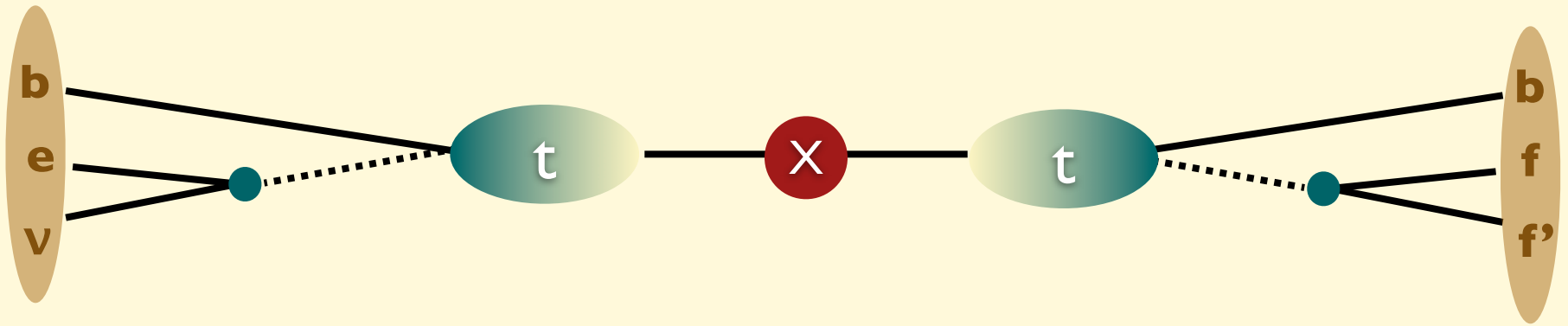
$$p_b = \frac{m_{\text{top}}^2 - m_W^2}{2 m_{\text{top}}}$$

$$p_f^{\text{max}} = \frac{m_W}{2} \frac{m_{\text{top}}^2 + m_W^2}{2 m_{\text{top}} m_W}$$

Boosting the top ...

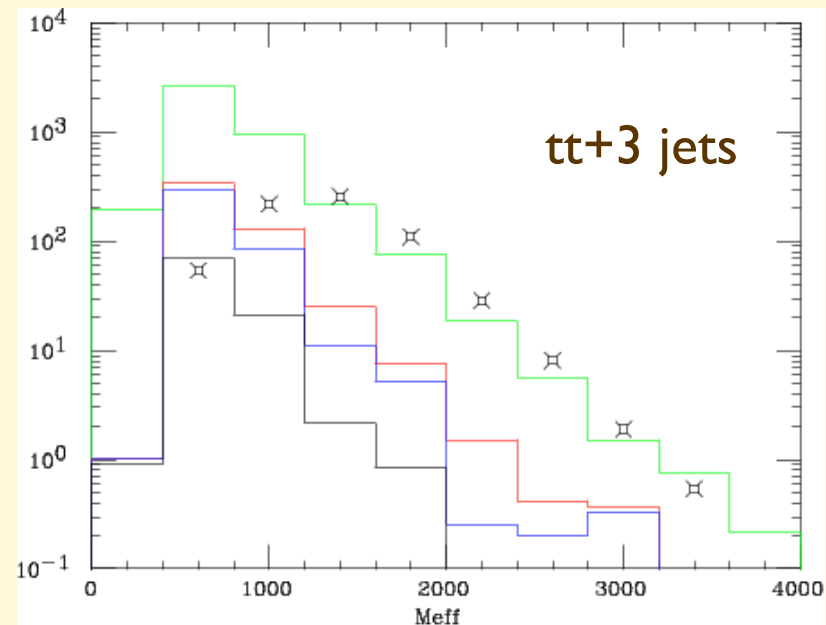
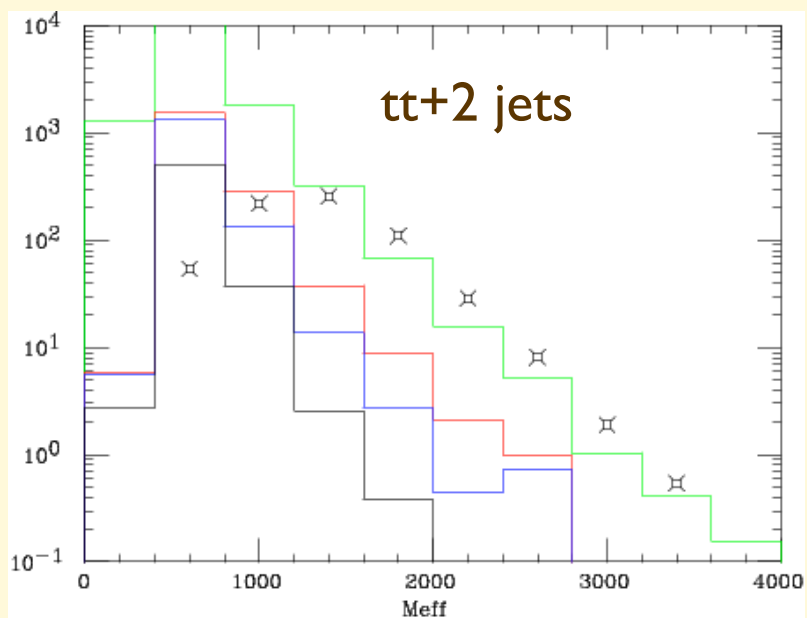
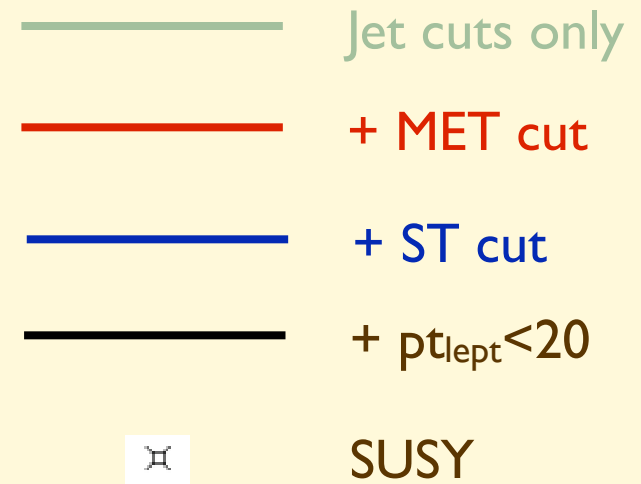
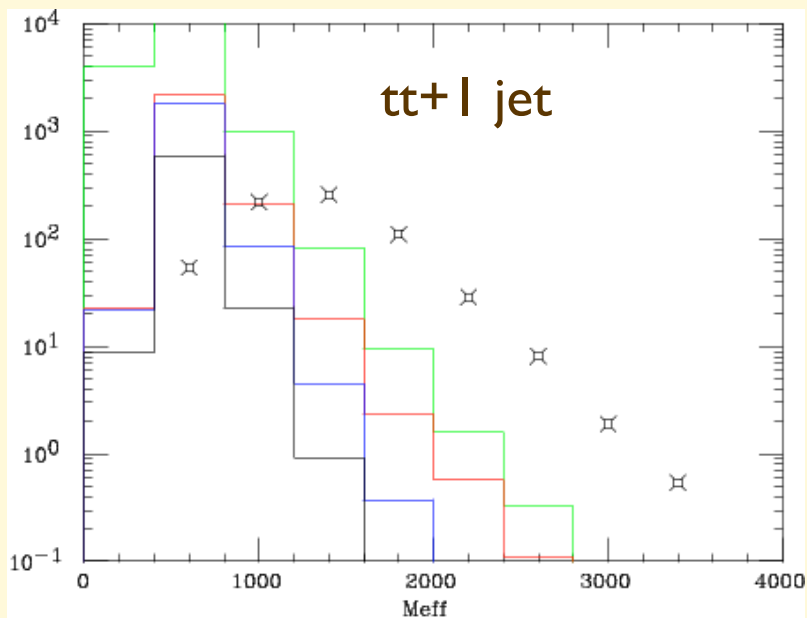


Top final states



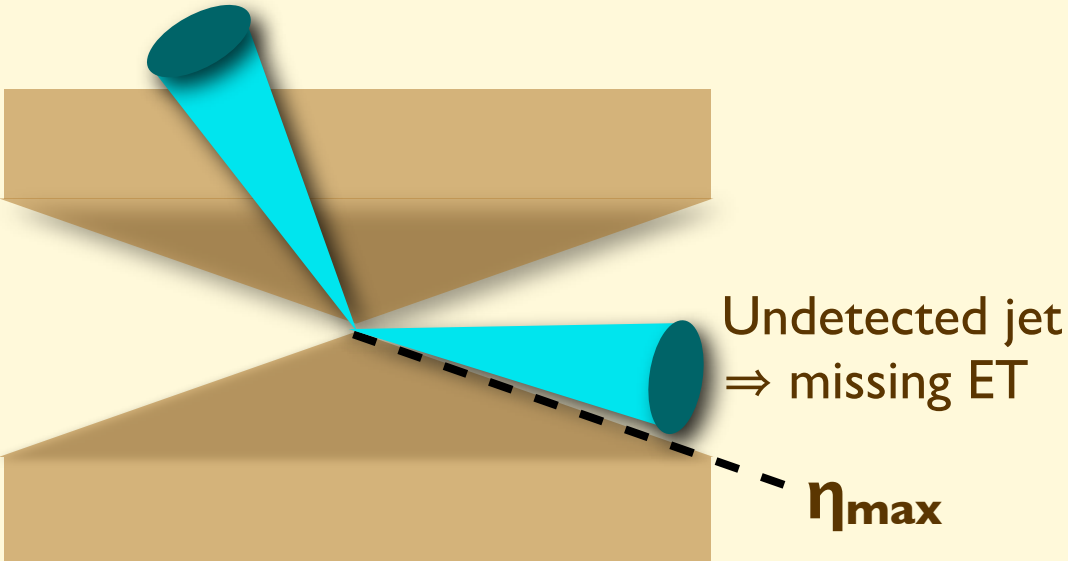
Large M_{eff} leads to highly collimated final states

Sphericity and multi-jet cuts very effective against the leading-order t - \bar{t} contribution!

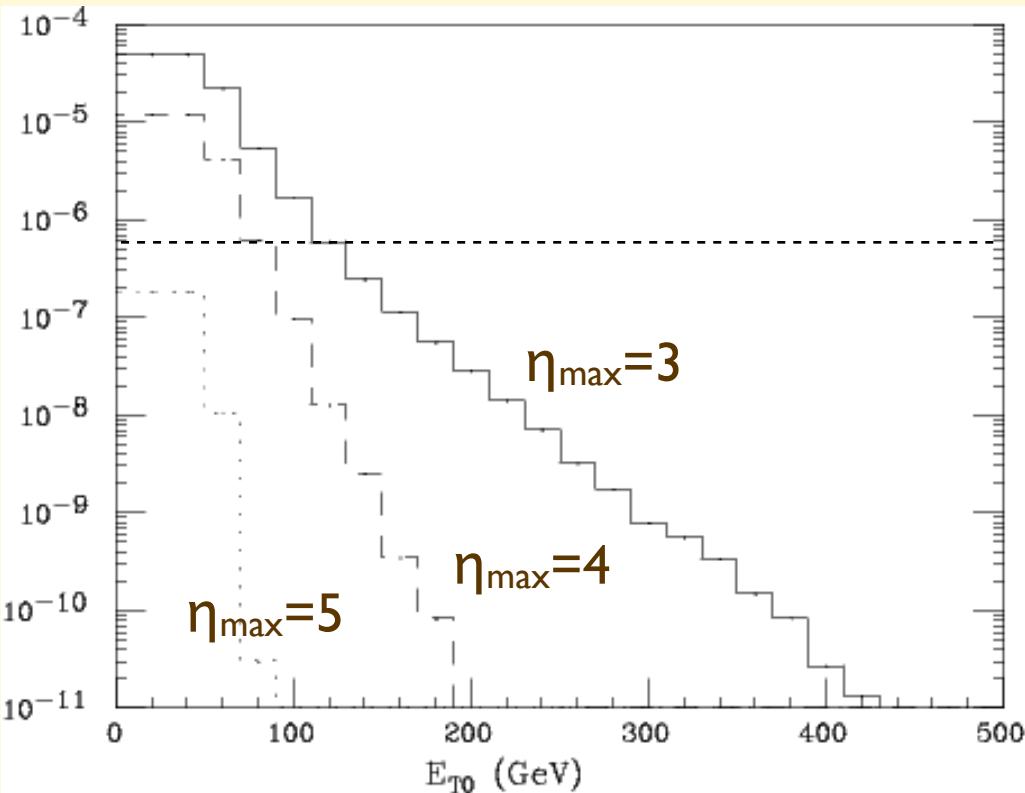


All jet multiplicities contribute at approximately the same level!!

Instrumental sources of missET: incomplete calorimeter η coverage



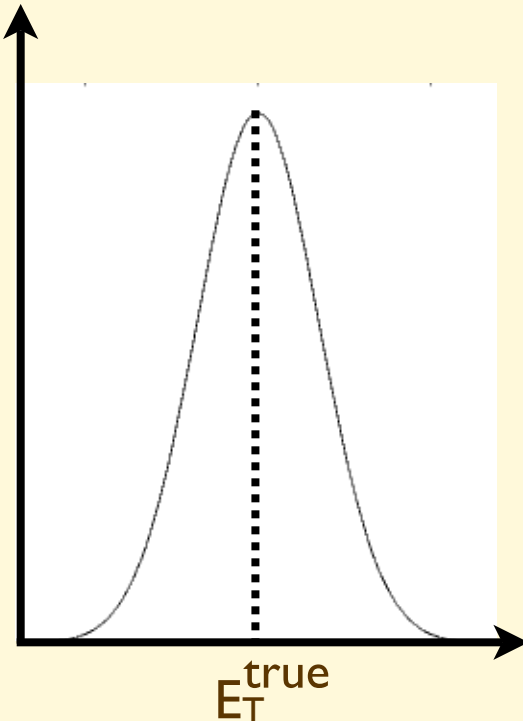
$\sigma(\text{jet-jet with MET} > E_{T0}) / \sigma(pp \rightarrow X)$



cfr:
 $\sigma(W \rightarrow l\nu) / \sigma(pp \rightarrow X) \approx 6 \times 10^{-7}$

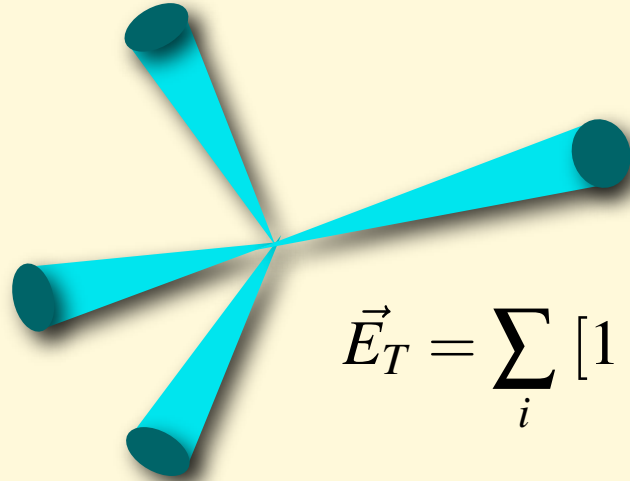
NB:
 At $L = 10^{34} \text{ cm}^{-2} \text{ s}^{-1}$,
 $\langle N(\text{pp collisions}) \rangle \approx 20$
 => **probability 20x larger**

Instrumental sources of missET: jet energy resolution



$$\text{Prob}[p_T] \propto \exp -\frac{(p_T - p_T^{\text{true}})^2}{\sigma^2}$$

$$\sigma = C\sqrt{E_T^{\text{true}}/\text{GeV}}, \quad C = O(1)$$

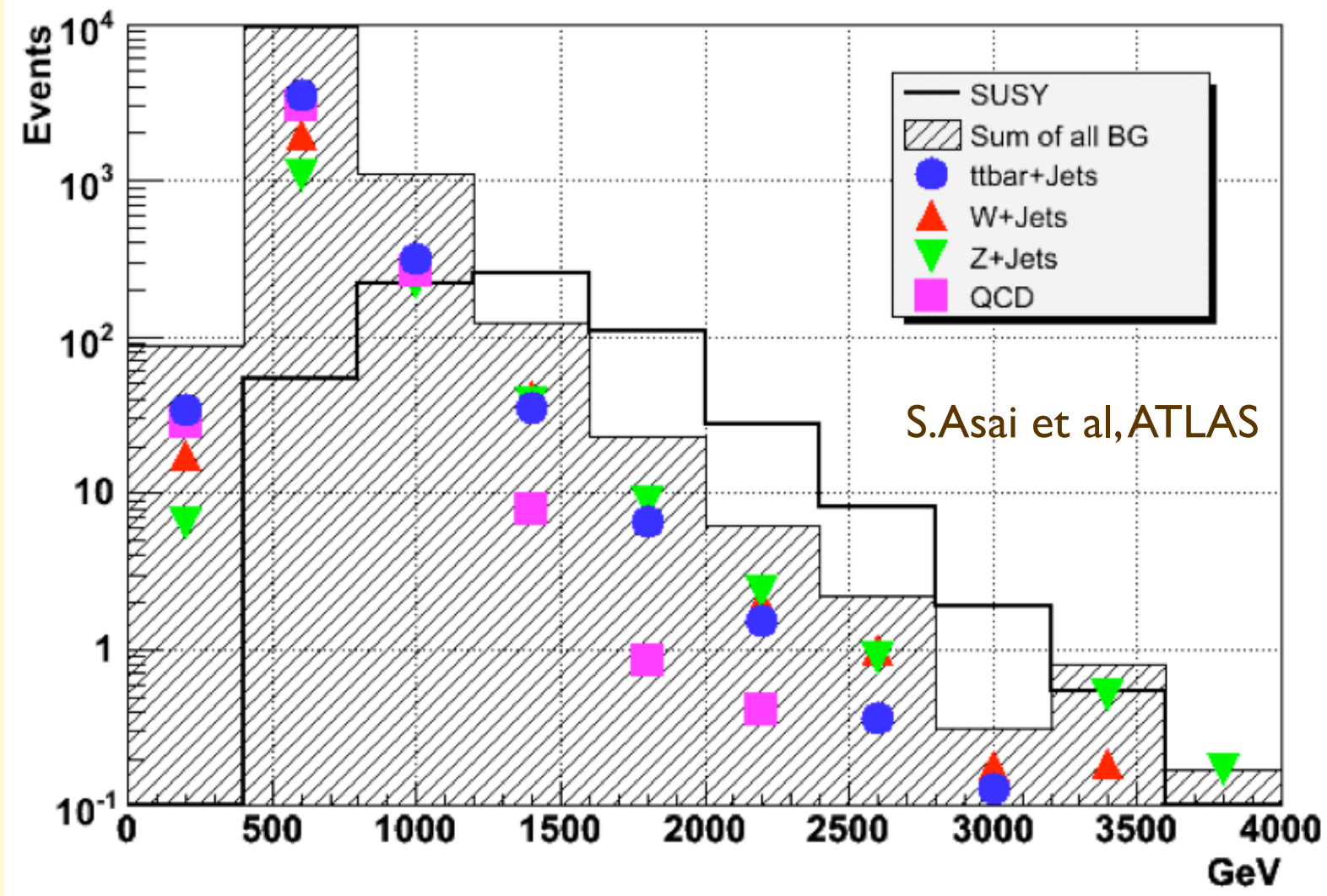


$$\vec{E}_T = \sum_i [1 + \delta_i] \vec{p}_{T,i}^{\text{true}} = \sum_i \delta_i \vec{p}_{T,i}^{\text{true}}$$

$$\langle |\vec{E}_T|^2 \rangle = \sum_{i,j} \langle \delta_i \delta_j \rangle \vec{p}_{T,i} \cdot \vec{p}_{T,j} \quad \langle \delta_i \delta_j \rangle = \frac{C^2}{p_{T,i}} \delta_{ij}$$

$$\langle \text{MET} \rangle = C \sqrt{\sum_i p_{T,i}}$$

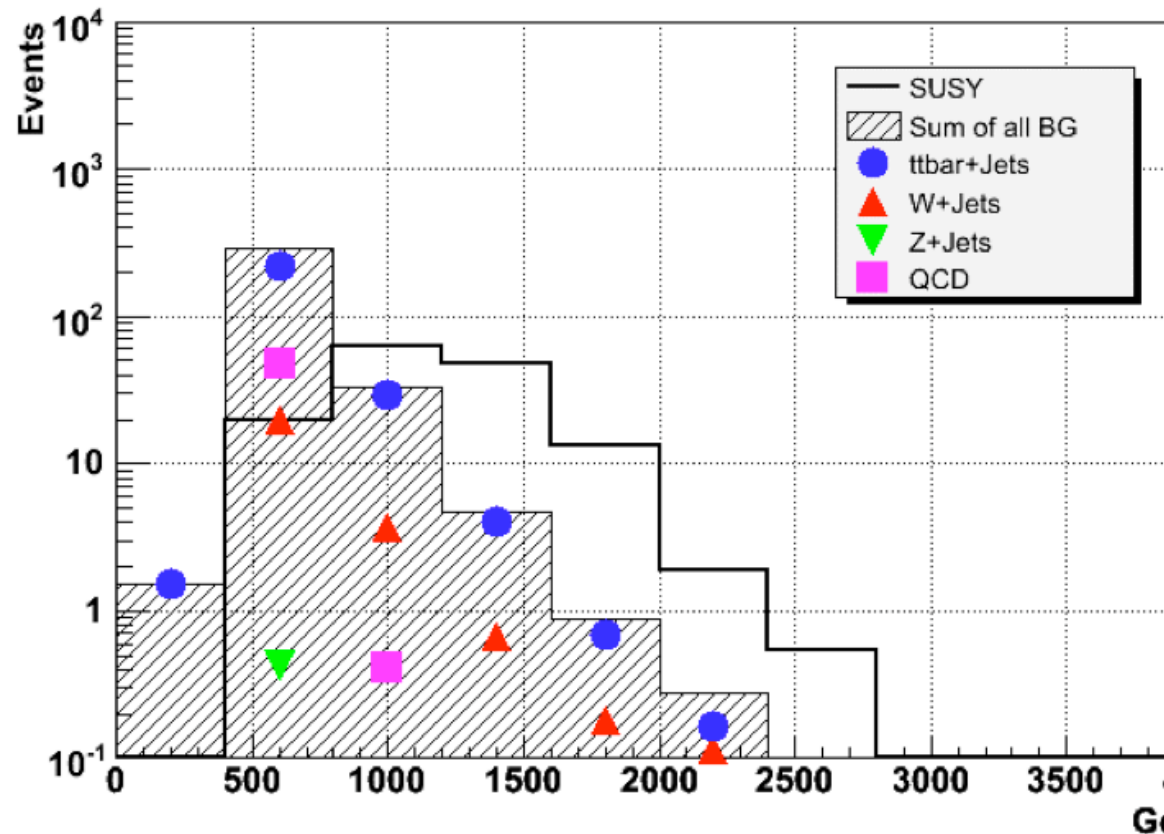
Overall result, after the complete detector simulation, etc....



Adding leptons ...

S.Asai et al, ATLAS

Effective Mass 1lepton SUSY



Missing Et Fast SUSY 2lepton mode DS MET>100GeV

